

IONOTHERMAL SYNTHESIS
A NEW SYNTHESIS METHODOLOGY USING IONIC LIQUIDS AND EUTECTIC
MIXTURES AS BOTH SOLVENT AND TEMPLATE IN ZEOTYPE SYNTHESIS

Emily Ruth Parnham

A Thesis Submitted for the Degree of PhD
at the
University of St Andrews



2006

Full metadata for this item is available in
St Andrews Research Repository
at:

<http://research-repository.st-andrews.ac.uk/>

Please use this identifier to cite or link to this item:
<http://hdl.handle.net/10023/10224>

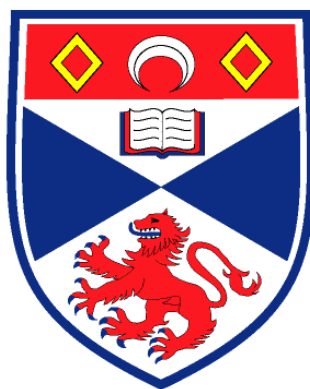
This item is protected by original copyright

Ionothermal Synthesis

A new synthesis methodology using ionic liquids and eutectic mixtures as both solvent and template in zeotype synthesis.

A thesis submitted in application for the title of Ph.D. by

Emily Ruth Parnham M.Sci. (Chem.)



University of St Andrews

June 2006

Declaration

I, Emily Ruth Parnham, hereby certify that this thesis, which is approximately 33,000 words in length, has been written by me, that it is the record of work carried out by me and that it has not been submitted in any previous application for a higher degree.

Date

Signature of candidate

I was admitted as a research student in September 2003 and as a candidate for the degree of a Ph.D. in September 2004; the higher study for which this is a record was carried out in the University of St Andrews between 2003 and 2006.

Date

Signature of candidate

I hereby certify that the candidate has fulfilled the conditions of the Resolution and Regulations appropriate for the degree for Ph.D. in the University of St Andrews and that the candidate is qualified to submit this thesis in application for that degree.

Date

Signature of supervisor

In submitting this thesis to the University of St Andrews I understand that I am giving permission for it to be made available for the use in accordance with the regulations of the University Library for the time being in force, subject to any copyright vested in the work not being affected thereby. I also understand that the title and abstract will be published, and that a copy of the work may be made and supplied to any *bona fide* library or research worker.

Date

Signature of candidate

Courses Attended

The School of Chemistry at St Andrews University requires that a postgraduate attend a number of taught courses. The courses attended were:

Crystallography Dr. P. Lightfoot

Electron Microscopy Dr. W. Zhou

Irvine Review Lectures – 2003

Publications

Ionic liquids and eutectic mixtures as solvent and template in synthesis of zeolite analogues.

E.R. Cooper, C.D. Andrews, P.S. Wheatley, P.B. Webb, P. Wormald and R.E. Morris, *Nature*, 2004, **430**, 1012

A new methodology for zeolite analogue synthesis using ionic liquids as solvent and template.

E.R. Cooper, C.D. Andrews, P.S. Wheatley, P.B. Webb, P. Wormald and R.E. Morris, *Studies in Surface Science and Catalysis, Part A*, 2005, **158**, 247

The ionothermal synthesis of SIZ-6 – a layered aluminophosphate

E.R. Parnham, P.S. Wheatley and R.E. Morris, *Chem. Commun.*, 2006, **4**, 380

The ionothermal synthesis of cobalt aluminophosphate zeolite frameworks.

E.R. Parnham and R.E. Morris, *J. Am. Chem. Soc.*, 2006, **128**, 2204

Ionothermal materials synthesis using unstable deep eutectic solvents as template delivery agents.

E.R. Parnham, E.A. Drylie, P.S. Wheatley, A.M.Z. Slawin and R.E. Morris, *Angew. Chemie*, 2006, **118**, 1

1-alkyl-3-methyl imidazolium bromide ionic liquids in the ionothermal synthesis of aluminium phosphate molecular sieves

E.R. Parnham and R.E. Morris, *Chem. Mater.*, submitted

Acknowledgements

I thank Prof. R.E. Morris for being my Ph. D. supervisor. I would also like to thank Dr. Paul Wheatley and Dr. Paul Webb for so patiently answering so many questions at the start of my project, Dr. Simon Teat, Dr. John Warren and Dr. Tim Prior for their technical help and crystallographic knowledge while at the SRS in Daresbury. Thanks also go to Dr. David Apperley at the EPSRC solid state NMR service, Prof. Alex Slawin for crystallography data collected at St Andrews, Dr Phil Wormald for the solid state NMR data collected at St Andrews and to the technical staff at St Andrews University, Mrs. S. Williamson (CHN analysis), Mrs. M. Smith (NMR) and Mr. R. Blackley (SEM/EDXS).

Many thanks also go to all those friends from St Andrews and back home who have tried so hard to keep me sane over the past three years; taking me out clubbing and bringing bottles of wine round to my flat – especially when the Ph. D. blues arrived! A big special thanks goes to Lynn, Lyndsey and Aoife for stopping their Ph. D.'s to work so hard on organising the best hen night ever for me and helping out so much with my wedding. Thanks must also be given to Stuart Miller for reading through the whole of this thesis. Cannot wait to return the favour!

I thank EPSRC for funding this work.

A special thanks also go to my family for helping me through the past years of study, especially to my sister Rowan and little nephews Sam and Peter for making me smile so much. I would also like to thank my now husband, Ben, for standing by and supporting me for the past three years.

Abstract

The aim of this thesis was to research the new synthesis methodology of ionothermal synthesis, used for the synthesis of zeolite type materials, mainly aluminophosphates. An ionic liquid or eutectic mixture is to act as both the organic template and the solvent, hence eliminating the space filling effects in the reaction from the water.

Initial reactions were carried out using the ionic liquid 1-ethyl-3-methylimidazolium bromide which acted as the solvent and template in the production of four three-dimensional structures and one layered structure. The addition of cobalt into the aluminophosphate framework was investigated and resulted in three different cobalt-aluminophosphates being synthesised, including one new zeolite framework.

Experiments were carried out into the effect of altering the imidazolium cation alkyl chain. It appears likely that in the presence of fluoride, some of the imidazolium cations undergo a metathesis reaction forming 1,3-dimethylimidazolium which acts as a template in the formation of an aluminophosphate. Preliminary investigations have also been started into the effects of changing the ionic liquid anion from bromide to phosphorus hexafluoride and bis((trifluoromethyl)sulfonyl)amide. The use of these anions resulted in the production of several different one and two-dimensional structures.

The use of eutectic mixtures as solvent and template was also investigated as a cheaper, more easily synthesised solvent than the ionic liquids. The results show a new methodology of eutectic mixtures acting as template delivery agents through the slow, *in situ* decomposition of the urea derivative of the eutectic mixture. This synthesis method resulted in the formation of nine one and two-dimensional aluminophosphates.

Table of Contents

1: Introduction

1.1: Zeolites and Zeolite Analogues	1
<i>1.1.1: Background</i>	1
<i>1.1.2: Synthesis</i>	6
<i>1.1.3: Organic Guest Molecules. Structure directing agents, templates or space fillers?</i>	13
<i>1.1.4: Solvent</i>	15
<i>1.1.5: The Fluoride Route</i>	17
1.2: Ionic Liquids	19
<i>1.2.1: Background</i>	19
<i>1.2.2: Are Ionic Liquids Really Green?</i>	21
<i>1.2.3: Synthesis</i>	22
<i>1.2.4: Water Content</i>	25
<i>1.2.5: pH and pK_a</i>	27
<i>1.2.6: Eutectic Mixtures</i>	29
1.3: References	31

2: Aims

2.1: Synthesis of zeolite analogues using ionic liquids and eutectic mixtures as the solvent and template	37
2.2: Characterisation	39
2.3: References	40

3: Experimental and Analytical Techniques

3.1: Hydrothermal/Ionothermal Synthesis	41
3.2: Moisture Sensitive Techniques	43
3.3: X-ray Diffraction	43
3.3.1: <i>Introduction and X-ray Generation</i>	43
3.3.2: <i>Crystallographic Space Groups</i>	45
3.3.3: <i>Diffraction of X-rays by Crystals</i>	47
3.3.4: <i>Single Crystal X-ray Diffraction</i>	51
3.3.5: <i>Powder X-ray Diffraction</i>	52
3.3.6: <i>Synchrotron Radiation</i>	53
3.4: Nuclear Magnetic Resonance (NMR)	55
3.5: Thermogravimetric Analysis (TGA)	58
3.6: CHN Analysis	58
3.7: Scanning Electron Microscopy (SEM) combined with Energy Dispersive X-ray Spectroscopy (EDXRS)	59
3.8: References	60

4: 1-ethyl-3-methylimidazolium bromide as solvent and template in the synthesis of AlPOs

4.1: Aims	61
4.2: Introduction (1-alkyl-3-methylimidazolium cation)	61
4.3: Experimental – Ionothermal synthesis of AlPOs	63
4.3.1: <i>Synthesis of 1-ethyl-3-methylimidazolium bromide</i>	63
4.3.2: <i>Synthesis of zeolite analogues in sealed autoclaves</i>	64
4.3.3: <i>Synthesis of zeolite analogues in round bottom flasks</i>	65
4.3.4: <i>Recycling of ionic liquid</i>	65
4.3.5: <i>Experimental Details</i>	66

4.4: Results	68
4.4.1: <i>SIZ-1</i>	68
4.4.2: <i>SIZ-3</i>	74
4.4.3: <i>SIZ-4</i>	79
4.4.4: <i>SIZ-5</i>	83
4.4.5: <i>SIZ-6</i>	86
4.5: Discussion and Conclusion	92
4.6: References	95

5: 1-ethyl-3-methylimidazolium bromide as solvent and template in the synthesis of Co-AIPOs

5.1: Aims	97
5.2: Introduction – Addition of cobalt to aluminophosphates	97
5.3: Experimental – Ionothermal synthesis of Co-AIPOs	100
5.3.1: <i>Synthesis of Co-AIPOs</i>	100
5.3.2: <i>Experimental Details</i>	101
5.4: Results	102
5.4.1: <i>SIZ-7</i>	102
5.4.2: <i>SIZ-8</i>	106
5.4.3: <i>SIZ-9</i>	109
5.5: Discussion and Conclusion	110
5.6: References	112

6: Variations on the imidazolium cation used as solvent and template in AIPO synthesis

6.1: Aims	113
6.2: Introduction – Imidazolium cation variations	113

6.3: Experimental – Changing the imidazolium cation	115
6.3.1: <i>Synthesis of 1-propyl-3-methylimidazolium bromide</i>	115
6.3.2: <i>Synthesis of 1-isopropyl-3-methylimidazolium bromide</i>	115
6.3.3: <i>Synthesis of 1-butyl-3-methylimidazolium bromide</i>	116
6.3.4: <i>Synthesis of 1-pentyl-3-methylimidazolium bromide</i>	116
6.3.5: <i>Synthesis of 1,1'-dimethyl-3,3'-hexamethylene -diimidazolium dibromide</i>	117
6.3.6: <i>Synthesis of zeolite analogues in sealed autoclaves</i>	118
6.3.7: <i>Experimental Details</i>	119
6.4: Results	120
6.4.1: <i>Effect of lengthening ionic liquid alkyl chain on AIPO structure formation</i>	120
6.4.2: <i>Effect of ionic liquid alkyl chain branching on AIPO structure formation</i>	124
6.5: Discussion and Conclusion	126
6.6: References	129

7: Effect on AIPO synthesis of changing the ionic liquid anion

7.1: Aims	131
7.2: Introduction – Ionic Liquid Anions	131
7.3: Experimental	133
7.3.1: <i>Synthesis of 1-ethyl-3-methylimidazolium phosphorus hexafluoride</i>	133
7.3.2: <i>Synthesis of 1-ethyl-3-methylimidazolium bis((trifluoromethyl)sulfonyl)amide</i>	133
7.3.3: <i>Synthesis of zeolite analogues in sealed autoclaves</i>	134

7.3.4: <i>Experimental Details</i>	135
7.4: Results	136
7.4.1: β - NH_4AlF_4	136
7.4.2: $\text{Al}(\text{H}_2\text{PO}_4)_2\text{F}$	140
7.5: Conclusions and Discussions	143
7.6: References	146
8: Urea/Choline Chloride eutectic mixture as solvent in the synthesis of AIPOs	
8.1: Aims	147
8.2: Introduction – Eutectic Mixtures verse Ionic Liquids	147
8.3: Experimental	148
8.3.1: <i>Synthesis of choline chloride/urea eutectic mixture</i>	148
8.3.2: <i>Synthesis of zeolite analogues in sealed autoclaves</i>	148
8.3.3: <i>Experimental Details</i>	150
8.4: Results	151
8.4.1: <i>SIZ-2</i>	151
8.4.2: <i>AIPO-CJ2</i>	156
8.5: Discussion and Conclusion	158
8.6: References	159
9: Eutectic Mixtures as Template Delivery Agents	
9.1: Aims	160
9.2: Introduction – <i>In situ</i> generation of template	160
9.3: Experimental	162

9.3.1: <i>Synthesis of eutectic mixtures</i>	162
9.3.2: <i>Synthesis of aluminophosphate zeolite analogues in sealed autoclaves</i>	162
9.3.3: <i>Synthesis of gallium phosphate Zeolite-A (Structure 9)</i>	163
9.3.4: <i>Experimental Details</i>	164
9.4: Results	165
9.4.1: <i>Structure 1</i>	165
9.4.2: <i>Structure 2</i>	168
9.4.3: <i>Structure 3</i>	171
9.4.4: <i>Structure 4</i>	174
9.4.5: <i>Structure 5</i>	176
9.4.6: <i>Structure 6</i>	177
9.4.7: <i>Structure 7</i>	179
9.4.8: <i>Structure 8</i>	180
9.4.9: <i>Structure 9</i>	182
9.5: Discussion and Conclusions	184
9.6: References	186
10: Review, Conclusions and Future Work	
10.1: Summary and Conclusions	188
10.2: Future Work	196
10.3: References	202

Abbreviations

AlPO	Aluminophosphate
BASIL	Biphasic acid scavenging utilising ionic liquids
BMI	1-buty-3-methylimidazolium
CCD	Charge coupled device
CCLRC	Central Laboratory of the Research Councils
Co-AlPO	Cobalt aluminophosphate
D_nR	Double- n -ring
EDXRD	Energy dispersive X-ray diffraction
EMI	1-ethyl-3-methylimidazolium
ESI-MS	Electro spray ionisation - mass spectroscopy
EU	Eutectic mixture
IL	Ionic Liquid
iPrMI	1-isopropyl-3-methylimidazolium
IZA-SC	International Zeolite Association - Structure Commission
MAS-NMR	Magic angle spinning - nuclear magnetic resonance
PBU	Primary building unit
PeMI	1-pentyl-3-methylimidazolium
PNBU	Pre-nucleation building units
POSS	Polyhedral oligomeric silsesquioxanes
PrMI	1-propyl-3-methylimidazolium
PXRD	Powder X-ray diffraction
S_nR	Single- n -ring
SAXS	Small-angle X-ray scattering
SBU	Secondary building unit
SCXRD	Single crystal X-ray diffraction

SDA	Structure directing agent
SEM	Scanning electron microscopy
SIZ	St Andrews ionic liquid zeolite
SRS	Synchrotron Radiation Source
T	Tetrahedra or tetrahedral
TBU	Tertiary building unit
Tf ₂ N ⁻	bis-((trifluoromethyl)sulfonyl)amide
TGA	Thermal gravimetric Analysis
UV	Ultraviolet
WAXS	Wide-angle X-ray scattering
XRD	X-ray diffraction

Three letter zeolite codes as allocated by the International Zeolite Association

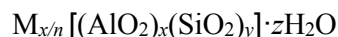
1: Introduction

1.1: Zeolites and Zeolite Analogues

1.1.1: Background

Zeolites are microporous solids that are commercially important in catalytic, adsorption and separation processes.¹ In 1756 Cronstedt reported the discovery of the first zeolite, the naturally occurring mineral stilbite.² On heating, stilbite was found to rapidly lose water, hence the name zeolite, derived from the Greek words “zeo” to boil and “lithos” stone.³ In the 1940s, Barrer⁴ (Imperial College, London) and Milton⁵ (Union Carbide, New York) hydrothermally synthesised independently the first zeolites, finding new (not naturally occurring) framework structures. To date approximately 40 natural zeolite structures³ and more than 130 synthetic framework types⁶ are known.

Zeolites are microporous, crystalline, aluminosilicates with a three-dimensional framework structure formed by corner sharing TO_4 tetrahedra (where T, the tetrahedral atom = Si or Al).⁷ Every apical oxygen is shared between two neighbouring tetrahedra giving a framework ratio of 2 oxygen atoms to every tetrahedral atom.³ The $AlO_{4/2}^-$ tetrahedra determine the framework charge, which is balanced by cations that occupy non-framework positions to attain electroneutrality. The general formula is:



Where x cations of valence M^{n+} charge balance the Al^{3+} .

The primary building unit (PBU) of a zeolite is the individual tetrahedral unit, TO_4 . The topology of all known zeolite framework types can be described in terms of a finite number of specific combinations of tetrahedra called "secondary building units" (SBUs)

as shown in Figure 1.1.⁸ In Figure 1.1, T atoms belonging to the TO_4 are located at each corner and the oxygens (not plotted for clarity) located near the mid-points of the lines joining each pair of T atoms hence each line represents a T-O-T linkage.

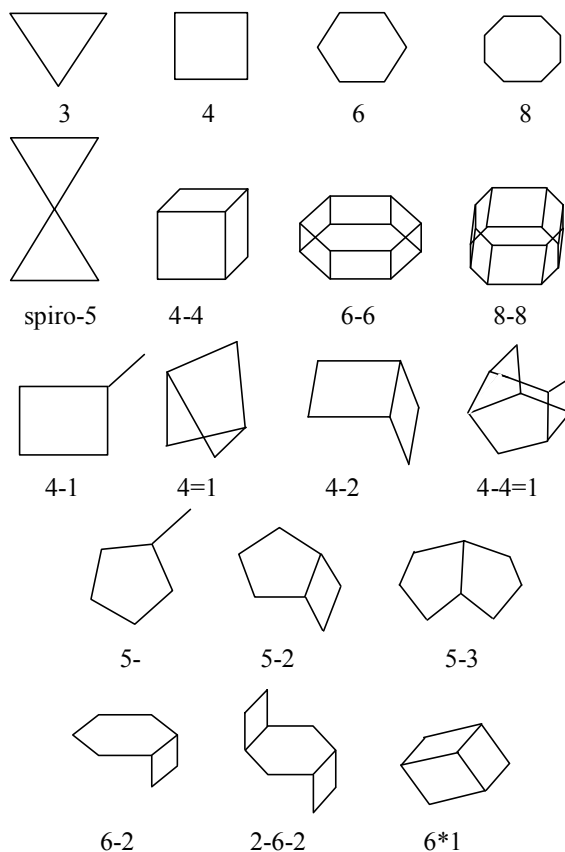


Figure 1.1: Secondary building units (SBUs) and their symbols.

The SBUs are combined together to form “tertiary building units” (TBUs). These TBUs may be considered in terms of large polyhedral building blocks which join together to form characteristic cages. An example of this is the sodalite cage (or β -cage) composed of 24T atoms: six 4-rings or eight (fused) 6-rings. The sodalite cages join together in different combinations to form a variety of framework types e.g. EMT, FAU, LTA and SOD (Figure 1.2). These three letter codes are assigned by the Structure Commission of the International Zeolite Association (IZA-SC) to all unique and confirmed zeolite framework topologies.

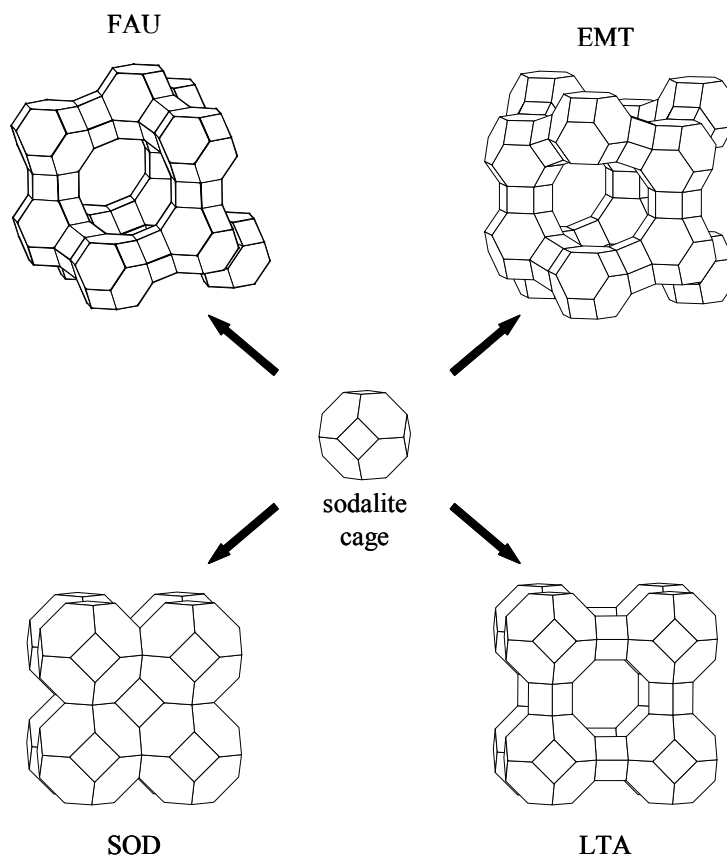


Figure 1.2: Framework types from linking of sodalite cages.⁹

The zeolite structure results in a regular array of channels and cavities on a molecular scale (ca. 3-15 Å).¹⁰ These channels and cavities can be filled with water or other guest molecules and selective separation is possible, hence the term “molecular sieve” is often used when discussing zeolites, although such behaviour is not exclusive to zeolites.

The term “molecular sieves” was introduced by McBain¹¹ in 1932 and in fact refers to a whole family of chemical materials, of which the zeolites is just one of the classes. He defined a molecular sieve as a family of materials with an internal pore structure capable of separating a mixture by absorbing molecules based on molecular size and shape differences.¹¹

Today the term “molecular sieve” is more broadly used to describe porous oxide materials with varying elemental composition. Their structure is the same as that of the zeolites but cations other than aluminium and silicon may occupy the tetrahedral sites. Table 1.1¹² shows a selection of cations which are presently known to be able to occupy the sites within molecular sieves. These cations must have the ability to occupy framework sites, but need not be isoelectronic with Si⁺⁴ or Al⁺³.

Cation	Oxide Charge
(M ⁺² O ₂) ⁻²	Be, Mg, Zn, Co, Fe, Mn
(M ⁺³ O ₂) ⁻¹	Al, B, Ga, Fe, Cr, Sc
(M ⁺⁴ O ₂) ⁻⁰	Si, Ge, Mn, Ti
(M ⁺⁵ O ₂) ⁺¹	P, As

Table 1.1: Cations that may form molecular sieve framework structures and the cation oxide charge possible.

The first class of molecular sieves synthesised which contained no silica were the aluminophosphates (AlPOs), synthesised by Flanigen and co-workers in the early 1980s.¹³ The AlPO framework consists of alternating Al³⁺ and P⁵⁺ sites giving a global framework charge zero,¹⁴ hence the AlPOs have no ion-exchange capacity, but they do still display many similar properties to those of the zeolites.¹⁵

It is however possible for the framework of the AlPOs to be very different to that of the aluminosilicate zeolites. The Al atoms in the AlPOs can adopt four, five and six coordination with oxygen.¹⁶ This is in contrast to the aluminosilicates where the Al only forms tetrahedral coordination. The tetrahedral P atoms can share one to four of its oxygen atoms with an adjacent Al in molecular sieve structures. Terminal P-O bonds are possible, resulting in an interrupted structure with a negatively charged framework with the Al/P ratio less than 1. Examples of this are AlPO-HDA with an Al:P ratio of 4:5¹⁷ and AlPO-CJ4 with an Al:P ratio of 1:2.¹⁸ These structural differences have lead

to many new framework architectures being discovered with over 200 open-framework aluminophosphate structures recently being compiled (May 2005) in an online database; <http://mezeopor.jlu.edu.cn/alpo/>.¹⁹

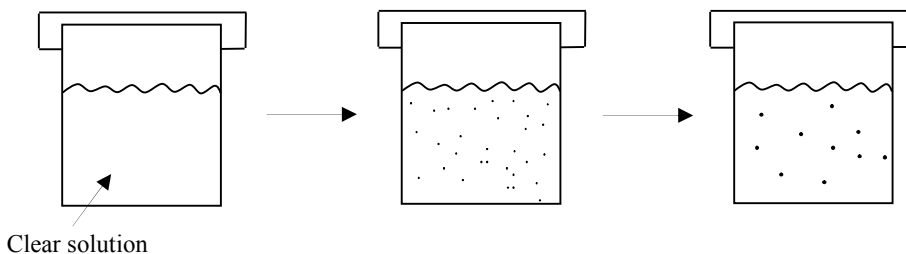
Another difference between the AlPOs and the aluminosilicates is the fact that the AlPOs normally only have an even number of T atoms in a ring. This is due to Löwenstein's rule which states that no two aluminium ions can occupy the centres of tetrahedral linked by one oxygen.²⁰ There is however little theoretical basis for this strict application of aluminium avoidance but rather a thermodynamic preference giving a strong tendency toward Al-O-Al bond avoidance.²¹ Bell *et al.* have calculated that compounds prepared by hydrothermal synthesis should support Löwenstein's rule, however the energy loss due to the direct Al-O-Al linkages could be overcome by thermal energies²² e.g. from high-temperature solid-state synthesis as in the formation of Cs₂Al₂P₂O₉.²³

1.1.2: Synthesis

The most commonly used route to synthetic molecular sieve synthesis is the hydrothermal method developed by Milton²⁴ and Barrer.²⁵ This involves the mixing of the reagents in water in the presence of an organic template then heating (< 250 °C) in an autoclave at autogenous pressure for a specific time. The synthesis of zeolites, is in general, very sensitive to the various reaction conditions including cation source, pH, water content, organic template, solvent, time, temperature, aging and stirring. The number of variables can make zeolite synthesis very difficult to reproduce and to add to the difficulties often varying just one component can end up changing several reaction conditions.

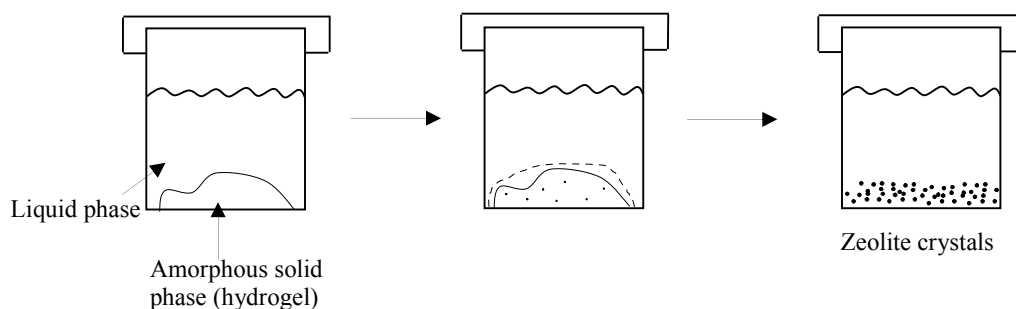
The zeolite crystallisation mechanism is not well understood due to its complexity and the difficulties of carrying out *in situ* experiments. This adds to the problems associated with zeolite synthesis especially in relation to attempts to synthesise and engineer new zeolite type structures. It is, however, accepted that there is probably not just one universal mechanism to describe all zeolite synthesis.³ At the two extremes of the proposed mechanisms Caullet and Guth²⁶ suggested the following:

- a) The solution-mediated transport mechanism e.g. Zeolite A.²⁷



This involves the diffusion of the aluminate and silicate species from the liquid phase to the nucleation site for crystal growth.

b) The solid-phase transformation mechanism e.g. ZSM-35 (FER) and ZSM-5.²⁸



This involves the solid hydrogel reorganizing “*in situ*” to form the zeolite structure.

Crystallisation from solution involves the formation of nucleation centres followed by subsequent growth of these nuclei to form the final crystalline product. There are several different opinions for the crystallisation mechanism with evidence to support each argument. It is however agreed that it is the formation of the initial small particles which is critical to the final solid formed.

Early ideas of a crystallisation mechanism came from Barrer’s concept of primary and secondary building units (Figure 1.1) pre-existing in solution then joining together to form the solid.²⁹ Breck later carried out a study using XRD measurements on the crystallisation of zeolite Na-A and Na-X.³⁰ He concluded that the nuclei may consist of preliminary building units of polyhedra (e.g. the hexagonal prism) as suggested by Barrer *et al.*²⁹ This idea caused much discussion as the existence of SBUs in the silicate solutions could not be shown unambiguously.³¹

In 2000, Bussian *et al.* demonstrated using electro spray ionisation mass spectrometry (ESI-MS) and ²⁹Si NMR that double-4-rings (D4R) were the dominant species present (88.3 %) in a silicate solution containing tetramethyl ammonium hydroxide.³² These D4R units can be isolated as a solid and belong to the class of materials known as the polyhedral oligomeric silsesquioxanes (POSS)³³ (Figure 1.3).

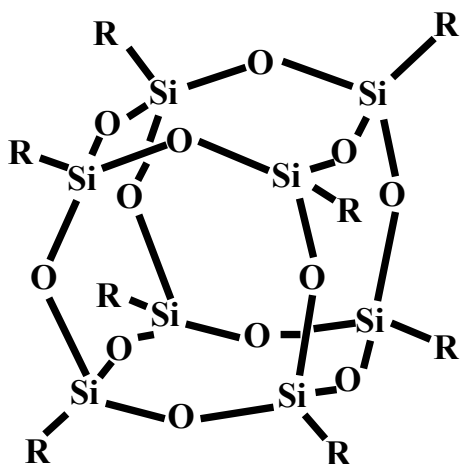


Figure 1.3: Cubic silsesquioxane

Morris *et al.* have since synthesised solvothermally and hydrothermally respectively the gallophosphate³⁴ D4R building unit occluding oxygen or fluoride and the germinate³⁵ analogue occluding fluoride within the D4R (Figure 1.4). Whilst these D4R SBUs can be isolated, there is still no conclusive evidence for the correlation between SBUs present in a zeolite structure and their role in the synthesis mechanism of the material. It cannot however be neglected that controlling the type of SBU present in the synthesis, then controlling how the SBUs condense together is an attractive mechanistic idea for the design and preparation of molecular sieves.³⁶

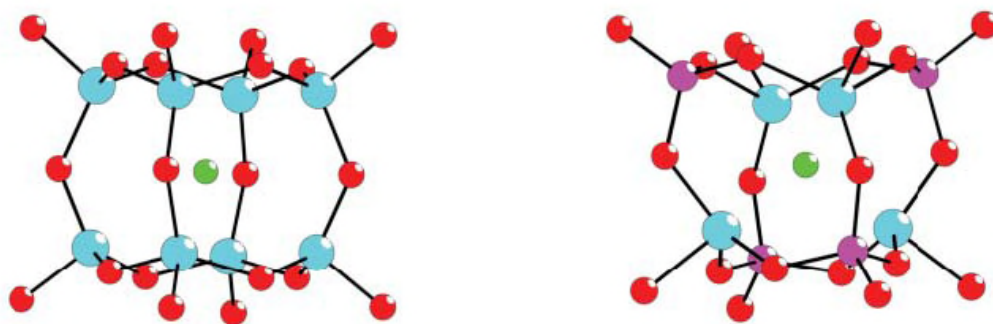


Figure 1.4: $\text{Ge}_8\text{O}_{16}\text{F}$ (left) and $\text{Ga}_4\text{P}_4\text{O}_{16}\text{F}$ (right) D4Rs.³⁶
Key: red = O, cyan = Ge/Ga, purple = P, green = F

Feréy *et al.* recently demonstrated, using *in situ* NMR techniques, that there are units in solution that can be identified during the formation of AlPO-CJ2 and these units are the building blocks for crystal formation (Figure 1.5).³⁷ This however does not full-fill Breck's conditions of being identical objects in solution and crystal, hence Feréy has called these units Pre-nucleation Building Units (PNBU) and not SBUs.³¹ The PNBU tetramer units undergo a rearrangement during nucleation and solid growth to produce a diagonal bridging connection, Al-X-Al (where X = F or OH) observed in the final AlPO-CJ2 structure.

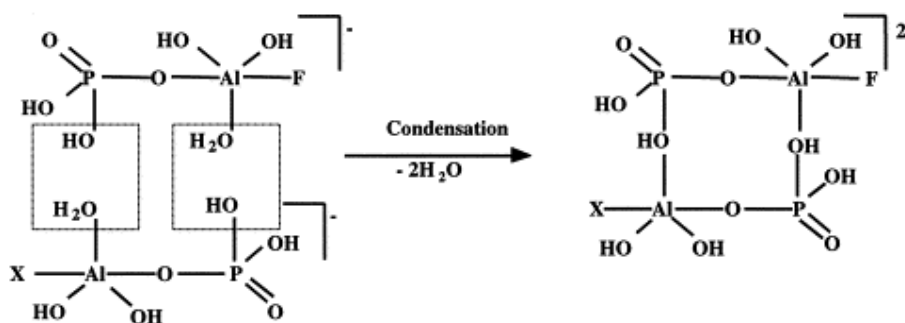


Figure 1.5: Cyclic tetramer (4R) formation of PNBU in AlPO-CJ2.³⁸

Oliver *et al.* proposed a model for aluminophosphates involving a transformation of linear chains to layers and then to a three dimensional structure through the hydrolysis-condensation process (Figure 1.6).³⁹ The evidence for this crystallisation mechanism came from the isolation of chains and layers in the same reaction composition as that which forms a three dimensional structure.

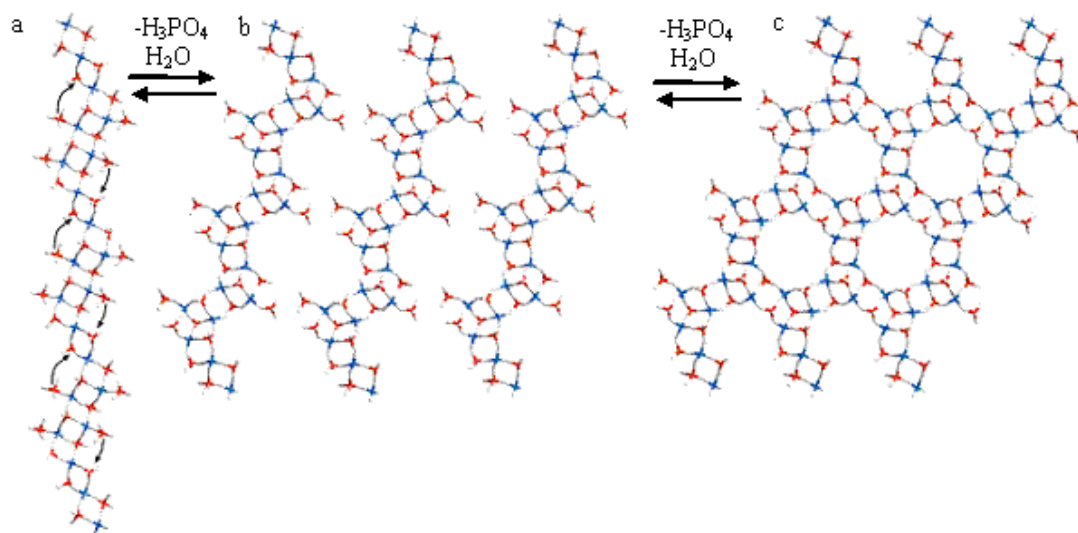


Figure 1.6: Formation of the capped AlPO-5 like layered structure
 a) The partial *trans* chain, b) Intrachain condensation creates an array of edge-sharing 4 and 6-rings, c) Condensation of the chains to form the 2-dimensional structure containing 12-rings.³⁹

The first *in situ* experiments carried out on aluminophosphates to provide experimental evidence for Oliver's proposed mechanism have been undertaken using a combination of X-ray scattering (SAXS/WAXS) and absorption techniques (UV-vis and Raman). Grandjean *et al.*⁴⁰ summarised zeolite formation in three stages:

- 1) a reaction of starting reagents to form a primary gel phase
- 2) condensation and aggregation in the secondary amorphous phases
- 3) nucleation and crystallisation of the AFI structure.

Gallium fluorophosphates have been studied *in situ* using the technique of time-resolved energy dispersive X-ray diffraction (EDXRD). During the hydrothermal synthesis of the three-dimensional ULM-3, a one-dimensional chain structure is observed before the rapid crystallisation to form ULM-3. The EDXRD data confirms the chain phase to be a solid precursor of the microporous ULM-3.⁴¹

Another method of producing layer to framework transformation is through calcination. Examples include the borosilicate molecular sieve ERB-1, framework topology MWW, which is formed through the calcination of a layered intermediate.⁴² The aluminosilicate ferrierite can be formed through the layered intermediate PREFER⁴³ and zeolite RUB-41, framework type code RRO, has been synthesised as a calcination product using a layered silicate, RUB-39, as precursor.⁴⁴ The AIPO-41, framework topology AFO, can be synthesised by calcination of [F, Tet-A]-AIPO-1. Wheatley proposed the idea that first the layers undergo a translation along the a and b axis of about 8.4 Å and 4.8 Å respectively followed by condensation in the c -direction to produce AIPO-41 (Figure 1.7).⁴⁵

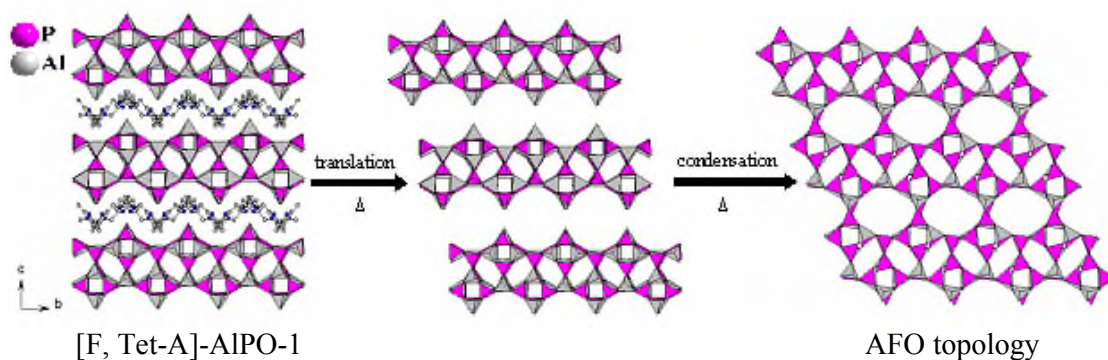


Figure 1.7: Transformation of [F, Tet-A]-AIPO-1 to AFO topology *via* calcinations.⁹

The addition of organic molecules, such as amines and alkyl quaternary ammonium ions, into the synthesis gel can affect both the rate of zeolite production and the actual chemical structure. XRD, MAS-NMR spectroscopy and ion exchange studies on the formation of ZSM-5 have provided direct evidence for the existence of preorganised inorganic-organic composite structures that resemble the channel interactions of the product to be formed.^{46,47} The inorganic-organic species are initially formed by the overlap of the hydration spheres of the inorganic/organic components with the release of water to give favourable van der Waals interactions. Aggregation takes place to give

nucleation. Crystal growth then takes place by the addition of the species to the surface of the growing crystal to give a layer-by-layer growth mechanism as illustrated in Figure 1.8. The organic SDA (Structure Directing Agent) is held tightly in the channels, often too big to escape the openings of the zeolite framework and can only be removed by calcination.

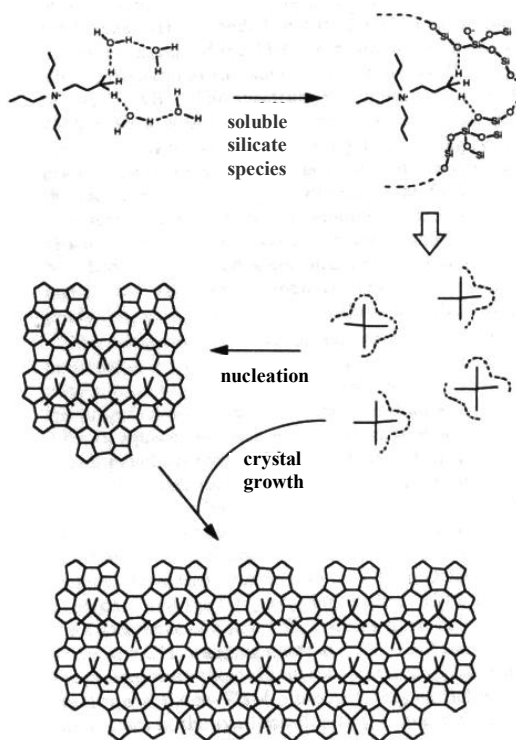


Figure 1.8: Mechanism of structure direction and crystal growth in the synthesis of TPA-Si-ZSM.⁴⁷

To date there is still much debate over the crystallisation mechanism of microporous solids, which appears to be very complex and poorly understood. There is experimental evidence to support the different mechanistic views and it is in fact very likely that there is more than one crystallisation mechanism to molecular sieve formation. The synthesis of new framework topologies still has to proceed through the screening of different conditions (cation source, pH, water content, organic template, time, temperature, aging and stirring) selected carefully using prior knowledge gained from known synthesis.

1.1.3: Organic Guest Molecules.

Structure directing agents, templates or space fillers?

In recent years, the most successful strategy used in synthesising new zeolite structures has been to vary the structure directing agent (SDA) used in the synthesis mixture.⁷ The role of the organic molecules in the synthesis gel has caused much discussion. Araya and Lowe⁴⁸ have made the distinction between the organic molecules acting as “pore fillers” versus “templates” in describing whether or not there is a structure-directing effect in operation. Here the word “templating” refers to the framework “wrapping” itself around the organic cation and the pore taking on the shape of the template like a “lock and key” relationship.⁴⁹ A “pore filler” however is just filling some of the space and the framework does not resemble the shape of the organic molecule. This would imply that many different organic molecules could potentially act as “pore fillers” in the same zeolite framework.

Davis and Lobo have made a further distinction between organic guest molecules acting as (i) space-filling species, (ii) structure-directing agents or (iii) templates.³ It is a question of specificity of a particular structure to a particular organic molecule which makes it possible to distinguish between space-filler and structure-directing agent. In ZSM-5 and ZSM-48 there are at least 22 and 13 different organic molecules used in their synthesis respectively.³ This is clearly an example of the organic guest molecules acting as space-fillers. Zeolites formed by organic molecules acting as structure-directing agents imply that a specific zeolite structure is synthesised *via* a single organic species. Examples of organic guest molecules acting as structure-directing agents include (i) N,N,N-trimethylammonium derivative of 1-adamantanamine in the synthesis of SSZ-24⁵⁰ and (ii) 1,4,7,10,13,16-hexaoxacyclooctane (18-crown-6) in the synthesis of hexagonal faujasite.⁵¹

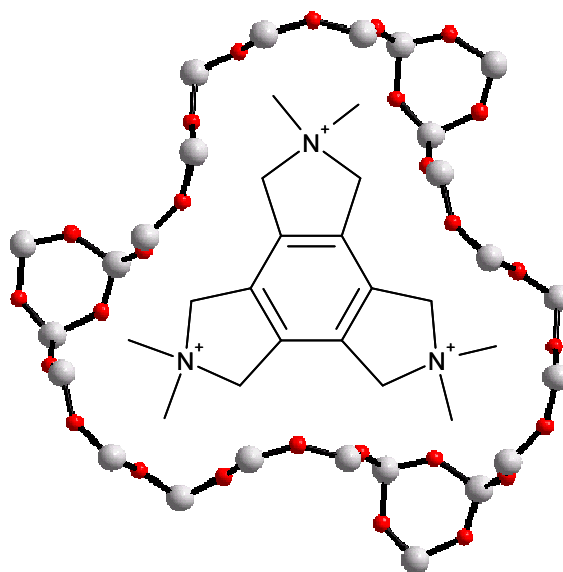


Figure 1.9: Trispyrrolidinium cation located within ZSM-18 (T-atoms grey and oxygens red)⁹

For an organic guest molecule to act as a “true template” the zeolite structure must adopt the geometric and electronic configuration that is unique to the templating molecule. Examples of this are very rare and in fact there appears to only be one example of “true templating” in the literature. This is ZSM-18 (MEI)⁵² which is templated by the trispyrrolidinium cation, which forms a close geometrical relationship with the framework structure as illustrated in Figure 1.9.

Being able to design new organic guest molecules that act as “true templates” in zeolite synthesis has become an important topic in the search for new zeotype structures.⁵³ (A zeotype is a material related to a zeolite but not necessarily having the strict Al/Si four co-ordination or porosity that is inherent of a zeolite material.) Lobo *et al.*⁵⁴ suggest that the selectivity of the structure-directing agent towards a specific zeolite structure increases as the size of the organic guest molecule is increased. They conclude that the most selective molecules are large, with more than 16 carbon and nitrogen atoms, and contain two or three charges per molecule.

One of the many challenges facing zeolite chemists is to synthesise a chiral zeolite framework. Chiral frameworks are of particular interest industrially due to their potential applications in heterogeneous catalysis and enantioselective separations. While there are several theoretical structures,⁵⁵ none as yet have actually been synthesised. Davis *et al.*³ suggest that to synthesise a chiral zeolite, a chiral template must be found and act as a “true template”.

1.1.4: Solvent

In the hydrothermal synthesis of zeolites, water is the solvent. Water does however appear to have other roles in the synthesis. It can act as a space filler in the porous lattice, it enhances the reactivity and lowers the viscosity of the mixture. So the water is not only a solvent but a reactant and a catalyst in T-O-T bond formation.⁵⁶

The quantity of water in a zeolite preparation appears to be very important. It has been reported that a minimum water content in the synthesis mixture is required to initiate the crystallisation process.⁵⁷ By controlling the amount of water in the same synthesis gel it has been possible to make zeolite omega, offretite, analcime and ferrierite.⁵⁶ In the synthesis gel with very little water present, the cations cannot be fully solvated by the water molecules. The consequence of this may be to alter the structure-directing behaviour of these cations and possibly lead to “true templating” as there will not be enough water present to act as a space filler.

Another possible zeolite synthesis route is the non-aqueous route. This tends to use organic solvents rather than water. To find suitable organic solvents for zeolite synthesis, their tendency to form hydrogen bonds must be considered. If the solvent forms hydrogen bonds which are too strong this will prevent the framework species and template from interacting hence preventing nucleation. An intermediate hydrogen bonding organic solvent is preferred.⁵⁷ Solvents such as hexanol, propanol, glycol, glycerol, sulfolane and pyridine have been examined.¹² Examples of zeolites synthesised include ZSM-48 and ZSM-39 which have been synthesised from mixed solvent, non-aqueous systems.⁵⁸ Silica-sodalite and aluminosilicate sodalites have been synthesised from ethylene glycol and propanol solvents. It is however often difficult to assess whether the reaction is actually brought about by the presence of small quantities of water, or whether it is the non-aqueous solvent playing a positive role and not just acting as a diluent or heat transfer medium.⁴⁹

1.1.5: The Fluoride Route

In 1978 Flanigen and Patton introduced a new route for synthesising zeolites that involved the use of F^- as a mineralising agent.⁵⁹ The OH^- which was traditionally used as a mineraliser is replaced by the F^- allowing crystallisation of zeolites at neutral or slightly acidic conditions, often resulting in large (in zeolite terms), good quality crystals. The larger crystals suggest that the mineralising power of the F^- is less than that of the OH^- so that the solubilities and effective super-saturations are lower. Further evidence for this is the higher temperature and longer reaction times usually required for fluoride based synthesis.⁴⁹ Typical fluoride sources include NH_4F , NH_4HF_2 and HF .

The fluoride route has also been extended to non-aluminosilicate synthesis. In AlPOs the F^- can act to charge balance the organic guest molecule as well as catalysing the formation of Al-O-P bond formation. The typical starting pH for an AlPO is slightly acidic to slightly alkaline (pH = 3-10) hence the pH conditions for the synthesis of phosphate-based materials in the presence of fluoride are close to those that would be used in its absence. The preferred fluoride source is HF due to the presence of cations like NH_4^+ producing undesirable side products with small pores templated by the NH_4^+ rather than the organic template e.g. AlPO-15 $NH_4Al_2OH(PO_4) \cdot 2H_2O$. During calcination the fluoride is removed along with the organic template.

The F^- can be either:

- (i) incorporated into the framework; for example in the triclinic fluorinated AlPO-CHA⁶⁰ where each six ring of the D6Rs contains one octahedral aluminium that connects to another octahedral aluminium of another D6R through two bridging fluorines, as demonstrated in Figure 1.20:

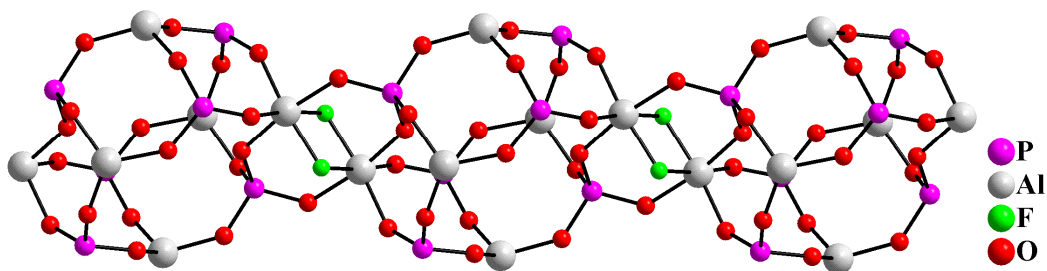


Figure 1.20: D6Rs linked by 4Rs in triclinic AlPO-CHA.

- (ii) incorporated into the small cages within the zeolite framework, usually inside a D4R cage. The fluoride ion can therefore be seen as a structure-director and has been shown through NMR studies to interact strongly with the framework atoms.¹⁰ Two examples of this are the silica AST and NON framework structures.⁶¹

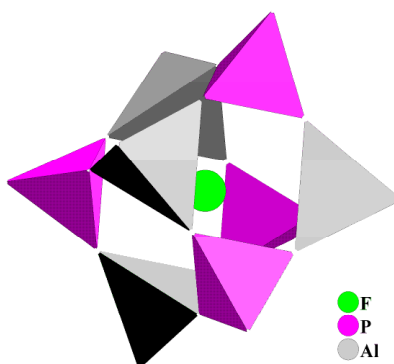


Figure 1.21: D4R with encapsulated fluoride

1.2: Ionic Liquids

1.2.1: Background

Ionic liquids, also known as room temperature molten salts,⁶² are liquids at ambient temperatures (less than 100 °C), that consist only of ions.⁶³ In 1914 ethylammonium nitrate was reported as the first room temperature ionic liquid with a melting point of 12°C.⁶⁴ It was synthesised by the addition of concentrated nitric acid to ethylamine, then the removal of water by distillation to give a pure salt.⁶⁵ In 1951 Hurley and Wier⁶⁶ developed low melting salts with chloroaluminate ions for low-temperature electroplating of aluminium. Throughout the 1970s and 1980s studies continued on these ionic liquids mainly for electrochemical applications.

In the 1980s ionic liquids were first proposed as solvents in organic synthesis.^{67,68} Acidic ionic liquids with chloroaluminate(III) ions proved to be effective solvents and catalysts in Friedel-Crafts reactions. Today ionic liquids are of industrial interest due to their unique solvent properties and lack of volatility. Currently the potential for substituting traditional organic solvents in chemical reactions is being researched,⁶⁹⁻⁷¹ since many traditional organic solvents are being banned for industrial use by the Montreal Protocol of 1989 due to the organic solvent's high volatility and/or toxicity.⁷² To date however there are only a few commercial processes where ionic liquids are used as the solvent in the reaction. They include the process operated by Eastman Chemical Company for the preparation of dihydrofurans,⁷³ and the BASIL process (Biphasic Acid Scavenging utilising Ionic Liquids) operated by BASF as part of a new route to precursors for photoinitiators that are used in UV-curable coatings.⁷⁴

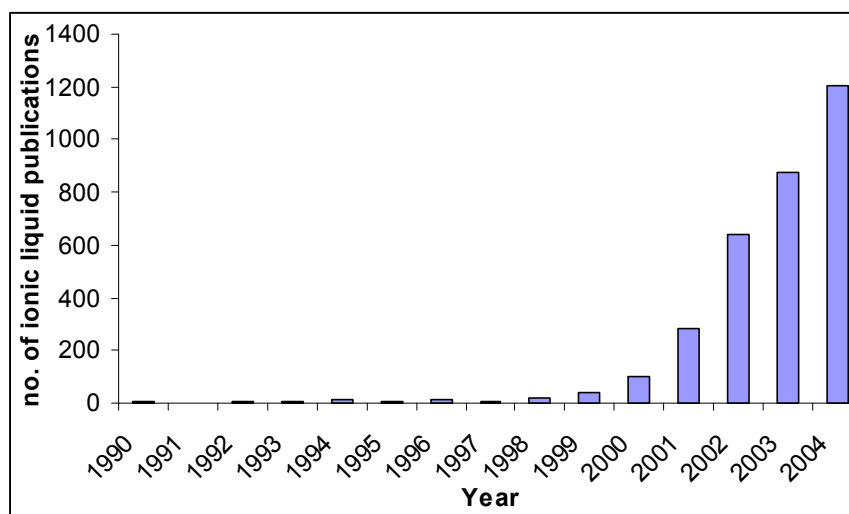


Figure 1.22: Yearly publications on ionic liquids – data produced from Scifinder

Since the mid 1990s there has been growing interest in the area of ionic liquids, and since the beginning of the 21st century there has been a boom in publications in this field (Figure 1.22). By 2004 over 500 ionic liquids had been synthesised and reported⁷⁵ with key researchers in the area predicting the actual number of possible ionic liquids to be of the order of 1 billion.⁷⁶ Some of the important properties of ionic liquids⁷⁷ which have made them of such academic and industrial interest are:

1. Excellent solvating properties for a wide range of organic, inorganic and polymeric materials. This means that unusual combinations of reagents can be brought into the same phase.⁷⁸
2. Little measurable vapour pressure therefore ionic liquids do not generally generate noxious volatile vapours and can be used effectively in high-vacuum systems. (It must however be noted that PF_6 and BF_4 salts undergo hydrolysis to produce HF.)⁷⁹
3. Non-flammability.
4. High thermal stability. Ionic liquids can show a liquid gap as large as 200 °C between their melting and decomposition temperatures.⁶²

1.2.2: Are Ionic Liquids Really Green?

Whilst the use of ionic liquids in industry may reduce the effects of solvents in air pollution due to their low volatility, the release of ionic liquids into aquatic environments may lead to water pollution due to their high solubility.⁸⁰ Provisional tests carried out on aquatic animals have shown that some ionic liquids are more toxic than conventional solvents such as methanol, dichloromethane and acetonitrile.⁸¹

Albrecht Salzer argued that ionic liquids are not green in *Chemical and Engineering News*, 2002, **80**, 4. Robin Rogers response to this argument is as follows:

“Salzer has not fully realized the magnitude of the number of potential ionic liquid solvents. I am sure, for example that we can design a very toxic ionic liquid solvent. However, by letting the principles of green chemistry drive this research field, we can ensure that the ionic liquids and ionic liquid processes developed are in fact green.”⁶⁵

Ionic liquid chemistry could be green as long as there is a drive for it to be green, with potentially harmful ionic liquids being disposed of carefully or even better recycled.

There is however another issue with ionic liquids and their environmental impact. Imidazole and haloalkanes, used in the synthesis of many ionic liquids, come from petroleum feed stocks, hence the origins of many ionic liquids are neither green nor sustainable.

1.2.3: Synthesis

Ionic liquids are made of two components, an organic or inorganic anion and a cation which is usually a large organic molecule. Some of the more commonly reported cations are shown in Figure 1.23. Examples of anions commonly used include halide ions, tetrafluoroborate (BF_4^-), tetrachloroaluminate (AlCl_4^-), hexafluorophosphate (PF_6^-) and bis((trifluoromethyl)sulfonyl)amide ($(\text{CF}_3\text{SO}_2)_2\text{N}^-$).⁷⁵

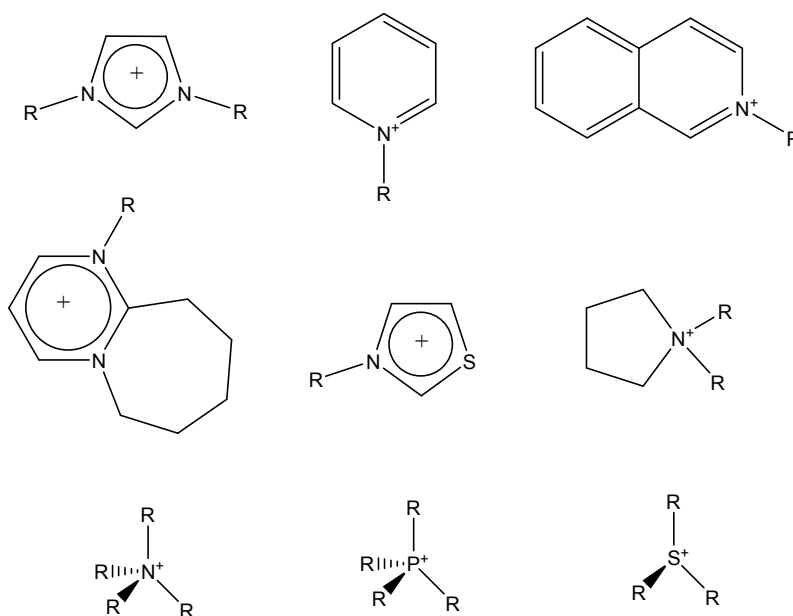


Figure 1.23: Important types of cations in ionic liquids.

By varying the anion and cation, the properties of an ionic liquid including viscosity, solvating ability, catalytic activity and melting point can be altered dramatically.^{82,83} For example, using 1-alkyl-3-alkylimidazolium cation and replacing the Br^- anion with the $(\text{CF}_3\text{SO}_2)_2\text{N}^-$ anion dramatically decreases the water solubility. This means that the solvents can be designed with a particular end use in mind, or to possess a particular set of properties, hence the term “designer solvents” is often used when describing ionic liquids.⁸⁴

Ionic liquids can be synthesised by the direct quaternisation of an amine or phosphine to yield the cation and desired anion (step 1; Figure 1.24). Examples of this are shown in Table 1.2 below.

Ionic liquid	Alkylation reagent	m.p. (°C)	Ref.
[EMIM] CF ₃ SO ₃ ^[a]	methyl triflate	-9	85
[EMIM] Br ^{- [a]}	Bromoethane	89	85
[Ph ₃ POc] OTs ^[b]	OcOTs	62	86

Table 1.2: Examples of ionic liquids that can be formed by direct quaternization. [a] EMIM = 1-ethyl-3-methylimidazolium; CF₃SO₃ = triflate anion. [b] Oc = octyl; Ts = H₃CC₆H₄SO₂ (tosyl).

If it is not possible to form the desired anion directly by the quaternisation reaction, then further steps must follow as illustrated in Figure 1.24.⁶³ The halide can be treated with a Lewis acid as illustrated in step 2a or the halide ion may be exchanged as illustrated in step 2b.

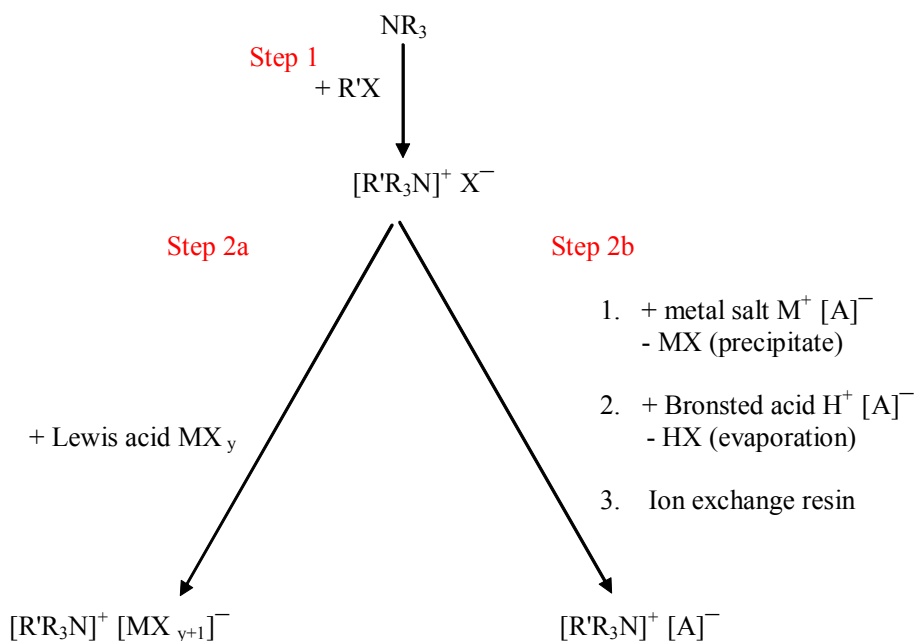
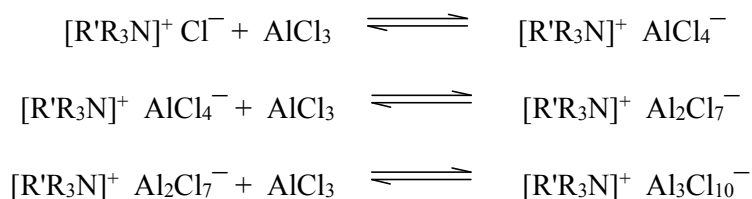


Figure 1.24: Possible synthesis paths for the preparation of ionic liquids from an amine.

In step 2a (addition of a Lewis acid) several anion species are often present in equilibrium.



When an excess of the Lewis acid is added, further acid-base reactions take place to form additional anion species. An example of this is the chloroaluminate melts:



Other Lewis acids used in this type of reaction to produce an ionic liquid include BCl_3 , CuCl and SnCl_2 .⁶⁵

Step 2b type reactions form ionic liquids which contain only one anion species when the exchange reaction is allowed to go to completion. To ensure high purity ionic liquid, it is essential to test for the presence of halide ions after ion exchange by using the silver nitrate test. Examples of ionic liquid anions formed in this way include BF_4^- , PF_6^- , NO_3^- .⁸⁷

1.2.4: Water Content

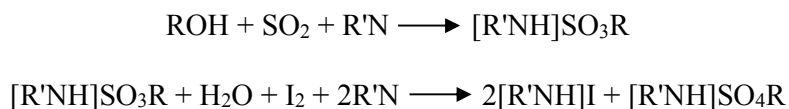
Many ionic liquids are hygroscopic and absorb significant amounts of water from the atmosphere,⁸⁸ hence even after a moderate drying process, water can still be found to be present.⁸⁹ In general, the hydrophobicity increases with the length of the alkyl chain and the larger the anion.⁹⁰

Recently there have been many publications of new ionic liquids that are both air and moisture stable. Dialkylimidazolium bis-((trifluoromethyl)sulfonyl)amides (Tf_2N^-) are reported to be hydrophobic,⁸⁵ but they still inevitably contain some water, even after a vigorous drying process.^{91,92} Rogers *et al.*⁸⁹ carried out studies on water content of dried hydrophobic and hygroscopic ionic liquids. As an example, 1-butyl-3-methylimidazolium Tf_2N^- is classed as a hydrophobic ionic liquid, but after drying still has 474 ppm water content; 1-butyl-3-methylimidazolium chloride is a hygroscopic ionic liquid and after drying still contains 2200 ppm water.

Infrared spectroscopy studies have been carried out to investigate the molecular state of water present in several ionic liquids. It was found that at low concentrations of water, the molecules are isolated or exist in small independent clusters. The water molecules form hydrogen bonds with the anion and the water content is in direct correlation with the strength of these hydrogen-bonds.⁸⁸ As the water content increases the viscosity decreases indicating that the water molecules reduce the electrostatic attractions between the ions. If water is present in equimolar amounts, the ionic liquid rearranges into a different internal order, into which more water molecules may be accommodated.⁹³ On further addition of water the ions become completely solvated and the water molecules are no longer hydrogen bonded to the salt.⁷² A continuous

water network appears which dramatically changes the mixture and its properties, such as polarity, viscosity and conductivity.⁹⁰

Karl Fischer titration⁹⁴ is one of the methods used to quantify the water content in ionic liquids. This titration is based on the following equation:



The alcohol reacts with sulfur dioxide and base to form an intermediate alkylsulfite salt. This is then oxidized by iodine thus consuming any water present. Once all the water is consumed, the presence of excess iodine is detected as a reddish-brown colour and a titration makes it possible to calculate the number of moles of iodine required to react with the water present.

Rather than using the titration method, the endpoint can also be determined by measuring the electrical conductance of the solution. This is called Coulometric Karl Fischer analysis.⁹⁵ As the Karl Fisher reagent reacts with water, the conductivity of the solution decreases with the endpoint being determined when the conductivity approaches zero. Coulometric Karl Fischer analysis is more widely used than the titration method for measuring water content in ionic liquids due to the greater sensitivity of the coulometric technique.⁷²

1.2.5: pH and pK_a

Measuring the Brønsted acidity of ionic liquids has proved to be non-trivial. According to the Brønsted-Lowry classification, an acid is a proton donor and a base is a proton acceptor. This definition makes no mention of the solvent and applies even if there is no solvent.

To date, pK_a measurements of ionic liquids have only been measured using water^{96,97} or alcohols⁹⁸ as the solvent. The pK_a is a measurement which quantifies the tendency of a molecule to lose its hydrogen atom as an acidic proton.⁹⁶ The pK_a value depends on the solvent used since the equilibrium of dissociation of a Brønsted acid depends on the interaction of the acid and its conjugate base with the solvent molecules hence the pK_a value is only meaningful if the solvent used is specified. pK_a is related to pH by the following equation:

$$\text{pK}_a = \text{pH} + \log \frac{[\text{HA}]}{[\text{A}^-]}$$

Fei *et al.*⁹⁹ have synthesised several carboxylic acid functionalised imidazolium salts which are Brønsted acids. The following reaction (Figure 1.25) shows that on treatment of mild base the corresponding zwitterion is formed:

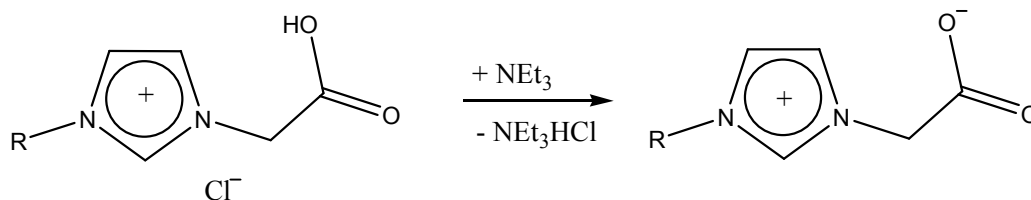


Figure 1.25: A carboxylic acid functionalised imidazolium salt reacting with mild base to form the corresponding zwitterions.

The pK_a values of several of these carboxylic acid ionic liquids dissolved in water were calculated by titration with KOH. It was found that in general the stronger acids had higher melting points. This was attributed to the increased hydrogen-bonding capabilities of the various anions tested.

Thomazeau *et al.*⁹⁷ proposed an acidity scale based on Brønsted acids in non-chloroaluminate ionic liquids. The Brønsted acidity was calculated from the determination of the Hammett acidity function using UV visible spectroscopy. It was shown that by altering the ionic liquid it was possible to change the acidity of a mixture when the same amount of an acid was added to it.

Many ionic liquids are Lewis acids and consequently used for this reason as catalysts in organic synthesis. A Lewis acid is an electron pair acceptor. The most common Lewis acid ionic liquids are composed of metal halides e.g. $AlCl_x$. All Brønsted acids are Lewis acids.

Yang *et al.*¹⁰⁰ reported a way of characterising the acidity of ionic liquids by using pyridine and ethanenitrile as IR probe molecules. Information from IR spectroscopy in the $1400-1700\text{ cm}^{-1}$ region for pyridine and the $2200-2400\text{ cm}^{-1}$ region for ethanenitrile allows the Lewis and /or Brønsted character of acidic ionic liquids to be distinguished and the strength of the Lewis acidity to be estimated. For the example of pyridine, the presence of a band near 1450 cm^{-1} indicates that the pyridine is co-ordinated to a Lewis acid site whilst a band near 1540 cm^{-1} indicates the formation of pyridinium ions resulting from the presence of a Brønsted acid site. It was concluded from the results that Lewis acidity increases in the order $CuCl < FeCl_3 < ZnCl_2 < AlCl_3$.

1.2.6: Eutectic Mixtures

Eutectic mixtures display unusual solvent properties that are very similar to those shown by the ionic liquids. High solubilities can be observed (depending on the eutectic mixture used) for inorganic salts, salts that are sparingly soluble in water, aromatic acids, and amino acids. Due to the high anion concentration these mixtures can also dissolve several metal oxides.¹⁰¹

The word eutectic comes from the Greek *eutēktos* meaning “easily melted”. A eutectic mixture is a mixture of two or more compounds which have a lower melting point than either of its constituents. Abbott *et al.*¹⁰¹ have shown that mixtures of substituted quaternary ammonium salts mixed with amides, acids, amines or alcohols¹⁰² can produce eutectics that are liquid at ambient temperature. An example is the urea/choline chloride mixture (ratio 1:2) which has a melting point of 12 °C which is much lower than that of either of the constituents (melting point choline chloride = 302 °C and urea = 133 °C) – Figure 1.26. The decrease in the melting point arises from the hydrogen bonding interaction between the urea molecules and the chloride ions.

The unusual solvent properties of eutectic mixtures are strongly influenced by hydrogen bonding.¹⁰² Generally it is the compounds capable of donating and accepting electrons or protons to form hydrogen bonds that show high solubilities.



Choline Chloride Urea Eutectic Mixture

Figure 1.26: Choline chloride and urea mixed in a 2:1 ratio respectively to give a eutectic mixture.

Advantages of using eutectic mixtures over ionic liquids is their ease of preparation in pure state and their relative non reactivity with water. Many are biodegradable and the toxicological properties of the components maybe well characterised. Eutectic mixtures based on urea and choline chloride are also far less costly than ionic liquids. These properties make eutectic mixtures a versatile alternative to ionic liquids.

1.3: References

1. P.A. Barrett, M.A. Cambor, A. Corma, R.H. Jones and L.A. Villaescusa, *Chem. Mater.*, 1997, **9**, 1713
2. A.F. Cronstedt, *Akad. Handle., Stockholm*, 1756, **17**, 120
3. M.E. Davis and R.F. Lobo, *Chem. Mater.*, 1992, **4**, 756
4. R.M. Barrer, *J. Chem. Soc.*, 1948, 127
5. D.W. Breck, W.G. Eversole, R.M. Milton, T.B. Reed and T.L. Thomas, *J. Am. Chem. Soc.*, 1956, **23**, 5963
6. M. Tagliabue, L.C. Carluccio, D. Ghisletti and C. Perego, *Catal. Today*, 2003, **81**, 405
7. P.A. Cox, J.L. Casci and A.P. Stevens, *Faraday Discuss.*, 1997, **106**, 473
8. The International Zeolite Association website (www.iza-online.org)
9. P.S. Wheatley, 'Synthesis of Open Framework Materials Using Azamacrocycles as Structure Directing Agents', Thesis, St. Andrews, 2003
10. C.S. Cundy and P.A. Cox, *Chem. Soc. Rev.*, 2003, **103**, 663
11. J.W. McBain, 'The Sorption of Gases and Vapours by Solids', Rutledge and Sons, 1932
12. R. Szostak, 'Molecular Sieves Principles of Synthesis and Identification', Van Nostrand Reinhold, 1989
13. S.T. Wilson, B.M. Lok, C.A. Messina, T.R. Cannan and E.M. Flanigen, *J. Am. Chem. Soc.*, 1982, **104**, 1146
14. A.O.S. Silva, M.J.B. Souza and A.S. Araujo, *Int. J. Inorg. Mater.*, 2001, **3**, 461
15. A.S. Araujo, V.J. Fernandes, A.O.S. Silva and J.G. Diniz, *J. Therm. Anal.*, 1999, **56**, 151
16. J.H. Yu and R.R. Xu, *Acc. Chem. Res.*, 2003, **36**, 481

17. J. Yu, K. Sugiyama, S. Zheng, S. Qiu, J. Chen, R. Xu, Y. Sakamoto, O. Terasaki, K. Hiraga, M. Light, M.B. Hursthouse and J.M. Thomas, *Chem. Mater.*, 1998, **10**, 1208
18. W.F. Yan, J.H. Yu, Z. Shi and R.R. Xu, *Chem. Commun.*, 2000, 1431
19. Y. Li, J. Jiang, Z. Wang, J. Zhang and R. Xu, *Chem. Mater.*, 2005, **17**, 6086
20. W. Loewenstein, *Am. Miner.*, 1954, **39**, 92
21. J.L. Provis, P. Duxson, G.C. Lukey and S.J. van Deventer, *Chem. Mater.*, 2005, **17**, 2976
22. R.G. Bell, R.A. Jackson and C.R.A. Catlow, *Zeolites*, 1992, **12**, 870
23. Q. Huang and S. Hwu, *Chem. Commun.*, 1999, 2343
24. R.M. Milton, US 2 882 243, 1959
25. R.M. Barrer and P.J. Denny, *J. Chem. Soc.*, 1961, 971
26. J.-L. Guth and P. Caultet, *J. Chim. Phys.*, 1986, **83**, 155
27. S. Mintova, N.H. Olson, V. Valtchev and T. Bein, *Science*, 1999, **283**, 958
28. W.Y. Xu, J.Q. Li, W.Y. Li, H.M. Zhang and B.C. Liang, *Zeolites*, 1989, **9**, 468
29. R.M. Barrer, J.W. Baynham, F.W. Bultitude and W.M. Meier, *J. Chem. Soc.*, 1959, 195
30. D.W. Breck, 'Zeolite Molecular Sieves', Wiley, New York, 1974
31. F. Taulelle, *Solid State Science*, 2001, **3**, 795
32. P. Bussian, F. Sobott, B. Brutschy, W. Schrader and F. Schuth, *Angew. Chem. Int. Ed. Engl.*, 2000, **39**, 3901
33. P.G. Harrison, *J. Organomet. Chem.*, 1997, **542**, 141
34. D.S. Wragg and R. E. Morris, *J. Phys. Chem. Solids*, 2001, **62**, 1493
35. L.A. Villaescusa, P. Lightfoot and R. E. Morris, *Chem. Comm.*, 2002, 2220
36. R.E. Morris, *J. Mater. Chem.*, 2005, **15**, 931

37. F. Taulelle, M. Pruski, J. P. Amoureux, D. Lang, A. Bailly, C. Huguenard, M. Haouas, C. Gerardin, T. Loiseau and G. Ferey, *J. Am. Chem. Soc.*, 1999, **121**, 12148
38. F. Taulelle, M. Haouas, C. Gerardin, C. Estournes, T. Loiseau and G. Ferey, *Colloids Surf. A*, 1999, **158**, 299
39. S. Oliver, A. Kuperman and G.A. Ozin, *Angew. Chem. Int. Ed.*, 1998, **37**, 46
40. D. Grandjean, A.M. Beale, A.V. Petukhov and B.M. Weckhuysen, *J. Am. Chem. Soc.*, 2005, **127**, 14454
41. F. Millange, R. I. Walton, N. Guillou, T. Loiseau, D. O'Hare and G. Ferey, *Chem. Mater.*, 2002, **14**, 4448
42. R. Millini, G. Perego, W.O. Parker, G. Bellussi and L. Carluccio, *Microporous Mater.*, 1995, **4**, 221
43. L. Schreyeck, P. Caullet, J.C. Mougénel, J.L. Guth and B. Marler, *Microporous Mater.*, 1996, **6**, 259
44. Y. X. Wang, H. Gies, B. Marler and U. Müller, *Chem. Mater.*, 2005, **17**, 43
45. R.E. Morris, P.S. Wheatley, *J. Mater. Chem.*, 2006, **16**, 1035
46. C.D. Chang and A.T. Bell, *Catal. Lett.*, 1991, **8**, 305
47. S.L. Burkett and M.E. Davis, *J. Phys. Chem.*, 1994, **98**, 4647
48. A. Araya and B.M. Lowe, *Zeolites*, 1986, **6**, 111
49. C.S. Cundy and P.A. Cox, *Microporous Mesoporous Mater.*, 2005, **82**, 1
50. R.A. Vannordstrand, D.S. Santilli and S.I. Zones, *ACS Symp. Ser.*, 1988, **368**, 236
51. F. Delprato, L. Delmotto, J.L. Guth and L. Huve, *Zeolites*, 1990, **10**, 546
52. S.L. Lawton and W.J. Rohrbaugh, *Science*, 1990, **247**, 1319
53. A. Moini, K.D. Schmitt, E.W. Valyocsik and R.F. Polomski, *Zeolites*, 1994, **14**, 504

54. R.F. Lobo, S.I. Zones and M.E. Davis, *J. Inclusion Phenom. Mol. Recognit. Chem.*, 1995, **21**, 47
55. L. Li, J.H. Yu, Z.P. Wang, J.N. Zhang, M. Guo and R.R. Xu, *Chem. Mater.*, 2005, **17**, 4399
56. S.Y. Yang, A.G. Vlessidis and N.P. Evmiridis, *Microporous Mater.*, 1997, **9**, 273
57. R.E. Morris and S.J. Weigel, *Chem. Soc. Rev.*, 1997, **26**, 309
58. H. Qisheng, F. Shouhua and X. Ruren, *Chem. Commun.*, 1988, 1486
59. E.M. Flanigen and R.L. Patton, U.S. 4 073 864, 1978
60. M.M. Harding and B.M. Kariuki, *Acta Crystallogr. Sect. C: Cryst. Struct. Commun.*, 1994, **50**, 852
61. M.A. Cambor, L.A. Villaescusa and M.J. Diaz-Cabanas, *Top. Catal.*, 1999, **9**, 59
62. M.G. Del Popolo and G.A. Voth, *J. Phys. Chem. B*, 2004, **108**, 1744
63. P. Wasserscheid and W. Keim, *Angew. Chem., Int. Ed. Engl.*, 2000, **39**, 3773
64. P. Walden, *Bull. Acad. Sci.*, 1914, 405
65. P. Wasserscheid and T. Welton, 'Ionic Liquids In Synthesis', Wiley-VCH, 2003, Ch. 2
66. F.N. Hurley and T.P. Wier, *J. Electrochem. Soc.*, 1951, **98**, 207
67. J.A. Boon, J.A. Levisky, J.L. Pflug and J.S. Wilkes, *J. Org. Chem.*, 1986, **51**, 480
68. S.E. Fry and N.J. Pienta, *J. Am. Chem. Soc.*, 1985, **107**, 6399
69. P. Kubisa, *J. Polym. Sci., Part A: Polym. Chem.*, 2005, **43**, 4675
70. X. X. Han and D. W. Armstrong, *Org. Lett.*, 2005, **7**, 4205
71. A. Corma, H. Garcia and A. Leyva, *Tetrahedron*, 2005, **61**, 9848
72. K.R. Seddon, A. Stark and M.J. Torres, *Pure Appl. Chem.*, 2000, **72**, 2275
73. G.W. Philips, S.N. Falling, S.A. Godleskii and J.R. Monnier, U.S. 5 315 019, 1994
74. P.L. Short, *Chem. Eng. News*, 2006, **84**, 15
75. K.N. Marsh, J.A. Boxall and R. Lichtenthaler, *Fluid Phase Equilib.*, 2004, **219**, 93

76. M.J. Earle and K.R. Seddon, *Pure Appl. Chem.*, 2000, **72**, 1391
77. C. Baudequin, J. Baudoux, J. Levillain, D. Cahard, A.C. Gaumont and J.C. Plaquevent, *Tetrahedron: Asymmetry*, 2003, **14**, 3081
78. C.L. Hussey, *Adv. Molten Salt Chem.*, 1983, **5**, 185
79. R.P. Swatloski, J.D. Holbrey and R.D. Rogers, *Green Chem.*, 2003, **5**, 361
80. K.M. Docherty and C.F. Kulpa, *Green Chem.*, 2005, **7**, 185
81. C. Pretti, C. Chiappe, D. Pieraccini, M. Gregori, F. Abramo, G. Monni and L. Intorre, *Green Chem.*, 2006, **8**, 238
82. H. Tokuda, K. Hayamizu, K. Ishii, M. Susan and M. Watanabe, *J. Phys. Chem. B*, 2004, **108**, 16593
83. H. Tokuda, I. Kunikaza, M. Susan, S. Tsuzuki, K. Hayamizu and M. Watanabe, *J. Phys. Chem. B*, 2006, **110**, 2833
84. M. Freemantle, *Chem. Eng. News*, 1998, **76**, 32
85. P. Bonhote, A.P. Dias, M. Armand, N. Papageorgiou, K. Kalyanasundaram and M. Gratzel, *Inorg. Chem.*, 1996, **35**, 1168
86. N. Karodia, S. Guise, C. Newlands and J.-A. Anderson, *Chem. Commun.*, 1998, 2341
87. P.A.Z. Suarez, J.E.L. Dullius, S. Einloft, R.F. de Souza and J. Dupont, *Polyhedron*, 1996, **15**, 1217
88. L. Cammarata, S.G. Kazarian, P.A. Slater and T. Welton, *Phys. Chem. Chem. Phys.*, 2001, **3**, 5192
89. J.G. Huddleston, A.E. Visser, W.M. Reichert, H.D. Willauer, G.A. Broker and R.D. Rogers, *Green Chem.*, 2001, **3**, 156
90. C.G. Hanks and R.M. Lynden-Bell, *J. Phys. Chem. B*, 2003, **107**, 10873
91. S. Rivera-Rubero and S. Baldelli, *J. Am. Chem. Soc.*, 2004, **126**, 11788
92. A. Chaumont, R. Schurhammer and G. Wipff, *J. Phys. Chem. B*, 2005, **109**, 18964

93. K. Miki, P. Westh, K. Nishikawa and Y. Koga, *J. Phys. Chem. B*, 2005, **109**, 9014
94. K. Fischer, *Angew. Chemie.*, 1935, **48**, 394
95. T. A. Jennings, 'Lyophilization', CRC Press, 1999, p416
96. C.O. da Silva, E.C. da Silva and M.A.C. Nascimento, *J. Phys. Chem. A*, 1999, **103**, 11194
97. Z. Fei, D. Zhao, T.J. Geldbach, R. Scopelliti and P.J. Dyson, *Chem. Eur. J.*, 2004, **10**, 4886
98. E. Bogel-Lukasik and U. Domanska, *Green Chem.*, 2004, **6**, 299.
99. C. Thomazeau, H. Olivier-Bourbigou, L. Magna, S. Luts and B. Gilbert, *J. Am. Chem. Soc.*, 2003, **125**, 5264
100. Y.L. Yang and Y. Kou, *Chem. Commun.*, 2004, 226
101. A.P. Abbott, G. Capper, D.L. Davies, R.K. Rasheed and V. Tambyrajah, *Chem. Commun.*, 2003, 70
102. A.P. Abbott, D. Boothby, G. Capper, D.L. Davies, R.K. Rasheed, *J. Am. Chem. Soc.*, 2004, **126**, 9142

2: Aims

2.1: Synthesis of zeolite analogues using ionic liquids and eutectic mixtures as the solvent and template.

The aim of this project is to synthesise zeolite analogues, primarily aluminophosphates, using ionic liquids¹ and eutectic mixtures² as both the organic template and the solvent. Ionic liquids appear to be suitable for this role since many ionic liquid cations are chemically very similar to species that are already known as good templates (alkylimidazolium-, pyridinium-based ionic liquids etc). They are also relatively polar solvents, making them suitable for the dissolution of the inorganic components required for the synthesis. For the purpose of this work an ionic liquid is given the broader definition of, any salt that melts below the temperatures used in the synthesis of zeolites - typically 150-220 °C. The use of ionic liquids and eutectic mixtures as a solvent and template will be referred to as ‘ionothermal’ synthesis.³

The most commonly used route to molecular sieve synthesis is the hydrothermal method.⁴ This involves the mixing of the reagents in water, which acts as the solvent, then heating in a sealed autoclave at autogenous pressure for a specific time. The water does however appear to have other roles in the synthesis. It can act as a space filler in the porous lattice, it enhances the reactivity and lowers the viscosity of the mixture. So the water is not only a solvent but a reactant and a catalyst in T-O-T bond formation.⁵

In ionothermal synthesis the theory is that there are no other solvents added hence there are no other molecules present to act as space fillers during zeolite synthesis. This means that ionothermal synthesis could potentially remove the competition between

template-framework and solvent-framework interactions that are present in hydrothermal preparations.

The structure directing properties of templates are often not as specific as we would like. In a system where an ionic liquid acts as both solvent and template the negatively charged atoms at the surface of a growing framework will always be interacting primarily with the templating cation rather than with a mixture of template and solvent.

Figure 2.1 illustrates this schematically.

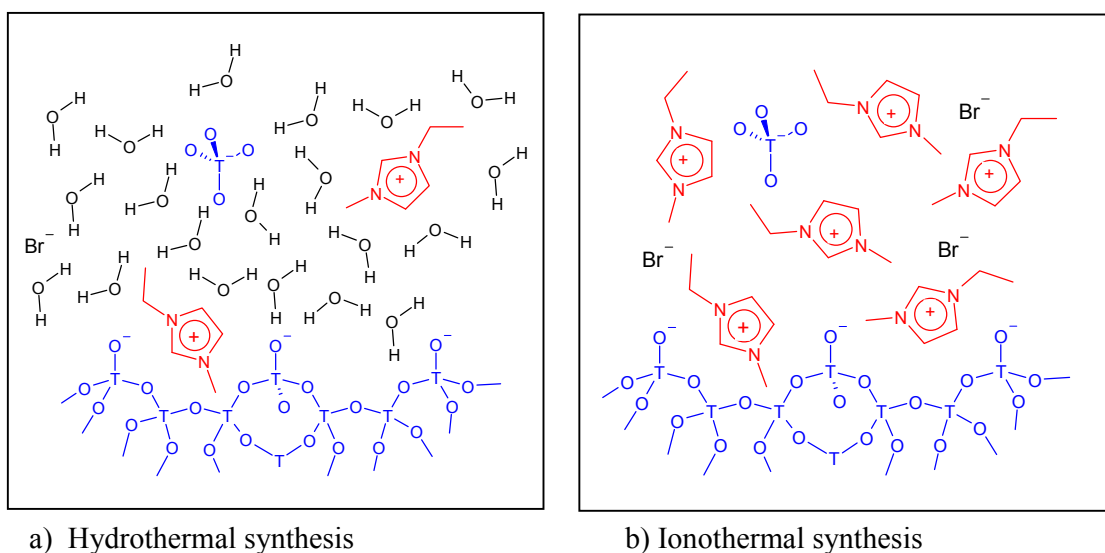


Figure 2.1: A schematic comparison between a hydrothermal and ionothermal synthesis.

Recent molecular modelling studies indicate that the structure of ionic liquids is characterised by long range correlations and distributions that reflect the asymmetric structures of the cations.⁶ Long range asymmetric effects of this kind potentially increase the likelihood of transferring chemical information from the template cation to the framework; a situation that is desirable if full control over the templating process is to be achieved. This distinguishes the potential of ionothermal synthesis further from hydrothermal synthesis where solvation/clathration by water reduces the range of effectiveness of the template structure.

Particular attention will be paid to the water content involved in the synthesis of the aluminophosphate molecular sieves and its affect upon the structures obtained. From the results, the role of the water in the synthesis of aluminophosphate molecular sieves will be considered and indeed, whether water is in fact necessary for successful synthesis. Using either the ionic liquid or eutectic mixtures as template and solvent is likely to produce a new synthesis mechanism for zeolite synthesis. This may potentially result in new framework structures being formed.

2.2: Characterisation

Characterisation of the molecular sieve structures will primarily be by single crystal X-ray diffraction techniques carried out in conjunction with powder X-ray diffraction, used to identify the phase/phases present. The crystals typically produced are too small to analyse by standard laboratory X-ray diffraction, hence synchrotron radiation is used in most cases. Solid state Nuclear Magnetic Resonance (NMR) is also used in the analysis of these materials in particular ^{13}C , ^{31}P , ^{27}Al and ^{19}F . This technique is especially useful in identifying the template present, especially in cases of high degree of disorder in the single crystal X-ray diffraction data. The physical properties are studied by Thermal Gravimetric Analysis (TGA) and CHN elemental analysis on phase pure materials.

2.3: References

1. P. Wasserscheid and W. Keim, *Angew. Chem., Int. Ed. Engl.*, 2000, **39**, 3773
2. A.P. Abbott, G. Capper, D.L. Davies, R.K. Rasheed and V. Tambyrajah, *Chem. Commun.*, 2003, 70
3. E.R. Cooper, C.D. Andrews, P.S. Wheatley, P.B. Webb, P. Wormald and R.E. Morris, *Nature*, 2004, **430**, 1012
4. R.M. Barrer, *J. Chem. Soc.*, 1948, 127
5. S.Y. Yang, A.G. Vlessidis and N.P. Evmiridis, *Microporous Mater.*, 1997, **9**, 273
6. M.G. Del Popolo and G.A. Voth, *J. Phys. Chem. B*, 2004, **108**, 1744

3: Experimental and Analytical Techniques

3.1: Hydrothermal/Ionothermal Synthesis

Natural zeolites are mostly found in regions of former or present magmatic activity. During the cooling process of a magmatic intrusion the dissolved ions, water-vapour, carbon dioxide and other volatile compounds are separated whilst trying to reach the earth's surface. This volatile phase crystallises during the cooling process losing its high pressure. Only at the lowest stage of pressure and temperature (27 - 55 °C), at the mildest conditions, called the hydrothermal state, is the environment right for the formation of the aluminosilicate zeolite phases. The water molecules are an active element during the zeolite formation process, as they are the solvent for the ionic species forming the later zeolite.

Synthetic hydrothermal zeolite formation mimics natural zeolite formation but is carried out under more severe conditions, but shorter time. It involves mixing together the reagents, usually the tetrahedron atom source, an organic structure directing agent, a mineraliser and the solvent water. This gel is then heated (< 220 °C) in a Teflon™ (polytetrafluoroethylene) lined steel autoclave (Figure 3.1) at high autogenous pressure (up to 15 atm at 200 °C)¹ for a period of time. These pressures can result in safety concerns, hence autoclaves are only ever filled to a maximum of 75 % of their capacity when cold. The product is recovered by vacuum filtration, washed and then sonicated if necessary to break-up the larger particles.

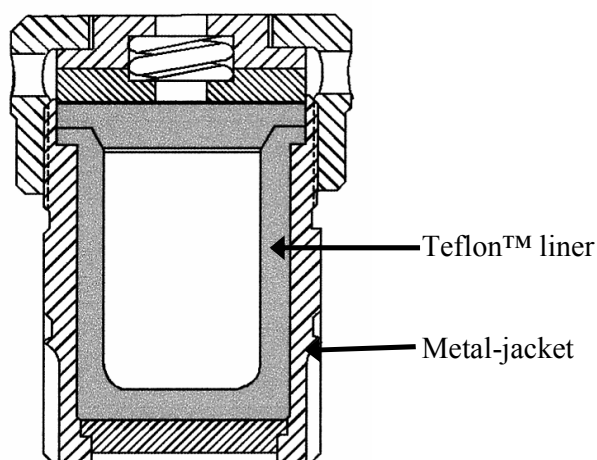


Figure 3.1: Cross section of an autoclave showing the Teflon™ liner and the metal jacket.²

Hydrothermal synthesis is an increasingly important preparative method for inorganic materials including open-framework and layered solids. This method offers many experimental variables including framework cations and source, mineraliser, structure directing agent, pH, time, temperature, pressure and agitation. These variables allow for the fine tuning of experimental conditions to enable a desired phase to be prepared. The use of solvent allows solids to be made rapidly and at lower temperatures (< 220 °C) than typically employed in solid-state chemistry.

Ionothermal synthesis is a new zeolite synthesis methodology to be investigated in the formation of synthetic zeolites and zeolite analogues. It is essentially the same as hydrothermal synthesis, except that the solvent (usually water) is replaced with an ionic liquid which acts as both the solvent and the structure directing agent. Another difference between ionothermal and hydrothermal synthesis arises due to ionic liquids having a vanishingly low vapour pressure which means the reactions are carried out at ambient pressure. This reduces the associated safety concerns that accompany hydrothermal synthesis in sealed autoclaves.

3.2: Moisture Sensitive Techniques

Standard Schlenk techniques, using argon as the purge gas, were utilised in the synthesis of ionic liquids due to their hygroscopic nature. The argon gas was passed through anhydrous calcium sulphate before use in order to ensure a dry environment. All glassware was oven-dried and purged three times with argon prior to use.

3.3: X-ray Diffraction

3.3.1: Introduction and X-ray Generation

X-ray diffraction data is traditionally of importance to chemists as a tool for crystal structure determination. The information obtained relates to the crystal lattice of the material, and can be used to help characterise the crystalline phases present. X-rays are diffracted by electrons and the information from an X-ray diffraction study concerns the electron density distribution.

X-rays are short-wavelength electromagnetic radiation with a wavelength, λ , in the range of 0.1 to 100 Å. X-rays are typically generated in the laboratory by bombarding a metal with high-energy electrons produced by heating a metal filament until it becomes white hot, emitting photo-electrons. The electrons rapidly decelerate as they enter the metal and collide with the metal atoms, generating radiation with a continuous range of wavelengths called Bremsstrahlung. Superimposed on this are a few high-intensity, sharp peaks (Figure 3.2) which are characteristic of the target material.

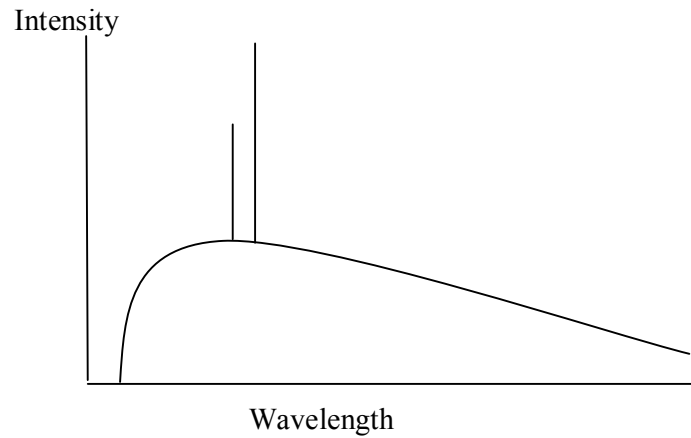


Figure 3.2: Bremsstrahlung background with high-intensity sharp transition peaks superimposed on it.

The high-intensity sharp peaks arise from the interaction of the incoming electrons with the electrons in the inner shells of the target material atoms as illustrated in Figure 3.3. This works by an incoming electron colliding with an electron in the inner shell K (i.e. a shell where $n=1$) transferring enough energy to eject it. Another electron from the higher energy shell (e.g. L shell, i.e. $n=2$) falls into the vacancy and emits the excess energy as an X-ray photon. The emitted X-ray photon has the energy that is equal to the difference between the upper and lower energy levels of the electron that filled the core hole.

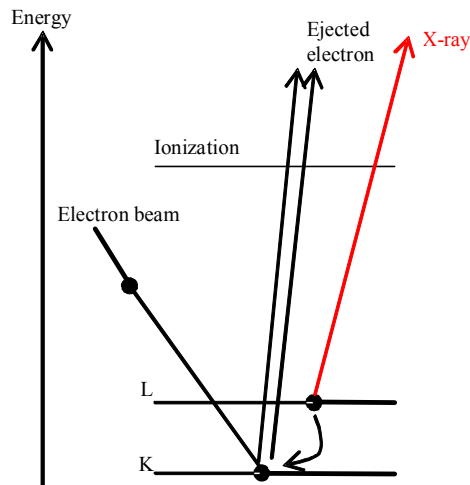


Figure 3.3: Generation of X-rays.³

3.3.2: Crystallographic Space Groups

In order to solve a crystal structure it is first necessary to assign a unit cell. This is the smallest repeating unit which shows the full symmetry of the crystal structure. There are seven unique crystal systems possible in three-dimensional crystal structures (Figure 3.4).

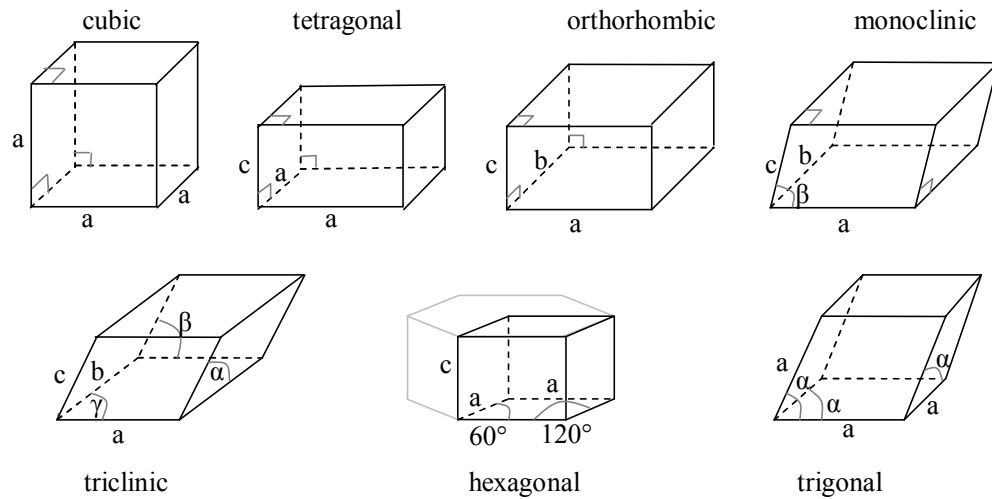


Figure 3.4: The seven crystal systems and their unit cell shapes

The unit cell of the crystal is repeated on a regular three-dimensional space lattice to form the complete crystal. This gives one lattice point per unit cell, resulting in a so-called primitive lattice, P. However sometimes it is more convenient to have more than one lattice point per cell, resulting in centred lattices (face centred, F; side centred, C or body centred, I). There are 14 different Bravais lattices which arise from all the possible centring in each crystal system.

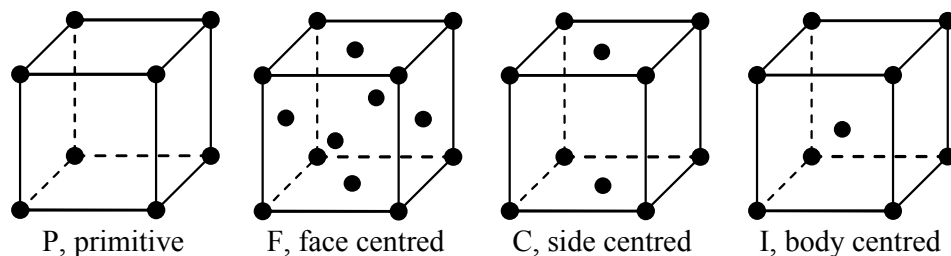


Figure 3.5: The four different lattice types.

Each crystal system is governed by the presence or absence of symmetry. A symmetry element is a physically identifiable point, line, or plane in a molecule about which symmetry operations are applied. A symmetry operation is a reflection in a plane, a rotation about a line or an inversion through a point which leaves the molecule afterwards with an identical appearance. All symmetry operations can be classified as proper rotations (rotations by a certain fraction of 360° about a rotation axis), or improper rotations (the combination of a rotation and a simultaneous reflection in a plane perpendicular to the axis and passing through the centre of the molecule). In three-dimensional crystals, a rotation or reflection can be combined with translation to give, respectively, screw axes and glide planes.

The total collection of all the symmetry operations for a molecule is called a point group, and each group has its own characteristic properties and a conventional symbol. These symmetry operations can be combined in 32 different ways giving 32 crystallographic point groups which are compatible with the periodic nature of crystals. The combined configuration of a crystallographic point group repeated on a Bravais lattice is a space group. A space group describes the symmetry of the atomic structure of the crystal. The total number of possible space groups is 230.

3.3.3: Diffraction of X-rays by Crystals

A crystal is made up of a three-dimensional regular arrangement of atoms with a repeating pattern. This leads to an internal periodicity that acts as a diffraction grating for the X-rays. The observed pattern is the result of the constructive and destructive interference of the X-rays scattered by all the regularly arranged atoms (Figure 3.6).⁴

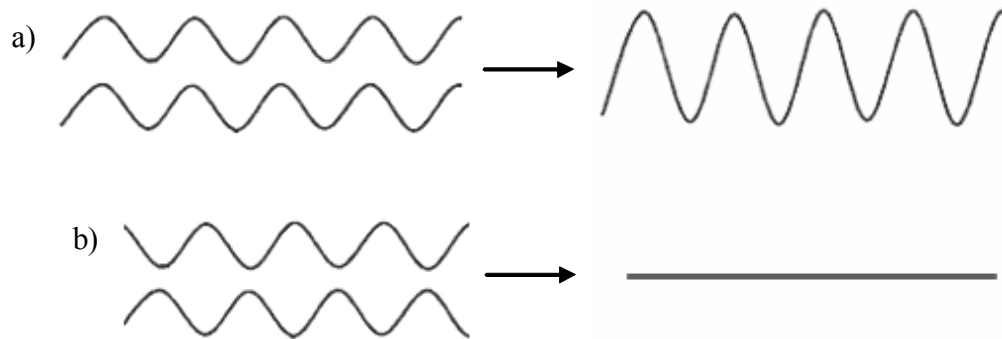


Figure 3.6: a) Constructive interference (waves exactly in phase),
b) Destructive interference (waves exactly out of phase)

To observe any diffraction intensity, there must be constructive interference between all the waves diffracted by the electrons in the crystal lattice (Figure 3.7). For constructive interference, the path length difference ($2d\sin\theta$) between scatterings from successive planes must be an integer number of wavelengths ($n\lambda$). θ is the incident angle and constructive interference is observed when the incident angle satisfies Bragg's law :

$$n\lambda = 2d\sin\theta$$

where n is the diffraction order 1, 2, 3,

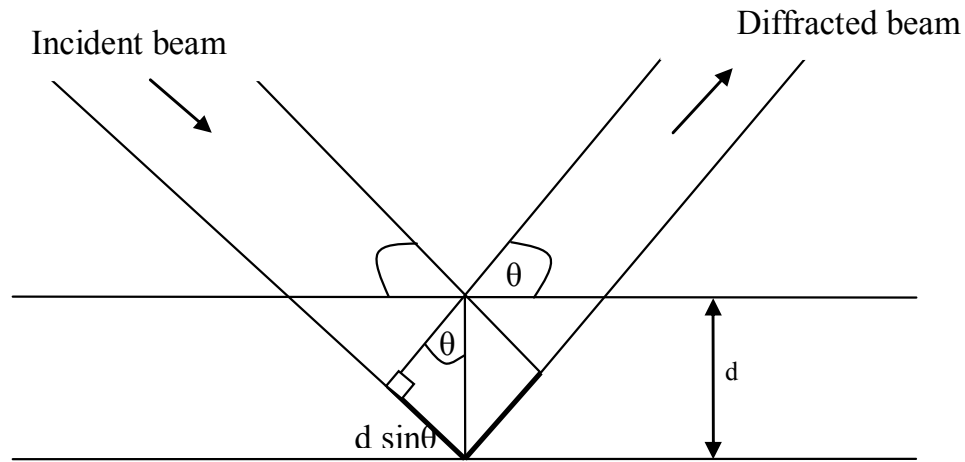


Figure 3.7: Diagram to show the derivation of the Bragg Equation

A diffraction pattern is the Fourier transform (known as the forward Fourier transform) of the crystal structure, corresponding to the pattern of waves scattered from an incident X-ray beam by a single crystal. Scattered X-ray intensity can be described mathematically by the following equation:

$$F(hkl) = \sum_j f_j(\theta) \cdot \exp(-8\pi^2 U_j \sin^2 \theta / \lambda^2) \cdot \exp[2\pi i(hx_j + ky_j + lz_j)]$$

Each reflection is a wave which is made up of an amplitude and a phase. This is represented by the complex number notation i . The summation is made over all the atoms in the unit cell, each of which has its appropriate atomic scattering factor f_j , a displacement parameter U_j , and coordinates (x_j, y_j, z_j) relative to the unit cell origin.⁵ This summation must be carried out for every diffracted wave.

In turn, the crystal structure is the Fourier transform (known as the reverse Fourier transform) of the diffraction pattern and is expressed in terms of electron density distribution.

$$p(xyz) = \frac{1}{V} \sum_{h,k,l} |F(hkl)| \cdot \exp[-2\pi i(hx + ky + lz)]$$

The term $1/V$ ($V =$ unit cell volume) must be included in order to give the correct units. Structure factors have units of electrons, but electron density is in $\text{e}\text{\AA}^{-3}$. The summation is over all values of h , k , and l but in practice reflections are measured only to a certain maximum Bragg angle. This is usually unimportant because the higher angle reflections are too weak to contribute significantly to the sums.

To work back to the electron density map, hence the molecular structure, it is necessary to know the phases of the data; the position of the wave crest and troughs relative to each other (Figure 3.8). This information cannot be measured and is commonly referred to as the phase problem. To overcome the phase problem, there are several methods, two of which will be discussed here; the Patterson synthesis and direct methods.⁵

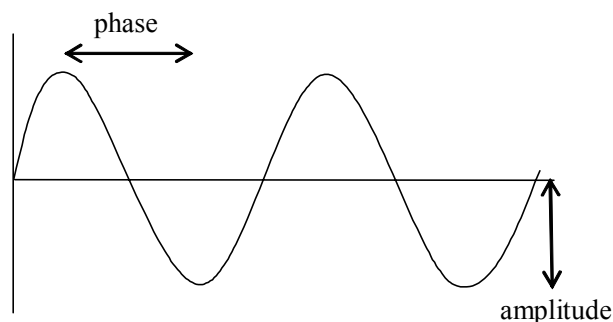


Figure 3.8: Amplitude and phase of a wave.

A Patterson map is produced when the Fourier transforms are carried out with the amplitudes squared and all phases set equal to zero i.e. all waves taken in phase. This map looks like an electron density map in that it has peaks of positive density in various positions, however these are not the positions of atoms but rather vectors between pairs of atoms. The Patterson peaks are proportional in size to the product of the atomic numbers of the two atoms concerned hence are usually broad with significant overlapping. The Patterson map shows where atoms lie in relation to each other, but not where they lie relative to the unit cell origin.

If a structure contains a few heavy atoms among a lot of lighter atoms, the Patterson map will show a few larger peaks standing out clearly above the general background. These heavy atoms can be located and this partial structure serves as an initial model to which forward Fourier transform calculations can be carried out to find the phases. Combining the calculated phases and the experimental amplitudes results in the reverse Fourier transform being possible. If the errors in the calculated phases are not too large, the electron density map will show the existing model structure plus some additional atoms. The model is thus improved and the process can be repeated with the new model.

The direct methods approach is a mathematical approach that makes it possible to extract phase data from the diffraction intensities. If it is assumed that a crystal is made up of small, discrete, similarly-shaped atoms that all have positive electron density, then there are statistical relationships between sets of structure factors. These statistical relationships can be used to deduce possible values for the phases by trial-and-error methods. The most important reflections are selected, and then the probable relationships among their phases are calculated by trying different phases to see how well the probability relationships are satisfied. For the most promising combinations, the Fourier transforms are calculated from the trial phases and the observed amplitudes. Unfortunately, the statistical relationships become weaker as the number of atoms increases, and direct methods are limited to structures with, at most, a few hundred atoms in the unit cell.

3.3.4: Single Crystal X-ray Diffraction

Single crystal X-ray diffraction has become an important, routine technique for the determination and proof of molecular structures. It is now possible to determine a structure in a matter of hours due to the high computing power of modern computers and the introduction of charge coupled device (CCD) detectors replacing the four-circle diffractometers.⁶

CCDs have high counting rates and good dynamic range combined with fast readout.⁷ CCD detectors use an X-ray sensitive phosphor to convert X-rays to visible light. This is coupled *via* lenses, image intensifiers and/or fibre optics to a charge coupled device which records the light signal. The visible light is recorded and stored in analogue form by a CCD chip until readout. In general, CCD detectors allow the user to examine the acquired diffraction image within seconds of recording the exposure.⁸

The first step to crystal structure determination is the selection of a suitable single crystal. This crystal is separated from the rest of the sample and any other crystalline material removed from the surface of the crystal by cleaning in oil. The crystals synthesised ionothermally are typically 30 x 30 x 10 μm in size, hence the crystals are too small to be mounted using a single glass fibre. Instead they are mounted on a two-stage fibre which consists of a \sim 1-2 mm strand of glass wool glued to a \sim 5 mm glass fibre attached to a pip. This pip is attached into a goniometer head and the crystal is aligned in the X-ray beam.

The unit cell is determined by collecting a series of unindexed reflections from different regions of reciprocal space. After least-squares refinement on the basis of all the

genuine reflections, the unit cell and metric symmetry can be determined usually by an automated process. The full data set is then collected and the integrated intensities are extracted from the raw frames using the orientation matrix to determine reflection positions. Using this data the structure can be solved using direct methods in the case of zeotypes.

3.3.5: Powder X-ray diffraction

For a crystalline powder with no preferential orientation, all sample orientations are present, thus all possible reflections are present to the incident beam. Diffraction intensity occurs when the Bragg equation is satisfied for any set of atomic planes in the sample thus giving concentric rings of scattering peaks corresponding to the various d-spacings in the crystal lattice. Solving crystal structures from powder patterns is non-trivial hence if it is possible to collect single crystal data for structure analysis this is the preferred technique.

During this project, powder X-ray diffraction patterns were collected for phase identification purposes only, on a STOE STADIP diffractometer using monochromated CuK_α ($\lambda = 1.54 \text{ \AA}$).

3.3.6: Synchrotron Radiation

Microporous materials, such as zeotypes, are often synthesised with crystals too small and too poorly scattering due to their large pore sizes for single crystal X-ray diffraction to be collected on an in-house X-ray diffractometer. A method to overcome this problem is to use synchrotron radiation. This is higher intensity, concentrated in a narrow angular range, polarised, with a wide spectral distribution tuneable with appropriate monochromating devices. It is delivered as a series of short pulses of less than nanosecond length.⁹

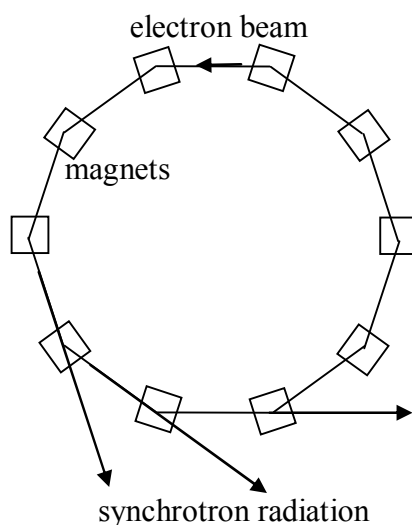


Figure 3.9: A schematic illustration of a storage ring

A schematic illustration of a storage ring is shown in Figure 3.9. When charged particles, in particular electrons or positrons, are injected into the storage ring (operated at high vacuum) and forced to move in a circular orbit by magnetic fields, photons are emitted. When the particles are moving at close to the speed of light these photons are emitted in a narrow cone in the forward direction, at a tangent to the orbit. In a high energy electron or positron storage ring, these photons are emitted with energies ranging from infra-red to short wavelength X-rays, from which a single wavelength of any value can be selected by a monochromator.⁵

Single-crystal X-ray diffraction was carried out at station 9.8 (Figure 3.10) at the CCLRC Daresbury Laboratory Synchrotron Radiation Source, Cheshire, UK. Experiments were carried out at low temperature (150 K) using a Bruker AXS SMART CCD area detector diffractometer with X-rays of wavelength set to between 0.68 and 0.71 Å.

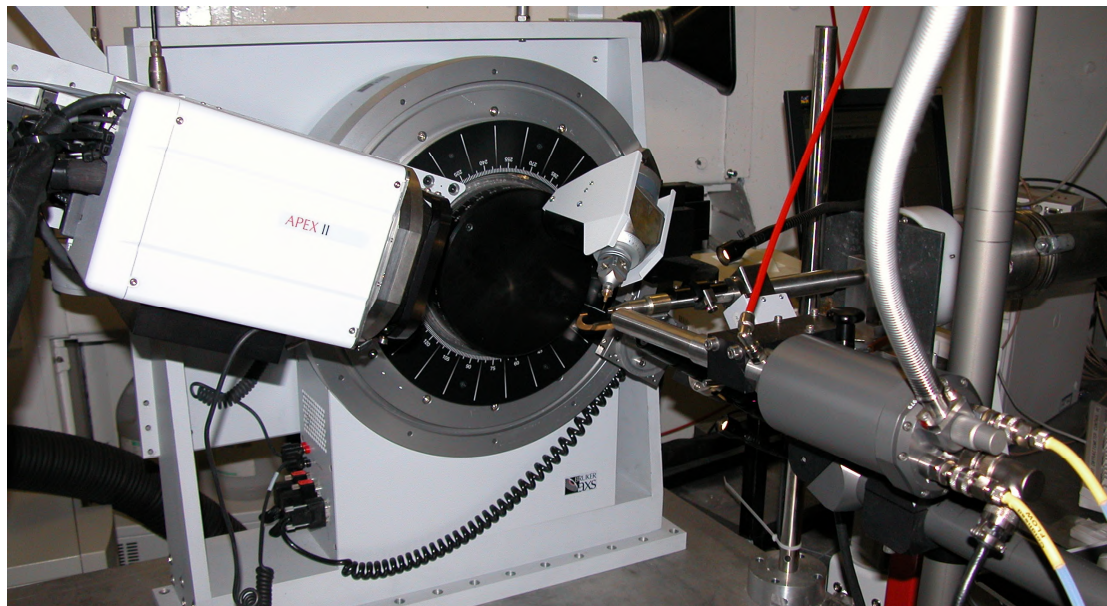


Figure 3.10: Station 9.8 of the SRS Daresbury

3.4: Nuclear Magnetic Resonance (NMR)

Solution state NMR is an important analytical technique routinely used in the identification and characterisation of organic molecules. ^1H and ^{13}C solution state NMR were carried out for the characterisation of the ionic liquids used in the ‘ionothermal’ synthesis using a Bruker Avance NMR spectrometer operating at 300 MHz for ^1H and 75.44 MHz for ^{13}C .

Electrons, protons and neutrons can be imagined as spinning on their axes. When the spins of the protons and neutrons comprising a nucleus are not paired, the overall spin of the charged nucleus generates a magnetic dipole along the spin axis. The intrinsic magnitude of this dipole is a fundamental nuclear property called the nuclear magnetic moment, μ .³ μ is a vector quantity and is proportional to the nuclear spin which is given the quantum number I .

$$\mu = \gamma I \quad (\gamma \text{ is the gyromagnetic ratio})$$

Since each isotope has a distinct gyromagnetic ratio the nuclear spins of each element will resonate at characteristic, distinct frequencies. I can take integral or half-integral values depending on the number of unpaired protons and neutrons. Examples include ^1H , ^{13}C , ^{19}F , and ^{31}P which have spin 1/2, ^2D and ^{14}N which have spin 1 and ^{27}Al which has spin 5/2. Nuclei that have spins greater than 1/2 are called quadrupolar.

Here we will consider a nucleus with spin quantum number $I = 1/2$. This may adopt either of two orientations when subjected to an applied magnetic field, B_0 ; +1/2 (i.e. spin up, aligned with an external magnetic field) or -1/2 (i.e. spin down, aligned against an external magnetic field). When there is no external magnetic field present, there is essentially no difference between up and down spin states. If a magnetic field is applied then it is more energetically favourable for the nucleus to align so that its magnetic

moment points in the same direction as the applied magnetic field (B_0). However, the difference between these energy levels is tiny, even in strong magnetic fields, so that the excess number of spins in the lower energy state is very small.

Irradiation of a sample with radio frequency energy corresponding exactly to the spin state separation of a specific set of nuclei will cause excitation of those nuclei in the $+1/2$ state to the higher $-1/2$ spin state. NMR is the absorption of radiation of energy equal to the difference between these levels. This frequency is known as the resonance or Larmor frequency.¹⁰ The detector measures the fluctuations in the magnetic field around the sample and this is then represented as the frequency spectrum or the chemical shift of the nuclei by Fourier transformation.

The frequency/chemical shifts are characteristically different for nuclei in different environments thus allowing the recognition of these environments. Examples include electronegative groups and the π -system of alkenes and aromatic compounds having a “deshielding “ effect and tend to move the NMR signals from neighbouring protons further “downfield” to higher ppm values. Nuclei which are non-equivalent and close to one another produce an additional magnetic field. This results in the splitting of a peak in the spectrum known as spin-spin coupling or J coupling.

Solid state NMR is an important technique used to aid in the characterisation of microporous materials. Unfortunately the spectra often have a lack of resolution with only broad signals being seen in the solid state NMR spectra, as the full effects of anisotropic or orientation-dependent interactions (the shielding, dipolar and quadrupolar interactions) are observed. To reduce this effect, high resolution NMR is used, which uses a number of special techniques/equipment including magic-angle spinning (MAS), cross polarization and enhanced probe electronics.

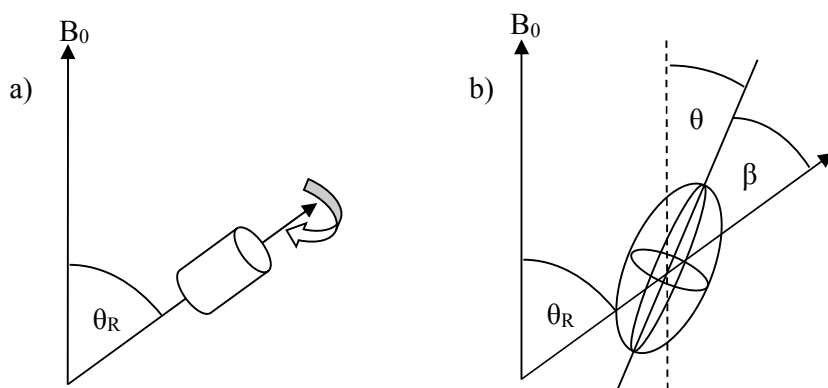


Figure 3.11: Representation of a) rotor spinning about an angle θ_R
 b) chemical tensor rotating with the sample.

Anisotropic dipolar interactions can be suppressed by introducing artificial motion on the solid. If a sample is spun about an angle θ_R with respect to the applied magnetic field, B_0 , then θ varies with time as the molecule rotates with the sample. The average of the orientation dependence of the nuclear spin interaction, under these circumstances can be shown as:

$$\langle 3\cos^2\theta - 1 \rangle = 1/2(3\cos^2\theta_R - 1)(3\cos^2\beta - 1)$$

Where the angles θ_R and β are defined in Figure 3.11.

If a sample is spun at an angle of $\theta_R = 54.74^\circ$ with respect to the external magnetic field, B_0 , then $3\cos^2\theta_R - 1 = 0$ hence the $\langle 3\cos^2\theta - 1 \rangle = 0$. Provided that the spinning rate is fast, so that θ is averaged, the interaction anisotropy averages to zero.

Cross polarisation involves transferring spin polarisation from abundant spins, I , such as ^1H or ^{19}F to dilute spins, S , such as ^{13}C or ^{15}N in order to enhance the signal to noise and reduce waiting time between successive experiments. This is achieved by the I and S spins precessing in their respective rotating frames at the same frequency, thus the Hartmann-Hahn condition, $\gamma_I B_I = \gamma_S B_S$ is satisfied. This results in a transfer of

resonance energy from the *I* to the *S* spins and results in an increase in intensity at the *S* spins of γ_I/γ_S .

Solid state NMR has been used to confirm the co-ordination of the Al and P sites analysed by single crystal X-ray diffraction. It has also confirmed the presence of F and helped to analyse structure directing agents within the microporous materials.

3.5: Thermogravimetric Analysis (TGA)

TGA is used to measure the loss of mass in microporous materials when heated under an atmosphere of either nitrogen or oxygen. The observed change in mass loss can provide information on the stability of the material and help to confirm a proposed molecular formula. Samples were examined using a TA Instruments 2960 TGA analyser.

3.6: CHN Elemental Analysis

C, H, N elemental analysis can give useful information on the organics present within a microporous material. Template identification can be assisted by examining the ratios of C, H and N. Elemental analysis was carried out using a Carlo Erba 1106 CHN Elemental Analyser.

3.7: Scanning Electron Microscopy (SEM) combined with Energy Dispersive X-ray Spectroscopy (EDXRS)

An SEM is essentially a high magnification microscope, which uses a focussed scanned electron beam to produce images of the surface of a sample.¹¹ Electrons generated from an electron gun enter the surface of the sample and generate many low energy secondary electrons by colliding with a sample atom electron and knocking it out of its shell. The intensity of these secondary electrons is governed by the surface topology of the sample. An image of the sample surface is therefore constructed by measuring the secondary electron intensity as a function of the position of the scanning primary electron beam.

In the process of producing secondary electrons, a 'hole' in an inner shell is left and the atom is not in a stable state. To stabilise the atoms, electrons from the outer shells drop in to the inner shells, releasing energy in the form of X-rays. These X-rays are characteristic in energy and wavelength not only to the element of the parent atom, but also the shell which lost the electron and the shell that replaced the electron. Since lower atomic number elements have fewer filled shells, they have fewer X-ray peaks. Each element has characteristic X-ray line(s) that allow a sample's surface elemental composition to be identified using the technique of EDXRS.

A Jeol JSM-5600 SEM integrated with an EDXRS system for analytical elemental analysis was used to confirm the presence and quantity of cobalt, silicon and fluorine in several of the zeotype materials synthesised.

3.8: References

1. H. Robson, 'Verified Synthesis of Zeolite Materials', Elsevier, Amsterdam, 2001
2. Parr product broacher, 'Sample Preparation Bombs', Bulletin 4700
3. P.W. Atkins, 'Physical Chemistry', Oxford University Press, New York, 1998
4. D.E. Sands, 'Introduction to Crystallography', Dover Publications, 1993
5. W. Clegg, 'Crystal Structure Dtermination', Oxford University Press, Oxford, 1998
6. H.F. Chung and D.K. Smith, 'Industrial Applications of X-ray Diffraction', Marcel Dekker Ltd, 1999
7. D. Turk and L. Johnson, 'Methods in Macromolecular Crystallography', IOS Press, 2001
8. S.M. Gruner and S. E. Ealick, *Structure*, 1995, **3**, 13
9. P. Coppens, 'Synchrotron Radiation Crystallography', Academic Press, London, 1992
10. J.A. Iggo, 'NMR Spectroscopy in InorganicChemistry', Oxford University Press, Oxford, 1999
11. I. Chorkendorff and J. W. Niemantsverdriet, 'Concepts of Modern Catalysis and Kinetics', Wiley-VCH, Weinheim, 2003, Ch. 4

4: 1-ethyl-3-methylimidazolium bromide as solvent and template in the synthesis of AlPOs.

4.1: Aims

This chapter describes the work carried out which aimed to investigate the use of the ionic liquid, 1-ethyl-3-methylimidazolium bromide as solvent and template in the synthesis of aluminophosphate zeotype analogues. The reactions were carried out containing minimal water content. Any effects on the structures produced by the addition of HF as a mineralising agent were considered.

4.2: Introduction (1-alkyl-3-methylimidazolium cation)



Figure 4.1: 1-alkyl-3-methylimidazolium cation

The 1-alkyl-3-methylimidazolium salts (Figure 4.1) are part of the family of ionic liquids. This means they are liquids at ambient temperatures (less than 100 °C), and exist as ionic species.¹ These properties mean that not only is there the possibility that they can be used as templates, but also as the solvent in the hypothesis of ionothermal synthesis of aluminophosphates.

Adams *et al.*² reported the synthesis of a mesoporous material using ionic liquids as templates in water. The use of 1-alkyl-3-methylimidazolium ($[C_n\text{mim}]^+$ where $n = 2-18$) was reported as the organic template in the synthesis of MCM-41. In this case the

liquid phase is predominantly molecular, and the salt acts as a surfactant and not as an ionic liquid.

Zones reported the use of four quaternized imidazole derivatives (Figure 4.2) as structure-directing organic cations in high-silica zeolite synthesis.³ Whilst these structures are not ionic liquids due to their melting point being too high, they do possess a very similar structure to the imidazolium based ionic liquids. In this work it was shown that the organocations could be structurally manipulated to give a very good templating effect in the synthesis of pentasil zeolites. It was shown that there was a close correlation between the imidazole structure and the zeolites pore size.

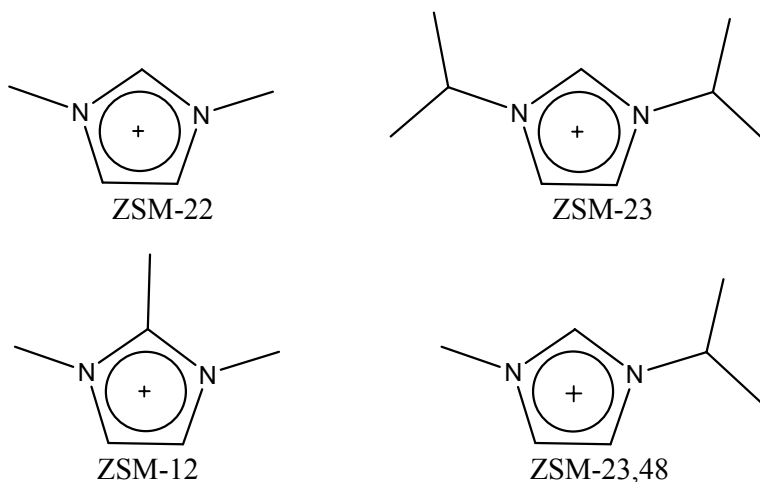


Figure 4.2: Quaternized imidazole derivatives and the zeolites phases that can be made from them.³

The reports of the imidazolium family acting as templates in the synthesis of mesoporous and microporous materials make the imidazoliums an appropriate starting material in the investigation of ionothermal synthesis.

4.3: Experimental – Ionothermal synthesis of AlPOs

4.3.1: Synthesis of 1-ethyl-3-methylimidazolium bromide – mp = 81 °C⁴

1-ethyl-3-methylimidazolium bromide is available commercially, but is expensive. Since the initial investigation into the synthesis of aluminophosphate molecular sieves was to be carried out using this ionic liquid, large amounts of it were required, hence it was synthesised from known literature procedures.⁵

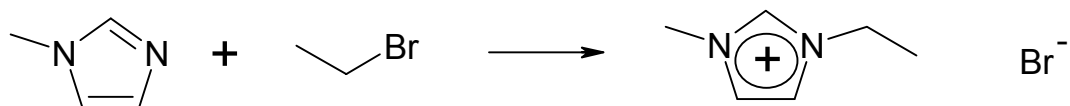


Figure 4.3: Synthesis of 1-ethyl-3-methylimidazolium bromide

Under inert atmosphere conditions, degassed ethylbromide (86.04 g, 0.790 mol, Avacado) was added to the redistilled N-methyl imidazole (49.86 g, 0.607 mol, Aldrich), with constant stirring. This was refluxed at 40 °C for 3 hours then allowed to cool to room temperature. Ethyl acetate was added and the product crashed out of solution. This was filtered, washed with ethyl acetate and dried under vacuum at 25 °C for 10 hours to give 1-ethyl-3-methylimidazolium bromide as a white solid. The product was stored under an inert atmosphere. Yield 94 %. ¹H-NMR (D₂O): δ 1.41 (t, 3H, CH₃, J = 7.3 Hz), 3.81 (s, 3H, NCH₃), 4.15 (q, 2H, NCH₂, J = 7.3 Hz), 7.38 (d, 2H, NC(H)C(H)N, J = 21.0 Hz), 8.66 (s, 1H, NC(H)N) ppm. ¹³C-NMR (D₂O): δ 14.68 (s, CH₃), 35.85 (s, NCH₃), 44.88 (s, NCH₂), 121.94, 123.52 (2 x s, NCCN), 135.63 (s, NCN) ppm. NMR comparable with literature values.⁶

4.3.2: Synthesis of zeolite analogues in sealed autoclaves

A typical synthesis procedure was as follows: a TeflonTM-lined autoclave (volume 23 ml) was charged with the ionic liquid or eutectic mixture, Al[OCH(CH₃)₂]₃ (Aldrich) and H₃PO₄ (85 wt% in H₂O, Aldrich). Distilled water or HF (48 wt% in H₂O, Aldrich) were added if required. The stainless steel autoclave was then heated in an oven to the required temperature. The reagent masses, temperatures and length of time left in oven needed to produce the optimum purity are as detailed in Table 4.1. These conditions were optimised by changing the reaction compositions (e.g. water content) slightly and then characterising the resulting products. After cooling the autoclave to room temperature the product was suspended in distilled water, sonicated, filtered by suction and washed with acetone.

Product	Mass of reagents added (g) (molar ratio of reagents)					Temp (°C)	Time (hrs)
	Al(OiPr) ₃	H ₃ PO ₄	HF	H ₂ O	IL		
SIZ-1	0.1018 (1.0)	0.1732 (3.0)	0.00 (0.0)	* (2.9)	4.05 (43)	150	66
SIZ-3	0.1013 (1.0)	0.1732 (3.0)	0.015 (0.73)	* (3.8)	4.07 (43)	150	68
SIZ-4	0.1054 (1.0)	0.1772 (3.0)	0.015 (0.70)	* (0.0)	3.82 (39)	150	68
SIZ-5	0.0465 (1.0)	0.0858 (3.1)	0.00 (0.0)	0.50(116)	2.03 (44)	150	19
SIZ-6	0.1000 (1.0)	0.1730 (3.1)	0.00 (0.0)	* (0.0)	4.25 (45)	200	96

* No extra water added in these preparations. Small amounts of water present come from the aqueous HF and H₃PO₄ solutions and the ionic liquid.

Table 4.1: Synthesis details and conditions for the preparation of materials using the ionic liquid (IL) 1-ethyl-3-methylimidazolium bromide.

In the case of the SIZ-4 and SIZ-6 synthesis the Al[OCH(CH₃)₂]₃, H₃PO₄ and HF (SIZ-4 only) were added to the TeflonTM liner. This was then heated to 50 °C on a hotplate for 2 hours to remove the water and any isopropanol formed during the initial reaction. This was confirmed by following the mass of the mixture until no more mass loss was observed. The ionic liquid was then added and the synthesis proceeded as normal.

4.3.3: Synthesis of zeolite analogues in round bottom flasks

SIZ-3 and SIZ-4 can be prepared in an open container using the conditions from Table 4.1. A round bottom flask, fitted with a condenser, magnetic stirrer and drying tube, was charged with the starting materials and then heated to the target temperature (150 °C) for the required length of time. The products were recovered as described in Chapter 4.3.2.

4.3.4: Recycling of ionic liquid

After filtering off the zeotype, the filtrate was centrifuged to remove any remaining small solid particles. The water and acetone were removed from the ionic liquid by rotary evaporation. The remaining product was dissolved in excess dichloromethane and magnesium sulphate added. This was stirred for 30 minutes then filtered under suction. The dichloromethane was removed by rotary evaporation. Ethyl acetate was added and the solidified ionic liquid precipitated from solution. This was filtered, then washed with ethyl acetate and dried under vacuum at 25 °C for 10 hours to give 1-ethyl-3-methylimidazolium bromide. Approximately 80 % of the mass of ionic liquid used in the original preparation can be recovered. Note however that some is used up as a template and so is not available for recycling and so the real recycling efficiency is greater than 80 %. The ionic liquid was characterised by ¹H NMR. The 1-ethyl-3-methylimidazolium bromide was then used successfully in the preparation of zeotypes SIZ-3 and SIZ-4.

4.3.5: Experimental Details

Structural Characterisation using X-ray diffraction

Single crystal X-ray diffraction data for SIZ-1, SIZ-3, SIZ-4 and SIZ-6 were collected on station 9.8 at the Synchrotron Radiation Source (SRS), Daresbury Laboratories, Cheshire, UK. The structures were solved using standard direct methods and refined using least-squares minimisation techniques against F^2 . CIF files are available for all structures on the accompanying CD. Framework phase identification for SIZ-5 was accomplished using powder X-ray diffraction (Stoe STADIP diffractometer, Cu $K\alpha$ radiation) as no suitable single crystals were prepared.

$\{^1\text{H}\}^{13}\text{C}$ CP MAS-NMR

Data for SIZ-1, SIZ-3, SIZ-4, SIZ 5 and SIZ-6 were collected at the University of St Andrews on a Varian Infinity plus spectrometer operating at frequencies of 500.156 MHz for ^1H and 125.759 MHz for ^{13}C . The samples were spun at the magic angle at 5 kHz. The spectra were collected with a proton 90 degree pulse of 3 μs , a contact time of 5 ms and a recycle time of 1 s.

^{31}P , ^{27}Al and ^{19}F MAS-NMR spectra

Data was collected for SIZ-1, SIZ-3, SIZ-4, SIZ-5 and SIZ-6 at the EPSRC Solid State NMR service facility at the University of Durham, UK on a 300 MHz Varian UNITY*Inova* with a 7.05 T Oxford Instruments magnet. The frequencies for data collection are 121.371 MHz (^{31}P), 78.125 MHz (^{27}Al) and 282.063 MHz (^{19}F). During data collection the samples were spun at 10 kHz (for ^{31}P , ^{27}Al) and 14 kHz for ^{19}F . ^{31}P NMR spectra were collected with proton decoupling using a recycle time of 300 s and a 20 ms acquisition time. Spectra were referenced to 85 % H_3PO_4 at 0 ppm. ^{27}Al NMR

spectra were collected without ^1H decoupling using a 20 ms acquisition time and a recycle time of 1 s. The spectra were referenced to 1M AlCl_3 at 0 ppm. ^{19}F MAS-NMR spectra were collected with a 10 ms acquisition time and a recycle time of 60 s. The chemical shift reference was CFCl_3 and there was no decoupling used.

Thermal analysis

Thermal analysis experiments were carried out at the University of St Andrews Facility for Characterisation of Solids using a TA Instruments 2960 TGA analyser. The samples were heated under flowing nitrogen up to $1000\text{ }^\circ\text{C}$ at $10\text{ }^\circ\text{C}$ per minute.

4.4: Results

4.4.1: SIZ-1

A novel structure type, SIZ-1 (St. Andrews Ionic Liquid Zeotype-1) was synthesised and its structure solved using single crystal X-ray diffraction on Station 9.8 at the Synchrotron Radiation Source, Daresbury. Crystal data and structure refinement details for SIZ-1 are given in table 4.2.

Table 4.2: Crystal data and structure refinement for SIZ-1

Identification code	SIZ-1
Empirical formula	$\text{Al}_4(\text{PO}_4)_5\text{H}_{1.5} \cdot 1.5(\text{C}_6\text{H}_{11}\text{N}_2)$
Formula weight	751.03
Temperature	150(2)K
Wavelength	0.6886 Å
Crystal system, space group	Triclinic, P-1
Unit cell dimensions	$a=9.162(5)\text{Å}$ $\alpha=75.038(5)^\circ$ $b=9.291(5)\text{Å}$ $\beta=75.244(5)^\circ$ $c=16.504(5)\text{Å}$ $\gamma=83.867(5)^\circ$
Volume	$1311.2(11)\text{Å}^3$
Z, Calculated density	2, 1.868 Mg/m ³
Absorption coefficient	0.458 mm^{-1}
F (000)	729
Crystal size	0.02 x 0.02 x 0.01 mm
Theta range for data collection	2.23 to 29.54 °
Limiting indices	$-13 \leq h \leq 13,$ $-13 \leq k \leq 12,$ $-23 \leq l \leq 18$
Reflections collected / unique	11742/6838 [R(int) = 0.0864]
Completeness to theta = 29.54 °	84.7 %
Refinement method	Full-matrix least-squares on F ²
Data / restraints / parameters	6838/11/455
Goodness-of-fit on F ²	0.950
Final R indices [I > 2σ(I)]	R1=0.0807, wR2=0.1916
R indices (all data)	R1=0.1499, wR2=0.2356
Extinction coefficient	0.013(2)
Largest diff. peak and hole	1.433 and -1.393 eÅ ⁻³

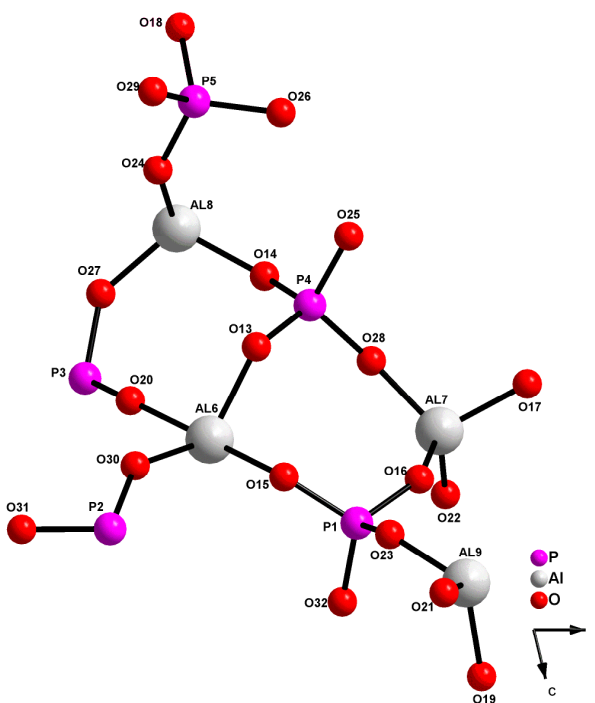


Figure 4.4: Asymmetric unit of SIZ-1 with the template molecules omitted.

The asymmetric unit of SIZ-1 (Figure 4.4) consists of four aluminium, five phosphorus, twenty oxygen, one and a half hydrogen with one and a half 1-ethyl-3-methylimidazolium molecules. This gives an empirical formula of $\text{Al}_8(\text{PO}_4)_{10}\text{H}_3 \cdot 3\text{C}_6\text{H}_{11}\text{N}_2$. The template has not been shown in the diagram of the asymmetric unit due to its disorder.

Once the framework atoms had been located and refined isotropically, peaks in the difference Fourier syntheses indicated the presence of three ionic liquid cations disordered in the channels of the structure (Figure 4.5). Overall occupancy factors for the three molecules refined to 0.48(1), 0.508(9) and 0.53(1), consistent (within the estimated errors) with the overall requirement for 1.5 cations per asymmetric unit to balance the charge on the framework. The final cycles of least-squares refinement included restraints to keep the aromatic parts of the template flat and chemically

equivalent distances in the template cation the same (FLAT and SADI restraints in the refinement program SHELXL-97).⁷ The final cycle of least-squares refinement also included a small (but significant) correction for extinction. The equivalent isotropic temperature factors for some of the atoms in the template are higher than usual, perhaps indicating some extra unresolved disorder of the template in the cavities.

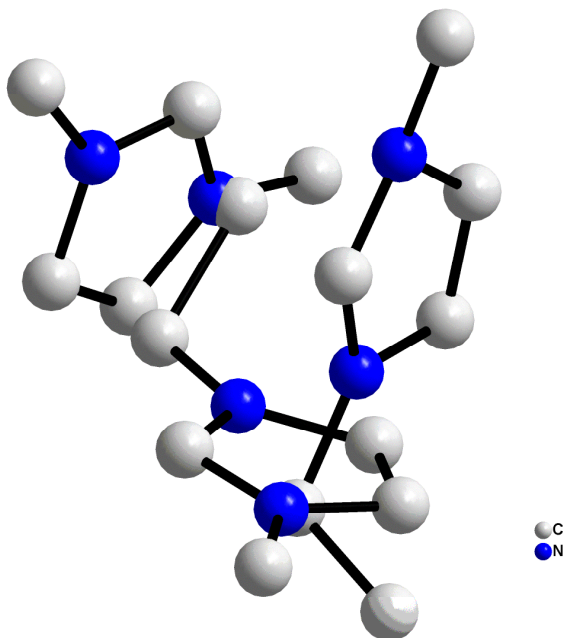


Figure 4.5: Disordered template in SIZ-1 pores.

The structure of SIZ-1 (Figure 4.6) consists of hexagonal prismatic units known as double six rings (D6Rs) joined to form layers that are linked into three-dimensional frameworks by units containing four tetrahedral centres (two phosphorus and two aluminium) known as single four rings (S4Rs).

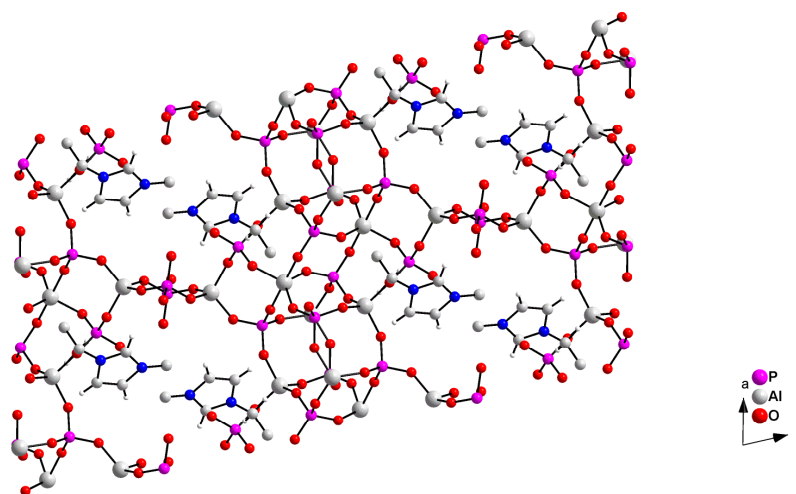


Figure 4.6: SIZ-1 framework. Only one out of the three templates has been shown.

The unusual feature of the SIZ-1 structure is that the Al:P ratio is not 1:1. The formula of the material is $\text{Al}_8(\text{PO}_4)_{10}\text{H}_3.3\text{C}_6\text{H}_{11}\text{N}_2$ but the Al-O-P alternation is maintained. The framework is therefore interrupted, with some unusual intraframework hydrogen bonding (Figure 4.7). The negative charge present on the framework (caused by the existence of terminal P-O bonds) balances the charge on the 1-methyl-3-ethyl imidazolium templates that are present in the pores. The overall structure of SIZ-1 (Figure 4.6 and 4.7) shows a two-dimensional channel system parallel to the *a*- and *b*-crystallographic axes.

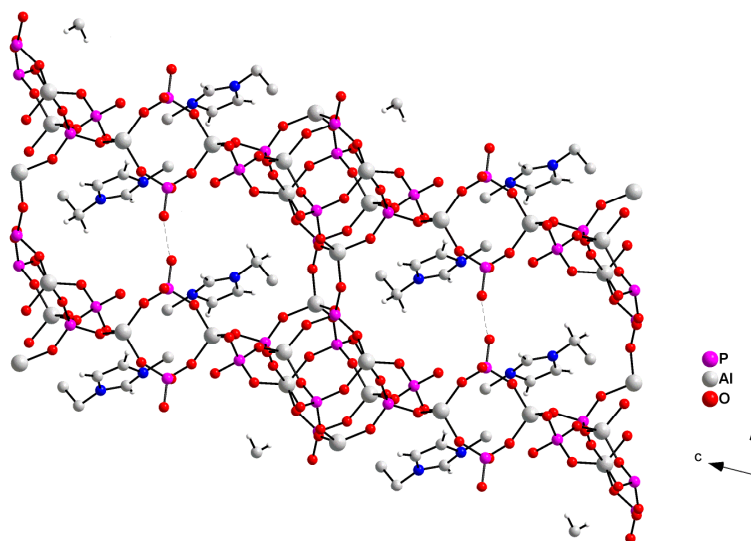


Figure 4.7: SIZ-1 framework showing intra framework hydrogen bonding.

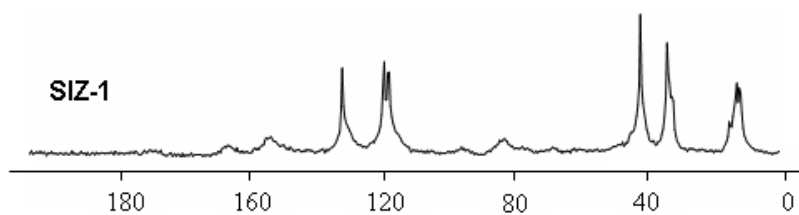


Figure 4.8: ^{13}C MAS-NMR of SIZ-1

It can be seen from the ^{13}C MAS-NMR (Figure 4.8) that the 1-ethyl-3-methylimidazolium template is present and intact within the SIZ-1 channels. This is consistent with the X-ray structure, where two out of the three terminal methyl groups could be located.

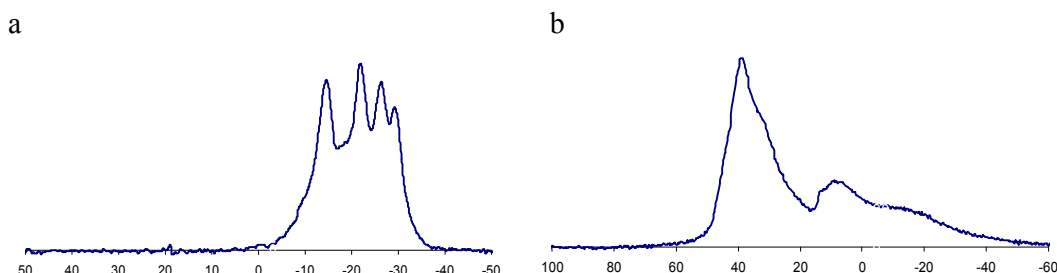


Figure 4.9: a = ^{31}P , b = ^{27}Al MAS-NMR of SIZ-1

Figure 4.9a gives the ^{31}P spectrum for SIZ-1. This shows a number of resonances in the region for tetrahedral phosphorus, as expected. The single crystal structure has five independent phosphorus sites, and the NMR shows at least four resolvable sites in a broad envelope between -14.6 and -29.3 ppm.

The ^{27}Al MAS-NMR (Figure 4.9b) spectrum shows evidence of tetrahedral aluminium, with intense resonances at around 40 ppm. There is also evidence of five co-ordinated aluminium, which is consistent with the X-ray data. It must be noted that the MAS-NMR peaks are relatively broad for SIZ-1, perhaps indicating that the sample has a degree of disorder.

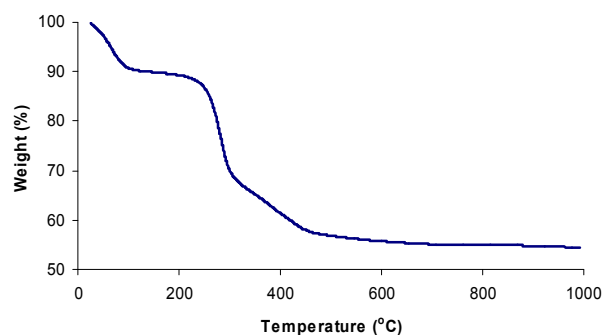


Figure 4.10: TGA experiment for SIZ-1

SIZ-1 TGA data shows an almost 10 % weight loss at just above room temperature, which is most likely due to weakly held species at the surface of the sample. It must be noted that SIZ-1 is relatively poorly crystalline, and while there are no other crystalline phases in the sample there may be some amorphous impurity that makes analysis of the TGA more difficult. However, the ~20 % weight loss at 250 °C for SIZ-1 is about correct for the removal of the imidazolium template (calc. 19.7 %). The further weight loss is then presumably due to the loss of water on condensation of the hanging P-OH units remaining after loss of the template.

Attempts to calcine SIZ-1 have not proved completely successful. If heated slowly at 1°C/min to 280 °C and held for 4 hrs, the product decomposes. However if SIZ-1 is heated to 250 °C under the same conditions for 12 hrs, it was found by CHN analysis that about 50 % of the template is removed and powder X-ray diffraction showed the structure still to be intact.

4.4.2: SIZ-3

Single crystal analysis of SIZ-3 indicated that the framework has the same topology as that of AIPO-11 (AEL).⁸ Crystal data and structure refinement details of SIZ-3 are given in Table 4.2. AIPO-11 is usually synthesised through the hydrothermal method, using amine or quaternary salts as templates,⁹ and was first synthesised by Wilson *et al.* in 1982.¹⁰ AIPO-11 has also been synthesised using the non-aqueous solvent system with ethylene glycol as the solvent.¹¹ The dry-gel conversion method¹² has also been used for the AIPO-11 synthesis which was carried out in the presence of only a small amount of external bulk water (which was necessary for the reaction).

Unfortunately, SIZ-3 is severely twinned and leads to several complications, some of which are yet unresolved, for example, many of the bond distances inferred from the average atomic positions are intermediate between those expected for Al-O and P-O bonds. This implies that the crystals are twinned in a fashion that produces an average structure where each T site is an average of Al and P occupancy. No twin refinements could successfully remove these problems and the single crystal structure can only be regarded as a gross representation of the framework structure. It is clear however, even from this refinement, that the framework is isostructural with AEL. Unfortunately, the template could not be located using this data (although ¹³C MAS-NMR confirms it is present and intact). However, a Fourier peak did show the presence of fluoride ions in the structure. This is, as far as we believe, the first time fluoride has been located in this framework. The final structure (Figure 4.11) was refined using the data produced from the program Squeeze contained within the PLATON¹³ package of crystallographic tools which excludes electron density from the pores. The final refinement yielded some large atomic displacement parameters, again indicative of the problems caused by twinning.

Table 4.2: Crystal data and structure refinement for SIZ-3.

Identification code	SIZ-3
Empirical formula	$\text{Al}_5(\text{PO}_4)_5\text{F} \cdot \text{C}_6\text{H}_{11}\text{N}_2$
Formula weight	739.92
Temperature	150(2) K
Wavelength	0.6886 Å
Crystal system, space group	Orthorhombic, Ibm2
Unit cell dimensions	$a = 13.292(2)$ Å $\alpha = 90^\circ$. $b = 18.469(4)$ Å $\beta = 90^\circ$ $c = 8.4212(16)$ Å $\gamma = 90^\circ$
Volume	$2067.3(7)$ Å ³
Z, Calculated density	4, 2.200 Mg/m ³
Absorption coefficient	0.618 mm^{-1}
F(000)	1360
Crystal size	0.02 x 0.02 x 0.01 mm
Theta range for data collection	1.83 to 29.53 °
Limiting indices	-14 ≤ h ≤ 12, -5 ≤ k ≤ 26, -11 ≤ l ≤ 12
Reflections collected / unique	3390 / 2323 [R(int) = 0.0317]
Completeness to theta = 29.53 °	80.0 %
Absorption correction	None
Refinement method	Full-matrix least-squares on F ²
Data / restraints / parameters	2323 / 1/ 147
Goodness-of-fit on F ²	1.086
Final R indices [I > 2σ(I)]	R1 = 0.0917, wR2 = 0.2576
R indices (all data)	R1 = 0.1083, wR2 = 0.2708
Largest diff. peak and hole	0.942 and -1.077 e. Å ⁻³

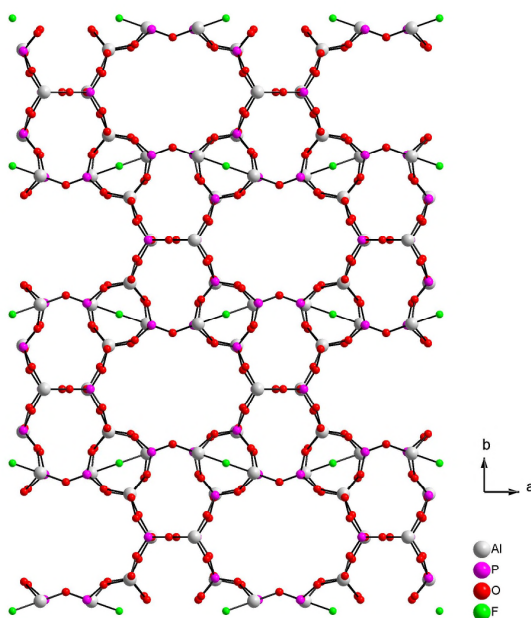


Figure 4.11: Ball and Stick of SIZ-3 along the c axis

The AlPO-11 framework structure is related to that of the AlPO-5 framework, but one set of four rings in the AlPO-5 framework has been removed. AlPO-11 exhibits a unidimensional channel system with 10-membered ring pores. These pores are elliptical in shape and each pore is isolated from the adjacent pore by a wall composed of linked 4- and 6-rings of alternate aluminium and phosphorous tetrahedral (Figure 4.11). The fluoride atom is observed in an AlO_4F unit, which forms an Al-F-Al linkage. This is shown in Figure 4.12 below.

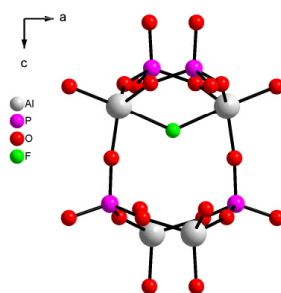


Figure 4.12: The location of fluoride in the structure of SIZ-3.

The template could not be located by the single crystal analysis due to the complications arising from the crystal twinning, but it can clearly be seen from the ^{13}C MAS-NMR (Figure 4.13) that the 1-ethyl-3-methylimidazolium template is present and intact within the AlPO-11 pores.

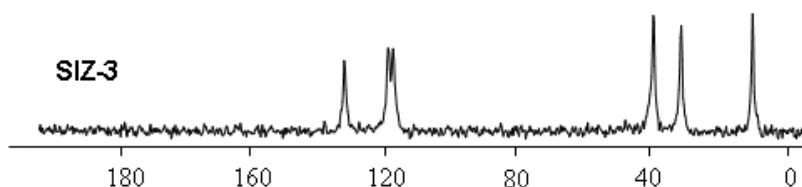


Figure 4.13: ^{13}C MAS-NMR of SIZ-3

The ^{31}P MAS-NMR (Figure 4.14) shows three resonances in a broad envelope from -20 ppm to -35 ppm. This is consistent with the expected three resonances from the XRD structure. The ^{27}Al NMR confirms the presence of the five coordinated aluminium required for the observed AlO_4F unit and the presence of fluoride in the material is confirmed by ^{19}F MAS-NMR (resonance centred at -118 ppm). The broad peak at about -150 ppm is probably due to impurity.

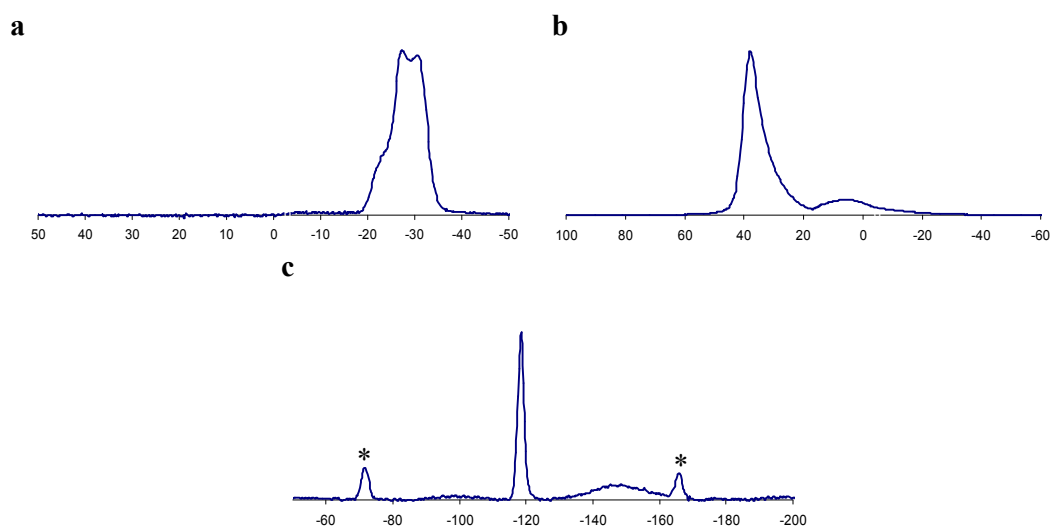


Figure 4.14: a = ^{31}P , b = ^{27}Al , c = ^{19}F MAS-NMR of SIZ-3.
Asterisks denote spinning sidebands.

SIZ-3 showed approximately the expected weight loss at between 250 – 440 °C of about 19 % (calc, 17.59 %) during TGA for the predicted chemical compositions from the XRD experiments. The one sharp weight loss at around 400 °C, can be attributed to the loss of the template and fluoride ions (Figure 4.15).

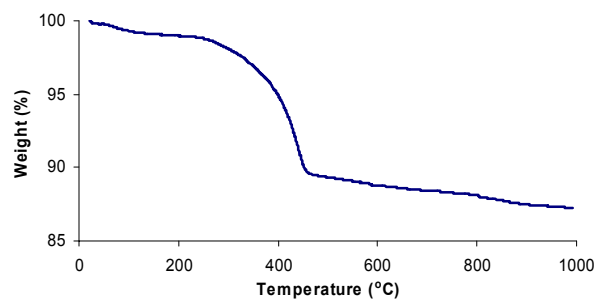


Figure 4.15: TGA experiment for SIZ-3

4.4.3: SIZ-4

The SIZ-4 structure appears to be a default structure that forms under many slightly different synthesis conditions. As the Teflon™ liners are porous, seeding of SIZ-4 has proved problematic due to previous product being trapped in the pores and being exposed with heating of the Teflon™. SIZ-4 has the same framework topology as the triclinic form of chabazite (CHA). Crystal data and structure refinement details of SIZ-4 are given in Table 4.3. The triclinic CHA was first synthesised by Guth¹⁴ and the structure solved independently by Simmen¹⁵ using powder data and Kariuki¹⁶ using single-crystal data. This structure has previously been synthesised from a fluoride route in a non-aqueous, solvent system media.¹⁷

Table 4.3: Crystal data and structure refinement for SIZ-4.

Identification code	SIZ-4
Empirical formula	Al ₃ (PO ₄) ₃ F.C ₆ H ₁₁ N ₂
Formula weight	496.02
Temperature	150(2) K
Wavelength	0.6886 Å
Crystal system, space group	Triclinic, P-1
Unit cell dimensions	a = 9.0897(9) Å alpha = 76.546(2)° b = 9.2075(9) Å beta = 87.299(2)° c = 9.2914(9) Å gamma = 89.411(2)°
Volume	755.45(13) Å ³
Z, Calculated density	2, 2.181 Mg/m ³
Absorption coefficient	0.520 mm ⁻¹
F(000)	500
Crystal size	0.04 x 0.02 x 0.01 mm
Theta range for data collection	2.19 to 29.33 °
Limiting indices	-12<=h<=11 -11<=k<=12 -12<=l<=12
Reflections collected/unique	5342/3930[R(int) = 0.0216]
Completeness to theta = 24.40 °	86.5%
Refinement method	Full-matrix least-squares on F ²
Data/restraints/parameters	3930 / 0 / 235
Goodness-of-fit on F ²	1.033
Final R indices[>2sigma(I)]	R ₁ = 0.0495, wR ₂ = 0.1363
R indices (all data)	R ₁ = 0.0528, wR ₂ = 0.1405
Largest diff. peak and hole	1.101 and -0.660 e. Å ⁻³

The asymmetric unit of SIZ-4 (Figure 4.16) consists of three aluminium, three phosphorus, twelve oxygen and one fluorine atom with one molecule of 1-ethyl-3-methylimidazolium. The terminal methyl group on the 1-ethyl-3-methylimidazolium seems to be severely disordered (probably over six possible sites) and was not refined in the final cycle of least-squares. Its presence however was confirmed by ^{13}C solid state NMR.

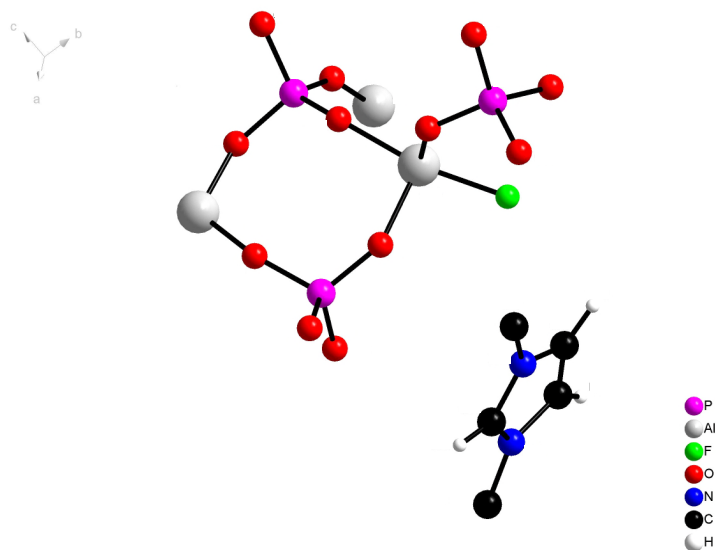


Figure 4.16: Asymmetric unit of SIZ-4.

The SIZ-4 CHA framework consists of double six-membered rings (D6Rs) of alternating aluminium and phosphorous tetrahedral. These are linked through four-membered rings to produce a three dimensional pore structure with eight-membered ring windows (Figure 4.17). Each six ring of the D6Rs contains one octahedral aluminium that connects to another octahedral aluminium of another D6R through two bridging fluorines.

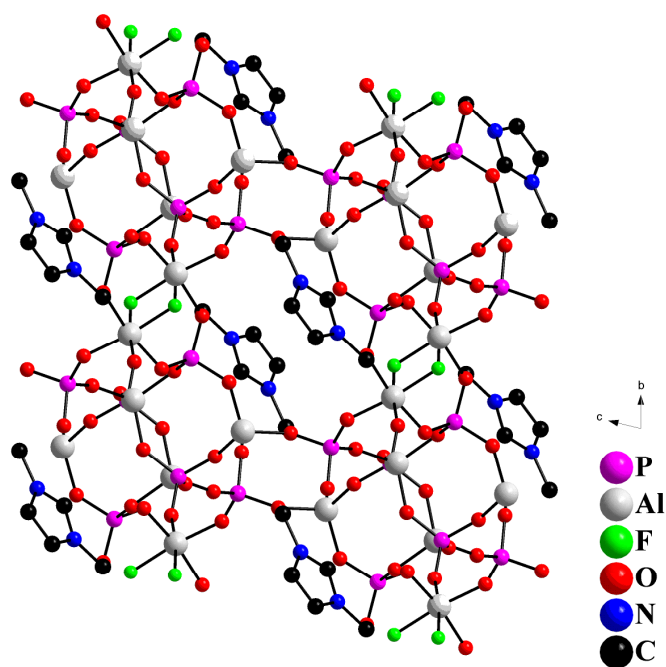


Figure 4.17: Ball and Stick of SIZ-4 along the a axis

The ^{13}C solid state NMR shows clearly that the 1-ethyl-3-methylimidazolium is intact in the zeolite cages (Figure 4.18). Also note the splitting of the methyl carbon from the ethyl group (~ 15 ppm), indicative of the disorder of this group, which is consistent with the X-ray structure. The disorder of the terminal carbon in the template of the structure indicates the possibility of using larger templates for this structure e.g. 1-isopropyl-3-methyl imidazolium cations.

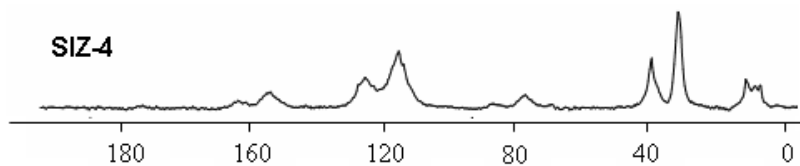


Figure 4.18: ^{13}C MAS-NMR of SIZ-4

In the ^{31}P MAS-NMR (Figure 4.19a), SIZ-4 has three major resonances (plus smaller ones from impurities) that are consistent with the structure. The ^{27}Al MAS-NMR (Figure 4.19b) shows clearly the octahedral (AlO_4F_2) coordination and the tetrahedral coordination. The presence of fluoride in the material is confirmed by ^{19}F MAS-NMR (resonance centred at -125 ppm).

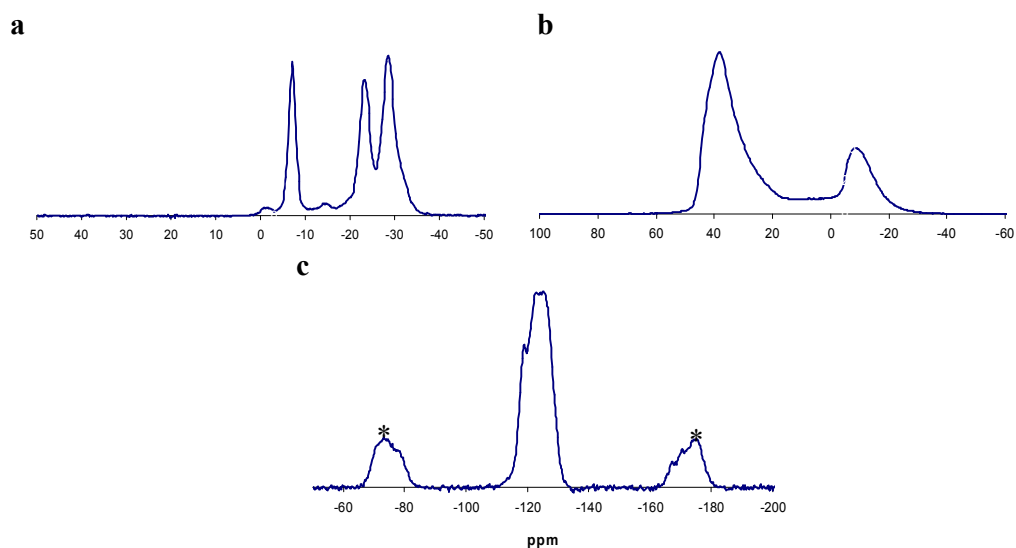


Figure 4.19: a = ^{31}P , b = ^{27}Al , c = ^{19}F MAS-NMR of SIZ-4. Asterisks denote spinning sidebands.

SIZ-4 showed approximately the expected weight loss during TGA (Figure 4.20) for the predicted chemical compositions from the XRD experiments. The one sharp weight loss of 24 % at around 400 °C, can be attributed to the loss of the template and fluoride ions (calc. 26.2 %).

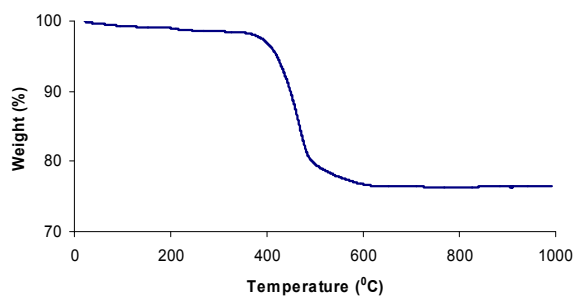


Figure 4.20: TGA experiment for SIZ-4

4.4.4: SIZ-5

X-ray powder diffraction (Stoe STADIP diffractometer, Cu K α radiation) was used to identify the framework structure of SIZ-5 as no suitable single crystals were prepared. The powder pattern is consistent with SIZ-5 having the same topology as zeolite AIPO-41 (AFO) which has orthorhombic lattice parameters 9.76 x 25.61 x 8.32 Å. It must however be noted that it was not possible to make this as a single phase and there is a large amount of dense phase present.

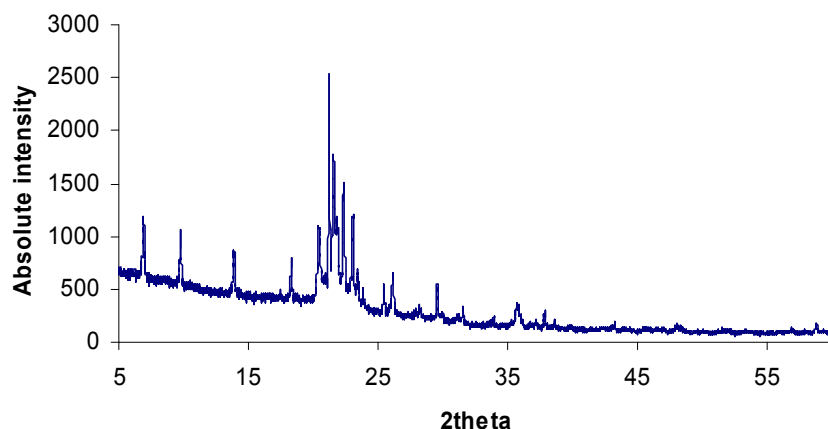


Figure 4.21: X-ray diffraction pattern of SIZ-5.

The synthesis of crystalline AIPO-41 was first reported by Lesch and Wilson¹⁸ in 1988 as a mixed phase product. It was synthesised under traditional hydrothermal synthesis conditions. Seeding the reaction produced the pure AIPO-41 phase. Clark *et al.*¹⁹ have reported the synthesis of AIPO-41 as a pure phase without the necessity of seeding by using a mixed solvent alcohol/water system.

The AIPO-41 structure has unidimensional 10-ring pores parallel to the *c*-axis direction (Figure 4.22). This is the same as in the SIZ-3 framework structure. The layer perpendicular to the *c* direction is connected by narsarsukite-type UDUD chains (linked

4-rings with sequence of tetrahedron interlayer directiveness up-down-up-down).²⁰ Again this is similar to SIZ-3, and both SIZ-3 and SIZ-5 framework structures are related to that of AlPO-5. The 10-ring pore in the AlPO-41 framework is not strictly elliptical, but rather a distorted elliptical pore.

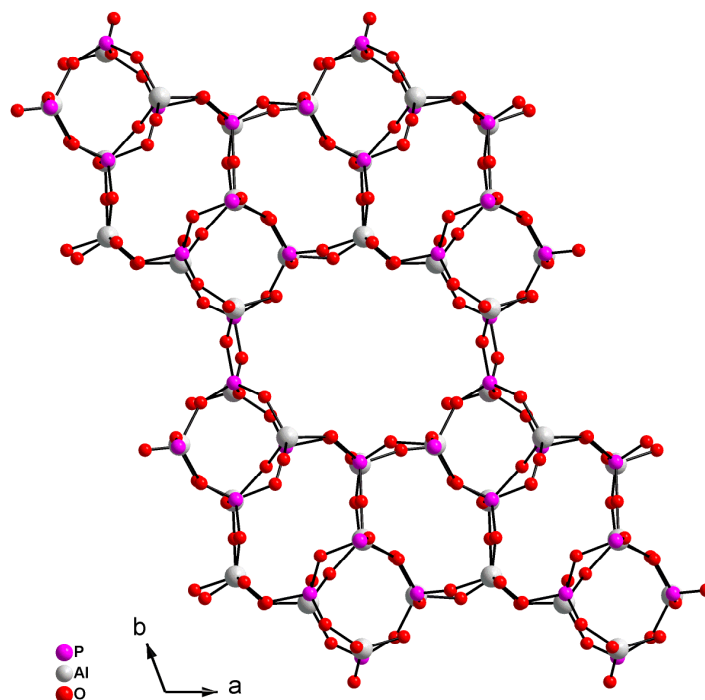


Figure 4.22: Ball and Stick of SIZ-5 along the *c*-axis¹⁸

The SIZ-5 ¹³C solid state NMR spectrum was collected on a very small sample and the large background signal is from the probe material. Despite this it is still possible to see that the 1-ethyl-3-methylimidazolium is intact in the zeolite pores (Figure 4.23).

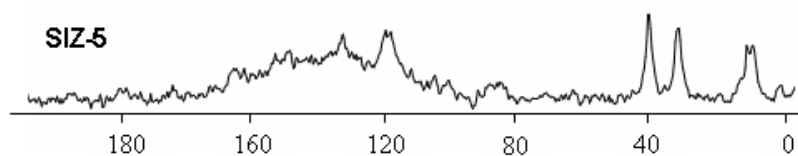


Figure 4.23: ¹³C MAS-NMR of SIZ-5

The SIZ-5 ^{31}P and ^{27}Al MAS-NMR (Figure 4.24) are similar to those previously reported for AIPO-41.²⁰ The slight broad peak in the ^{27}Al NMR at 10 ppm suggests the possibility of higher coordinated aluminium.

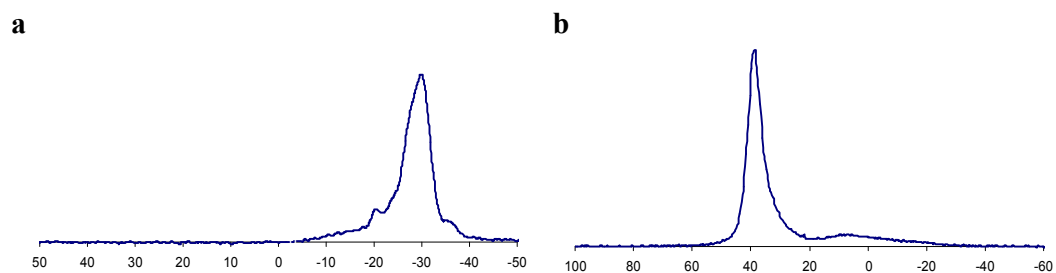


Figure 4.24: a = ^{31}P , b = ^{27}Al MAS-NMR for SIZ-5

SIZ-5 shows a weight loss of about 6 % at around 400 °C (Figure 4.25). This can be attributed to the loss of the template ions.

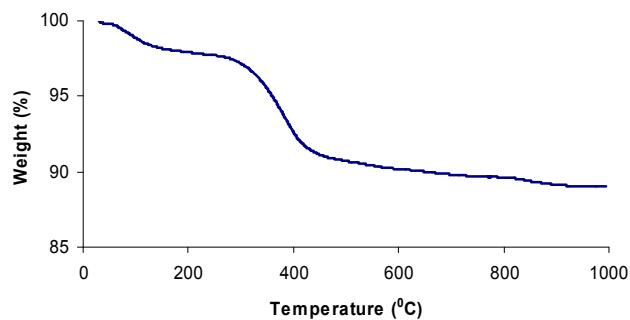


Figure 4.25: TGA experiment for SIZ-5

4.4.5: SIZ-6

An unusual, novel, layered structure type, SIZ-6, containing four, five and six coordinate aluminiums was synthesised and its structure solved using single crystal X-ray diffraction on Station 9.8 at the Synchrotron Radiation Source, Daresbury. Crystal data and structure refinement details for SIZ-6 are given in Table 4.4.

Table 4.4: Crystal data and structure refinement for SIZ-6.

Identification code	SIZ-6
Empirical formula	$\text{Al}_4(\text{OH})(\text{PO}_4)_3(\text{HPO}_4)(\text{H}_2\text{PO}_4)(\text{H}_2\text{O})_{0.2} \cdot \text{C}_6\text{H}_{11}\text{N}_2$
Formula weight	717.57
Temperature	150(2) K
Wavelength	0.6933 Å
Crystal system, space group	Orthorhombic, C mca
Unit cell dimensions	a=17.5472(14) Å alpha=90 ° b=18.0516(15) Å beta=90 ° c=35.560(3) Å gamma=90 °
Volume	11263.9(16) Å ³
Z, Calculated Density	16, 1.693 Mg/m ³
Absorption coefficient	0.443 mm ⁻¹
Crystal size	0.02 x 0.02 x 0.001 mm
Theta range for data collection	1.67 to 24.58 °
Limiting indices	-17<=h<=17, -18<=k<=18, -35<=l<=35
Reflections collected / unique	28464 / 3077 [R(int) = 0.0780]
Completeness to theta = 24.58 °	99.8 %
Refinement method	Full-matrix least-squares on F ²
Data / restraints / parameters	3077 / 0 / 297
Goodness-of-fit on F ²	1.114
Final R indices [I>2sigma(I)]	R1 = 0.0570, wR2 = 0.1365
R indices (all data)	R1 = 0.0717, wR2 = 0.1424
Largest diff. peak and hole	0.962 and -0.567 eÅ ⁻³

Unfortunately, the template could not be fully located using this data due to severe disorder (although ^{13}C MAS-NMR confirms it is present and intact). The final structure was refined using the data produced from the program Squeeze, contained within the PLATON¹³ package of crystallographic tools, which indicated that the total number of electrons unaccounted for by the $\text{Al}_4(\text{OH})(\text{PO}_4)_3(\text{HPO}_4)(\text{H}_2\text{PO}_4)(\text{H}_2\text{O})_{0.2}$ unit is approximately 58.8, which compares extremely well with the 61 electrons required by one 1-ethyl-3-methylimidazolium cation.

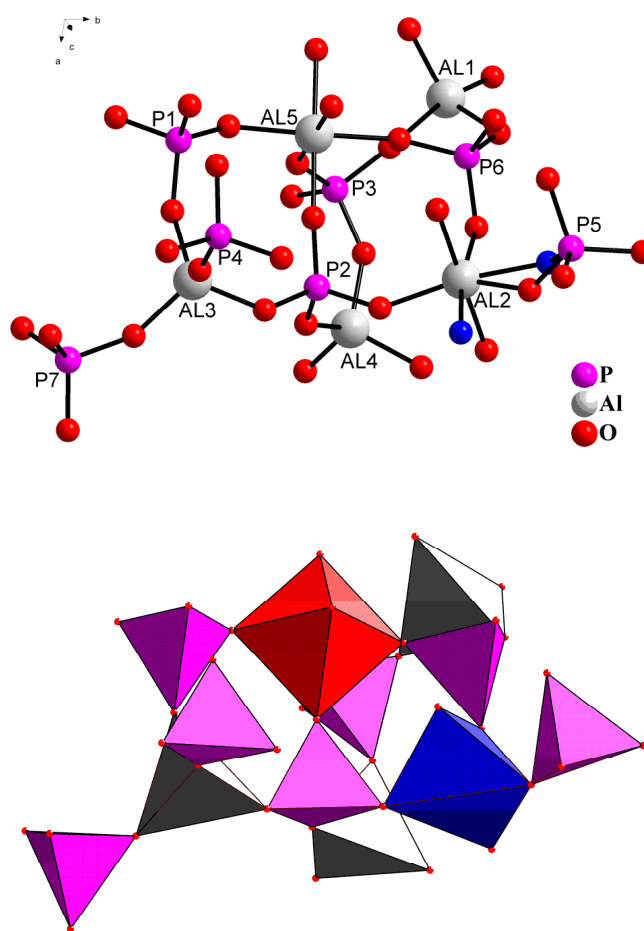


Figure 4.26: (Top) The asymmetric unit of SIZ-6 including the symmetry equivalent oxygen atoms to complete the coordination spheres. The minor atoms of the disorder present around Al2 are shown in blue. (Bottom) Polyhedral representation of the asymmetric unit showing three tetrahedral (grey), one octahedral (red) and one pentacoordinate (blue) aluminium (excluding minor component).

Figure 4.26 shows the asymmetric unit of SIZ-6 which consists of seven independent phosphorus and five aluminium atoms. All the phosphorus atoms show the expected tetrahedral coordination by oxygen. Three aluminium atoms have tetrahedral coordination by oxygen and one is in the centre of a regular octahedron. The remaining aluminium atom (Al2, Figure 4.26) is predominantly five coordinate, but the single crystal X-ray refinement revealed a Fourier peak that refined successfully as a partially occupied oxygen atom with an occupancy factor of 0.2. This indicates that about 80% of the asymmetric unit's Al2 is five coordinate but in the remainder it is six coordinate. The extra oxygen atom is most likely part of a water molecule remaining from the phosphoric acid source.

The bond distances and angles around the regular four and six coordinate aluminiums are as expected for such a structure but the coordination around the remaining aluminium is less regular. The disorder that is brought about by the presence or absence of the extra water molecule around Al2 leads to large anisotropic displacement parameters for two of the oxygens that form part of the coordination sphere of P5. The disorder affects the coordination sphere of P5 more than any other due to P5 having two hanging P-O bonds while the two other P-O bonds form part of an Al-O-P unit.

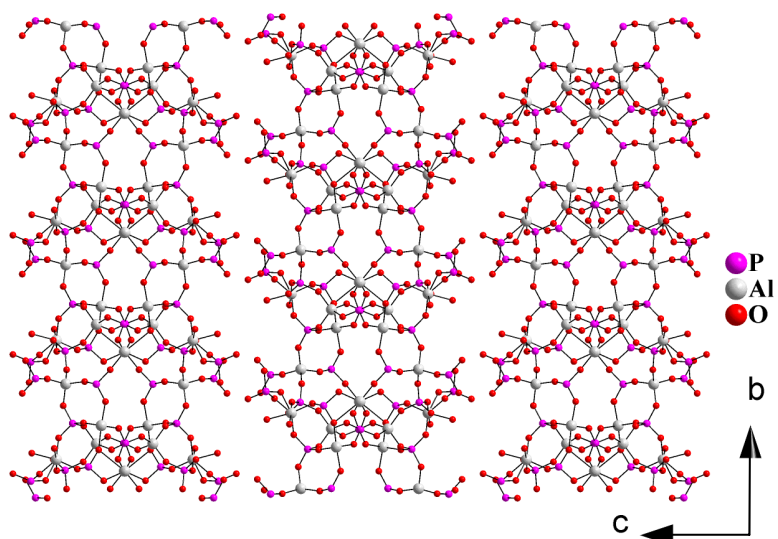


Figure 4.27: Ball and stick of SIZ-6 along the *a*-axis showing the thick aluminophosphate layers.

SIZ-6 comprises of 13.5 Å thick anionic aluminophosphate layers (Figure 4.27) as measured from the centres of the oxygens forming the surfaces of the layers. The layers consist of rings containing four, six and eight nodes (aluminium or phosphorus atoms). The eight-ring windows (Figure 4.28) are large enough to make the layers potentially porous to small molecules. The layers are held together *via* some relatively strong hydrogen bonding. This occurs because the H_2PO_4 groups, one from each adjacent layer, form dimeric units with O-O distances across the hydrogen bond of 2.441 Å.

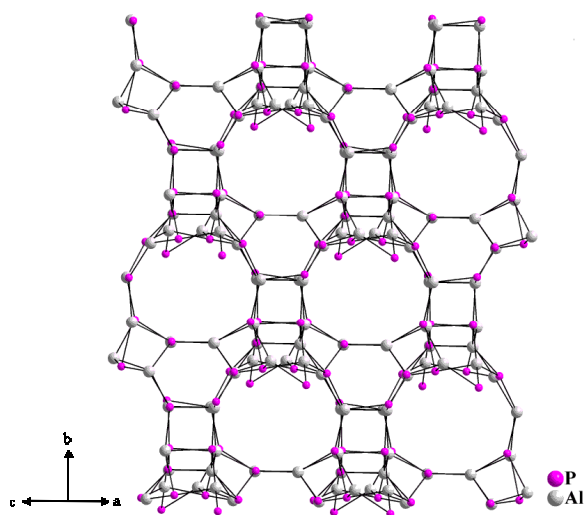


Figure 4.28: A view of a single layer showing the 8-ring windows. All oxygens are omitted for clarity.

The template could not be located by the single crystal analysis due to a high level of disorder between the aluminophosphate layers. It can clearly be seen however, from the ^{13}C MAS-NMR (Figure 4.29), that there are five distinct resonances in the expected regions to confirm the presence of the intact 1-ethyl-3-methylimidazolium template between the aluminophosphate layers.

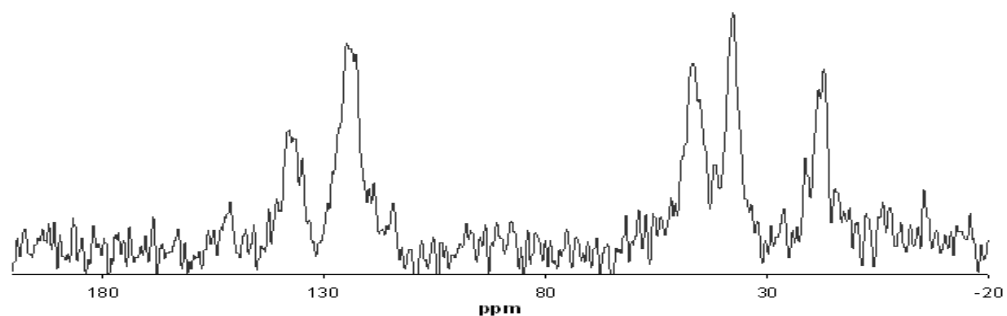


Figure 4.29: ^{13}C MAS-NMR of SIZ-6.

The ^{31}P MAS-NMR (Figure 4.30a) shows at least four resolved sites in a broad envelope between -6.6 and -34.4 ppm. The ^{27}Al MAS-NMR (Figure 4.30b) shows the octahedral coordination at -23.6 ppm, the tetrahedral coordination at 38.9 ppm and the five coordinate aluminium at 18.9 ppm.²¹

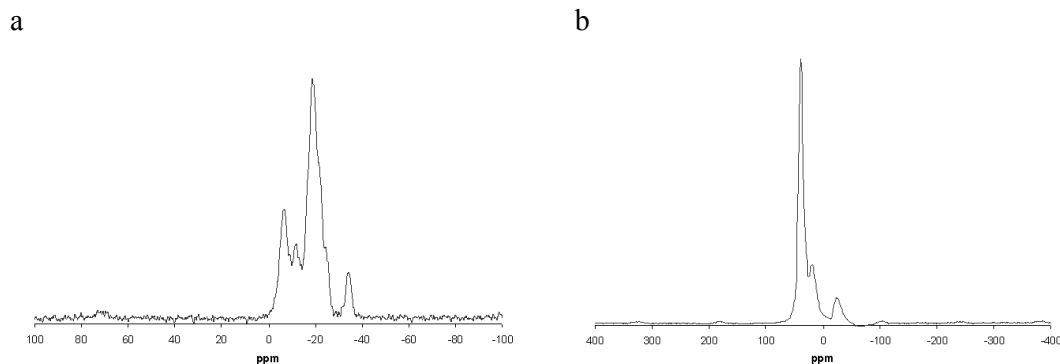


Figure 4.30: a = ^{31}P , b = ^{27}Al MAS-NMR for SIZ-6

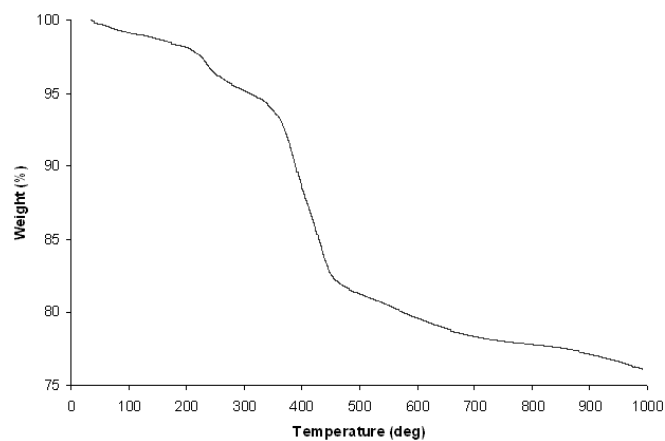


Figure 4.31: TGA experiment for SIZ-6

The TGA analysis (Figure 4.31) shows an initial mass loss of about 3.6 % between 200 and 300 °C which can be attributed to the water lost from condensation of the hanging P-OH bonds and the small amount of water bound to the aluminium in the sample (calc. ~3.0 %). The second mass loss between 350 and 450 °C of 16.3 % can be attributed to the loss of 1 mole of 1-ethyl-3-methylimidazolium per $\text{Al}_4(\text{OH})(\text{PO}_4)_3(\text{HPO}_4)(\text{H}_2\text{PO}_4)$ formula unit (calc. 15.5 %). Unfortunately the material breaks down after the condensation of the phosphate groups takes place.

4.5: Discussion and Conclusion

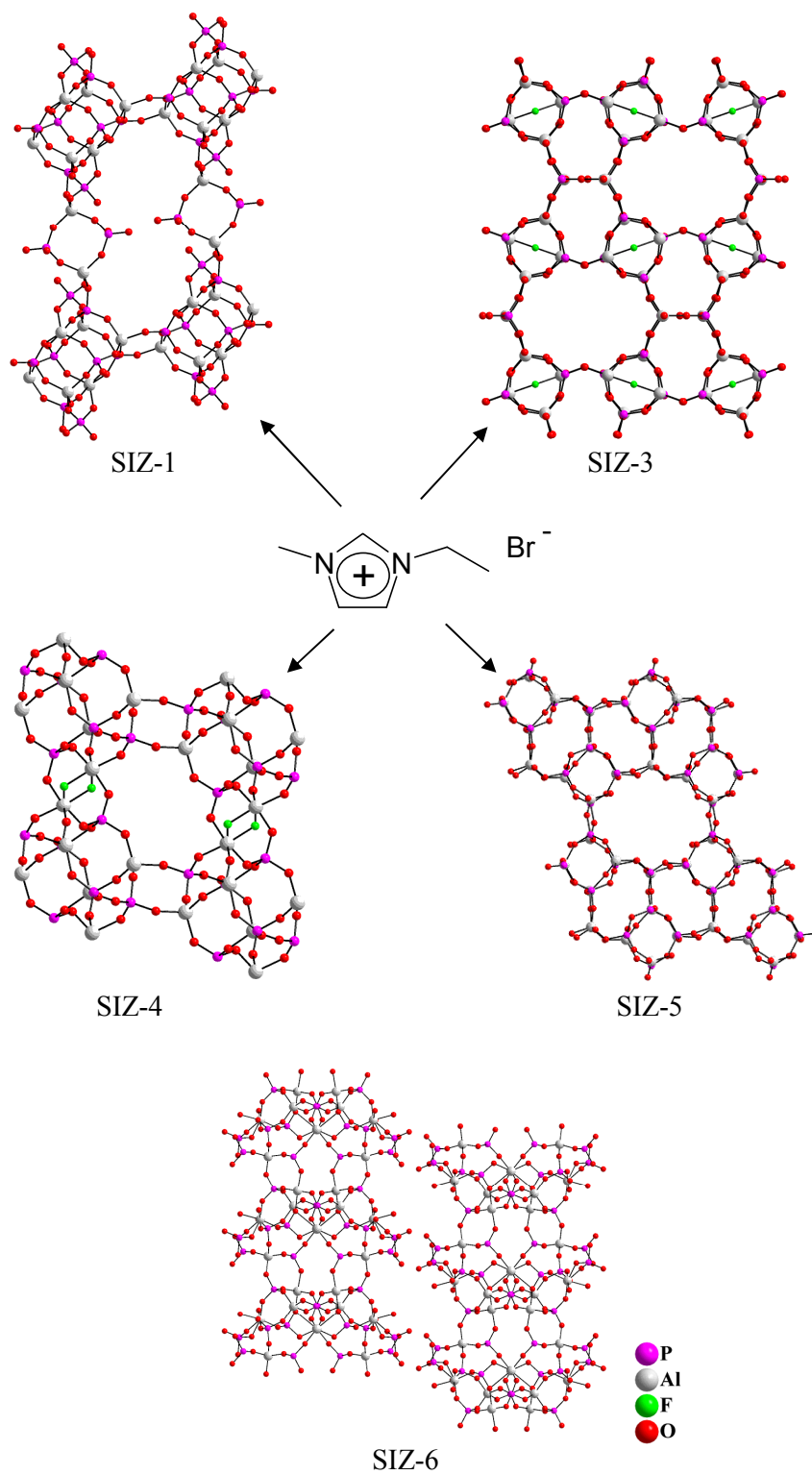


Figure 4.32: The four 3-dimensional aluminophosphates and the one layered aluminophosphate synthesised using 1-ethyl-3-methylimidazolium bromide as solvent and template.

Figure 4.32 shows the five structures synthesised ionothermally using 1-ethyl-3-methylimidazolium bromide as solvent and template. Ionic liquids have negligible vapour pressure and synthetic procedures can be carried out in open vessels (for SIZ-3 and SIZ-4) avoiding the high autogenous pressures (up to 15 atm at 200 °C) and associated safety concerns that accompany hydrothermal synthesis in sealed autoclaves. The ionic liquids can be recycled for further use.

Potentially the most important feature of this ionothermal synthesis mechanism is the removal of the competition between template-framework and solvent-framework interaction that is present in hydrothermal preparations. The structure directing properties of templates are often not as specific as we would like, but in a system where an ionic liquid is both solvent and template the negatively charged atoms at the surface of a growing framework will always be interacting primarily with the templating cation rather than with a mixture of template and solvent.

1-ethyl-3-methylimidazolium bromide is hygroscopic and it is almost impossible to dry it completely, hence there is always some water present in ionothermal synthesis. This is probably required to act as a catalyst for zeolite formation. Cammarata *et al.*²² and Hanke *et al.*²³ have carried out infrared and molecular dynamic studies which indicate that small amounts of water (molar ratios less than 10 %) are present as isolated molecules that interact very strongly with the anions of the ionic liquid. The interaction of water with the anions may be so strong that it is effectively shielded from interacting with the Al- and P- containing ions that are solubilised by the cations of the ionic liquid. The addition of further water to the reaction, so that it resulted in a water to ionic liquid molar ratio of 1 to 1 led to the synthesis of the dense AlPO phase, Berlinite (Al(PO₄)). If water is present in equimolar amounts, the ionic liquid rearranges into a different

internal order, into which more water molecules may be accommodated,²⁴ hence the properties of the ionic liquid are changed and it is no longer a true ionic liquid but rather a mixture of ionic liquid and water. The interactions between Al- and P- containing ions with the cations of the ionic liquid are likely to diminish due to the presence of water, resulting in the dense Berlinite phase.

Ionothermal synthesis allows a great deal of control over the mineralisers that are present in the solvent. Mineralisers, such as fluoride help solubilise the inorganic components and catalyse T-O-T bond formation (where T are the tetrahedral framework atoms). The ionic liquids are good solvents on their own, but adding fluoride increases their solvating power and can change the types of framework that are formed.

The ionic liquids solubilise the starting materials almost completely at the reaction temperatures, indicating that the synthesis mechanism is a crystallisation from solution rather than a solid-to-solid-transformation. The dependence of the products on water also gives some clues as to the mechanism of the reaction. With little water and no HF to act as mineralisers interrupted framework structures (SIZ-1 and SIZ-6) can be targeted. On addition of HF or water, condensed structures (SIZ-3, SIZ-4 and SIZ-5) are formed with no hanging bonds, hence there is the possibility of selectively targeting interrupted frameworks or fully condensed zeotypes.

4.6: References

1. P. Wasserscheid and W. Keim, *Angew. Chem., Int. Ed. Eng.*, 2000, **39**, 3773
2. C.J. Adams, A.E. Bradley and K.R. Seddon, *Aust. J. Chem.*, 2001, **54**, 679
3. S.I. Zones, *Zeolites*, 1989, **9**, 458
4. A. Elaiwi, P.B. Hitchcock, K.R. Seddon, N. Srinivasan, Y.M. Tan, T. Welton and J.A. Zora, *J. Chem. Soc., Dalton Trans.*, 1995, 3467
5. P. Wasserscheid and T. Welton, 'Ionic Liquids In Synthesis', Wiley-VCH, 2003, Ch. 2
6. P. Bonhote, A.P. Dias, M. Armand, N. Papageorgiou, K. Kalyanasundaram and M. Gratzel, *Inorg. Chem.*, 1996, **37**, 166
7. SHELXL97, Program for Crystal Structure Analysis (Release 97-2). G.M. Sheldrick, Institut für Anorganische Chemie der Universität, Tammanstrasse 4, D-3400 Göttingen, Germany, 1998
8. J. W. Richardson, J.J. Pluth and J.V. Smith, *Acta Crystallogr., Sect. B: Strut. Sci.*, 1988, **44**, 367
9. A.S. Araujo, V.J. Fernandes, A.O.S. Silva and J.G. Diniz, *J. Therm. Anal.*, 1999, **56**, 151
10. S.T. Wilson, B.M. Lok, C.A. Messina, T.R. Cannan and E.M. Flanigen, *J. Am. Chem. Soc.*, 1982, **104**, 1146
11. H. Qisheng, F. Shouhua and X. Ruren, *J. Chem. Soc., Chem. Commun.*, 1988, 1486
12. R. Bandyopadhyay, M. Bandyopadhyay, Y. Kubota and Y. Sugi, *J. Porous Mat.*, 2002, **9**, 83
13. A. L. Spek, *J. Appl. Crystallogr.*, 2003, **36**, 7
14. F. Guth, University de Haute Alasce, Mullhouse, France, 1989
15. A. Simmen, ETH, Zurich, Switzerland, 1992

16. M.M. Harding and B.M. Kariuki, *Acta Crystallogr. Sect. C: Cryst Struct. Commun.*, 1994, **50**, 852
17. S. Oliver, A. Kuperman, A. Lough and G.A. Ozin, *J. Mater. Chem.*, 1997, **7**, 807
18. D. A. Lesch and S. T. Wilson, European Patent Application, 254 275, 1988
19. H.W. Clark, W.J. Rievert and M.M. Olken, *Microporous Mater.*, 1996, **6**, 115
20. R.M. Kirchner and J.M. Bennett, *Zeolites*, 1994, **14**, 523
21. R.E. Morris, A. Burton, L.M. Bull and S.I. Zones, *Chem. Mater*, 2004, **16**, 2844
22. L. Cammarata, S.G. Kazarian, P.A. Salter and T. Welton, *Phys. Chem. Chem. Phys.*, 2001, **3**, 5192
23. C.G. Hanke and R.M. Lynden-Bell, *J. Phys. Chem. B*, 2003, **107**, 10873
24. K. Miki, P. Westh, K. Nishikawa and Y. Koga, *J. Phys. Chem. B*, 2005, **109**, 9014

5: 1-ethyl-3-methylimidazolium bromide as solvent and template in the synthesis of Co-AlPOs

5.1: Aims

This chapter describes the work carried out which aimed to investigate the incorporation of Co into the aluminophosphate zeotype frameworks using the ionothermal synthesis methodology previously described in Chapter 4. The addition of cobalt to an aluminophosphate structure leads to a charge imbalance in the framework hence producing sites which often have either acidic or redox properties. 1-ethyl-3-methylimidazolium bromide was used as both solvent and template in the reactions. Cobalt sources tested include cobalt acetate tetrahydrate, cobalt(II) hydroxide, cobalt(II) chloride, cobalt(II) bromide and cobalt(II) sulfate heptahydrate.

5.2: Introduction – Addition of cobalt to aluminophosphates.

The alternating Al^{3+} and P^{5+} zeolite frameworks of the type $\text{Al}(\text{PO}_4)$ i.e. Al:P ratio 1:1 are chemically inert.¹ If however a charge imbalance occurs in the framework by the incorporation of a heteroatom with similar size and coordination but a different charge, the framework may become chemically active. Such a modification to the framework charge often leads to the generation of sites which have either acidic or redox properties which are of particular interest for the design of new catalysts.² The economic importance for industry of synthesising new and improved catalysts has led to continuous attempts to extend the range of catalytically active microporous materials available.³ An example of the possible catalytic activity is the reported Co-AlPO and Mn-AlPO catalysts which act as regioselective heterogeneous catalysts for the oxidation

of linear alkanes. This process uses molecular oxygen as the reagent rather than the more expensive sacrificial oxidants such as organic hydroperoxides.⁴

The degree of incorporation of heteroatoms into an AIPO structure is dependent upon the particular structure,⁵ however it is possible to have some control by varying the charge and geometry of the structure-directing molecules.^{6,7} Examples of transition metals incorporated into the AIPO family of molecular sieves include Ti, V, Cr, Mn, Fe, Cu, Co, Zn.⁵ The Co-AIPO system however is of particular interest due to the large concentration of Co^{2+} which can be incorporated into the framework to give structures with a relatively high framework charge density. A particular example of this is the UCSB-6Co where about 45 % of the Al^{3+} sites are replaced by Co^{2+} .⁸ UCSB-6Co has the highest framework transition-metal concentration of any large-pore zeotype structure.

In general, for Co-AIPOs, tetrahedral Co and Al atoms occupy the same crystallographic sites, alternating with the P sites. Single Crystal X-Ray Diffraction (SCXRD) data can be used to calculate the $\text{Co}^{2+}/\text{Al}^{3+}$ ratio for each individual tetrahedral site. Since the X-ray scattering factors of cobalt and aluminium are significantly different it is possible to calculate the $\text{Co}^{2+}/\text{Al}^{3+}$ ratio from the refinement of the occupancy factors. However an often more reliable but indirect method of calculating the $\text{Co}^{2+}/\text{Al}^{3+}$ ratio of individual tetrahedral sites has been proposed by Feng *et al.*⁶ using the metal-oxygen bond distances.

Co-O and Al-O bond distance are approximately 1.93 Å and 1.74 Å respectively. A bond distance closer to 1.93 Å would therefore indicate the dominance of cobalt on that site and vice versa. Feng *et al.*⁶ examined the relationship between the occupancy factor

and the average bond lengths for each Co (Al) site. The following equation was deduced for well-refined structures:

$$\text{bond length} = 1.74 + 0.19 \times \text{occupancy of cobalt}$$

This relationship is more reliable than the refinement of the occupancy factors due to occupancy factors being affected by other aspects such as thermal parameters and disorder.

5.3: Experimental - Ionothermal synthesis of Co-AlPOs

The synthesis of zeolites, is in general, very sensitive to the various reaction conditions including cation source, pH, water content, organic template, solvent, time, temperature, aging and stirring. The addition of a cobalt source will, most certainly alter several of these conditions. Initial reactions were carried out using commercially available cobalt sulphate heptahydrate, cobalt bromide and cobalt hydroxide. Cobalt hydroxide produced the most promising initial results hence it was used to carry out further investigations into the ionothermal synthesis of Co-AlPOs.

5.3.1: Synthesis of Co-AlPOs

A typical synthesis procedure was as follows: A Teflon™ lined autoclave (volume 23 ml) was charged with 0.172 g H₃PO₄ (85 wt% in H₂O, Aldrich), 0.107 g Al[OCH(CH₃)₂]₃ (Aldrich), 0.079 g Co(OH)₂ (Avocado), 4.00 g 1-ethyl-3-methylimidazolium bromide (IL) (synthesis previously reported in Chapter 4.2) and 0.015 g HF (48 wt% in H₂O, Aldrich). Initial molar ratios for Al[OCH(CH₃)₂]₃ : H₃PO₄ : HF : IL : Co(OH)₂ : H₂O were 1 : 2.9 : 0.69 : 40 : 1.6 : 3.6. The stainless steel autoclave was heated to 170°C for 3 days. After cooling the autoclave to room temperature the product was suspended in distilled water, sonicated, filtered by suction and washed with acetone. The product was a blue, crystalline solid and contained three phases, SIZ-7 (minor), SIZ-8 (major) and SIZ-9 (minor), as a physical mixture.

5.3.2: Experimental Details

Structural Characterisation using X-ray diffraction

Single crystal X-ray diffraction data for SIZ-7, SIZ-8 and SIZ-9 were collected on station 9.8 at the Synchrotron Radiation Source (SRS), Daresbury Laboratories, Cheshire. The structures were solved using standard direct methods and refined using least-squares minimisation techniques against F^2 . CIF files are available on the accompanying CD for all structures.

Elemental analysis using a scanning electron microscope

A Jeol JSM-5600 scanning electron microscope (SEM) integrated with an Energy Dispersive X-rays (EDX) system for analytical elemental analysis was used to confirm the presence of cobalt in isolated crystals of SIZ-7, SIZ-8 and SIZ-9.

5.4: Results

5.4.1: SIZ-7

A novel Co-AIPO zeolite framework structure, SIZ-7, was synthesised and its structure solved using single crystal X-ray diffraction on Station 9.8 at the Synchrotron Radiation Source, Daresbury. Crystal data and structure refinement details for SIZ-7 are given in Table 5.1.

Table 5.1: Crystal data and structure refinement for SIZ-7

Identification code	SIZ-7
Empirical formula	$\text{Co}_{13.44}\text{Al}_{18.56}(\text{PO}_4)_{32}$
Formula weight	4331.81
Temperature	150(2) K
Wavelength	0.6910 Å
Crystal system, space group	Monoclinic, C 2/c
Unit cell dimensions	a = 10.2959(4) Å alpha = 90 ° b = 14.3715(5) Å beta = 91.0940 (10) ° c = 28.5990(10) Å gamma = 90 °
Volume	4231.0(3) Å ³
Z, Calculated density	1, 1.700 Mg/m ³
Absorption coefficient	1.561 mm ⁻¹
F(000)	2108
Crystal size	0.05 x 0.05 x 0.04 mm
Theta range for data collection	1.38 to 29.99 °
Limiting indices	-14<=h<=14, -20<=k<=20, -41<=l<=41
Reflections collected / unique	24429 / 6637 [R(int) = 0.0340]
Completeness to theta = 29.99 °	99.00%
Refinement method	Full-matrix least-squares on F ²
Data / restraints / parameters	6637 / 0 / 217
Goodness-of-fit on F ²	1.063
Final R indices [I>2sigma(I)]	R1 = 0.0547, wR2 = 0.1705
R indices (all data)	R1 = 0.0668, wR2 = 0.1775
Largest diff. peak and hole	1.140 and -0.881 e Å ⁻³

Unfortunately, the template could not be fully located and identified using this data due to severe disorder. The final structure was run through the program Squeeze, contained within the PLATON⁹ package of crystallographic tools, to remove the scattering caused by the residual electron density in the ‘solvent accessible volume’ of the structure. The final refinement was carried out on this data.

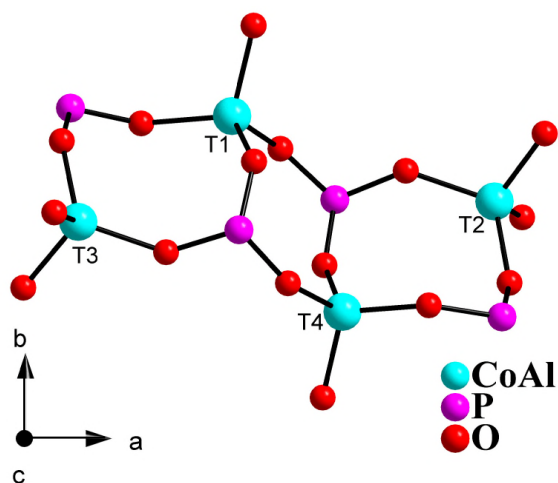


Figure 5.1: Asymmetric unit of SIZ-7

The asymmetric unit of SIZ-7 (Figure 5.1) consists of four cobalt/aluminium sites, four phosphorus and sixteen oxygen. The refined cobalt/aluminium bond distances indicate that there is some preferential ordering of the cobalt ions onto the T1 site. As discussed in section 5.1, an observed interatomic distance of nearer to 1.93 Å for the Co/Al disordered T site indicates a site predominantly occupied by cobalt. In the case of the T1 site (Figure 5.1) the T-O bond distances range from 1.856(4) Å to 1.891(4) Å with an average of 1.877 Å. Using the equation derived by Feng *et al.*:⁶

$$\text{occupancy of cobalt} = (\text{bond length} - 1.74) / 0.19$$

This indicates that the T1 site is approximately 72% occupied by cobalt. In contrast, the observed interatomic distances around T2 (1.798(4) to 1.833(3) Å, average = 1.814 Å), T3 (1.795(3) to 1.823(3) Å, average = 1.810 Å) and T4 (1.767(4) to 1.788(3) Å, average

($d = 1.778 \text{ \AA}$) indicate lower Co occupancies of $\sim 39\%$, 37% and 20% respectively. In the final cycle of least squares refinement the relative Co/Al occupancies were fixed at these levels. This gives an empirical formula of $\text{Co}_{13.44}\text{Al}_{18.56}(\text{PO}_4)_{32}$.

SIZ-7 is a novel framework structure which joins a family of related zeolites that includes the PHI¹⁰, GIS¹¹ and MER⁶ structure types. SIZ-7 can be described as consisting of double-crankshaft chains (Figure 5.2) which run parallel to the crystallographic a -axis. This same double crankshaft chain is found in the frameworks of PHI, GIS and MER and it is the manner in which these chains are connected which defines the type of framework formed (Figure 5.3).

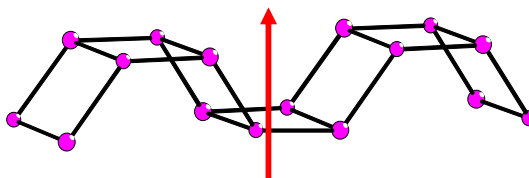


Figure 5.2: The double crankshaft chain present in SIZ-7, PHI, MER and GIS zeolite frameworks.

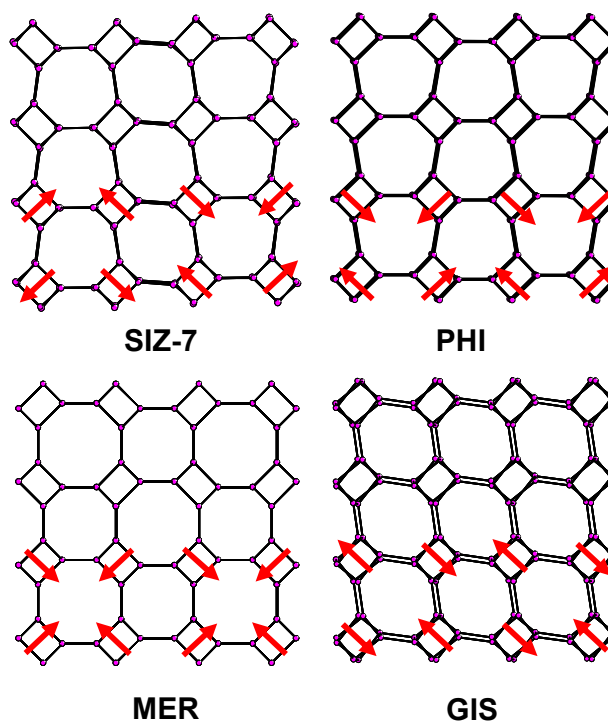


Figure 5.3: The crankshaft chains run into the plane of the paper and the red arrows indicate the relative orientations of the chains in the various structures. For clarity only the tetrahedral nodes in the structures are shown.

The way the double crankshaft chains are connected in SIZ-7 leads to a one-dimensional small pore zeolite structure with windows into the pores delineated by rings containing eight tetrahedral atoms (known as 8-ring windows). The repeat distance in the a -direction is 10.2959 (4) Å and equals one repeat unit of the double crankshaft chain. These chains are linked *via* four rings in both the b - and c - directions to form the 8-ring windows. The relative orientation of neighbouring chains means that there are two types of 8-ring channels. The two different windows are of similar size (3.66×3.26 Å and 3.40×3.52 Å) but are different in shape (this is most clearly seen in Figure 5.4). In the b -direction the same type of 8-ring (3.66×3.26 Å) channel is repeated, leading to a repeat unit in this direction of 14.3715 (5) Å while in the c -direction the two types of channel alternate, leading to an approximate doubling of the unit cell dimension in this direction to 28.599 (1) Å.

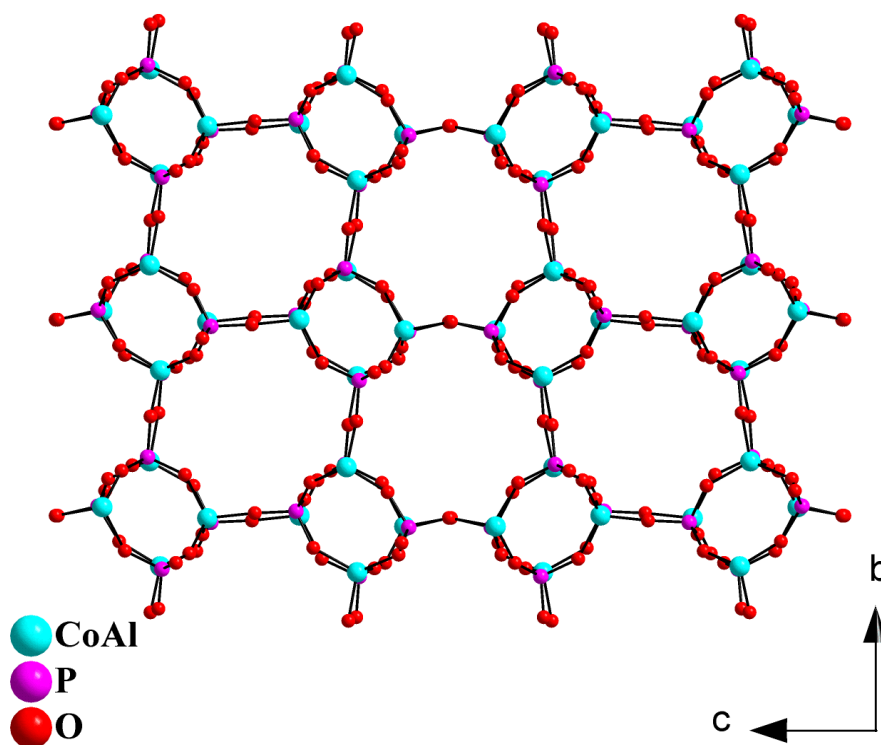


Figure 5.4: A view of SIZ-7 parallel to the a -axis showing the two different 8-ring windows.

5.4.2: SIZ-8

SIZ-8 has the same framework topology as AlPO-18 (AEI). This structure has been previously synthesised hydrothermally with and without cobalt incorporated into the structure.¹²⁻¹⁴ Many catalytic studies have been carried out for Co-AEI and it has been found to have interesting redox and acid properties.¹² Co-AEI has also been used as a selective catalyst in the conversion of methanol to light olefins¹⁵ and in the liquid phase selective oxidation of linear alkanes by molecular oxygen.⁴ Crystal data and structure refinement details of SIZ-8 are given in Table 5.2.

Table 5.2: Crystal data and structure refinement for SIZ-8

Identification code	SIZ-8
Empirical formula	Co _{5.84} Al _{18.16} (PO ₄) ₂₄
Formula weight	3113.39
Temperature	150(2) K
Wavelength	0.6910 Å
Crystal system, space group	Orthorhombic, C 2/c
Unit cell dimensions	a = 13.9992(18) Å alpha = 90 ° b = 12.7628(17) Å beta = 90 ° c = 18.680(3) Å gamma = 90 °
Volume	3337.5(8) Å ³
Z, Calculated density	1, 1.549 Mg/m ³
Absorption coefficient	1.049 mm ⁻¹
F(000)	1522
Crystal size	0.07 x 0.07 x 0.05 mm
Theta range for data collection	2.35 to 30.78 °
Limiting indices	-20 ≤ h ≤ 20, -18 ≤ k ≤ 18, -27 ≤ l ≤ 26
Reflections collected / unique	19156 / 5386 [R(int) = 0.0478]
Completeness to theta = 33.09 °	98.20 %
Refinement method	Full-matrix least-squares on F ²
Data / restraints / parameters	5386 / 0 / 163
Goodness-of-fit on F ²	1.088
Final R indices [I > 2σ(I)]	R1 = 0.0445, wR2 = 0.1381
R indices (all data)	R1 = 0.0543, wR2 = 0.1427
Largest diff. peak and hole	0.788 and -0.676 e. Å ⁻³

Unfortunately, the template was severely disordered; however it was still possible to identify, before the final refinement, several 5-membered rings, presumably from the 1-ethyl-3-methylimidazolium cation. The final structure was refined using the data produced from the program Squeeze contained within the PLATON⁹ package of crystallographic tools.

SIZ-7 and SIZ-9 are isolated crystals. This means that the bulk of the sample is SIZ-8. The sample was dissolved in an approximately 3M HCl solution. This dissolves the Co-AlPO framework, leaving any organic molecules present intact in solution. A ¹H-NMR (D₂O) was run and this confirmed the major organic product present to be the 1-ethyl-3-methylimidazolium cation (see section 4.3.1 for full NMR data). Whilst this confirms the presence of the 1-ethyl-3-methylimidazolium cation, it does not unambiguously prove that it is present as a template.

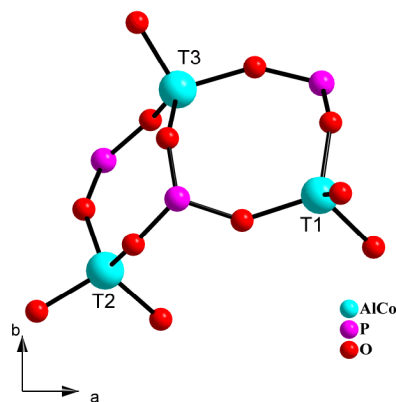


Figure 5.5: Asymmetric unit of SIZ-8

The asymmetric unit of SIZ-8 (Figure 5.5) consists of three shared cobalt/aluminium sites, three phosphorus and twelve oxygen. The refined cobalt/aluminium bond distances gave Co occupancy for T1, T2 and T3 as about 28%, 28% and 17% respectively. In the final cycle of least squares refinement the relative Co/Al occupancies were fixed at these levels. This gives an empirical formula of $\text{Co}_{5.84}\text{Al}_{18.16}(\text{PO}_4)_{24}$.

The SIZ-8 AEI framework consists of double six-membered rings (D6Rs) of alternating cobalt/aluminium tetrahedral sites and phosphorous tetrahedral. The framework can be described as a stacking of layers of tilted D6R linked through four-membered rings to produce a three-dimensional pore structure consisting of pear-shaped cages (made from six 8-rings and twelve 4-rings) and a three-dimensional eight-ring channel system with a slight elliptical cross section. The SIZ-8 AEI structure is related to the SIZ-4 CHA structure. In the AEI structure the tilted D6R layers have an alternating direction of tilt whereas in the CHA structure the D6R layers all tilt in the same direction throughout the structure (Figure 5.6).

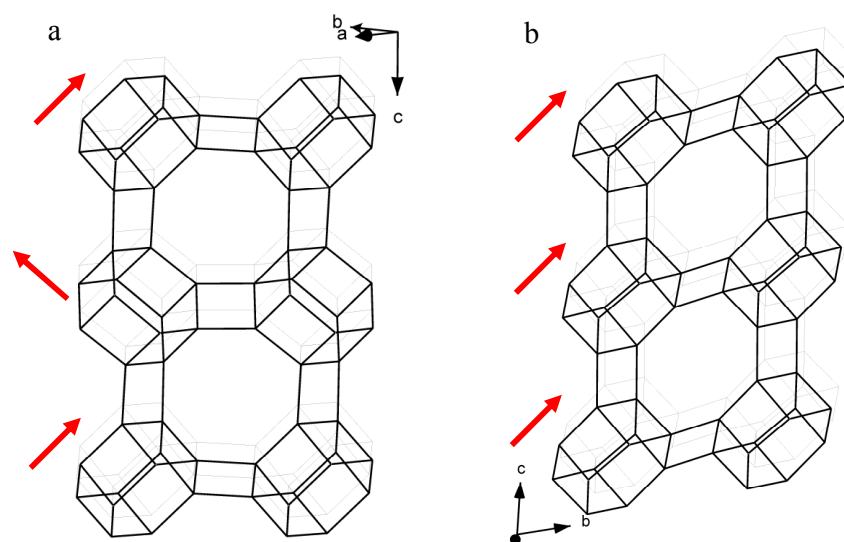


Figure 5.6: The framework topology of: (a) AEI and (b) CHA. The red arrows indicate the relative orientation of the D6R layers. The oxygen atoms are omitted for clarity.

The close structural relation between the SIZ-8 AEI structure and the SIZ-4 CHA structure could explain why, in some syntheses, the CHA structure forms instead of the AEI framework. A small alteration in the experimental conditions, such as mixing of starting materials can lead to the preferential formation of the CHA structure over the AEI structure. It must also be noted (as previously reported in section 4.4.3) that the CHA structure appears to be a default structure, and that once formed in a Teflon™ liner, keeps forming due to possible seeding effects from CHA trapped in the Teflon™.

5.4.3: SIZ-9

SIZ-9 has the same framework topology as naturally occurring sodalite (SOD). Its framework topology was identified and solved using single crystal X-ray diffraction on Station 9.8 at the Synchrotron Radiation Source, Daresbury. Unit cell data for SIZ-9 is as follows; cubic, P-43n, $a = 8.934(6) \text{ \AA}$. SIZ-9 was found to be analogous to the sodalite Co-AlPO framework previously synthesised and characterised, reporting a Co:Al ratio of 0.5:2.⁶

SIZ-9 is made up of sodalite cages, also known as β -cages, which are truncated octahedra made up of six 4-membered rings and eight 6-membered rings. These cages are joined together by the direct fusing of the 4-membered rings¹⁶ to give the SIZ-9 SOD structure

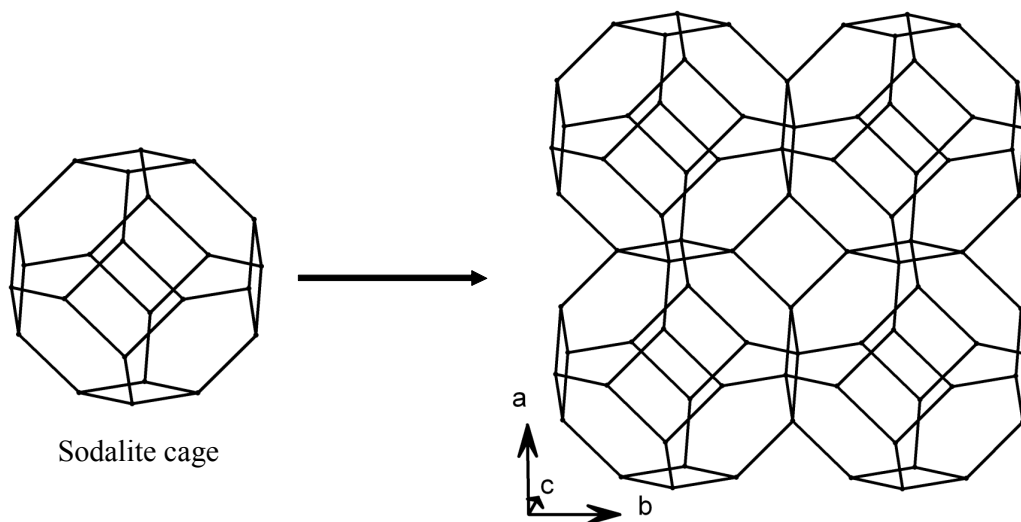


Figure 5.7: The sodalite cages join together by the direct fusing of the 4-membered rings to give the SIZ-9 SOD structure. The oxygen atoms are omitted for clarity.

5.5: Discussion and Conclusion

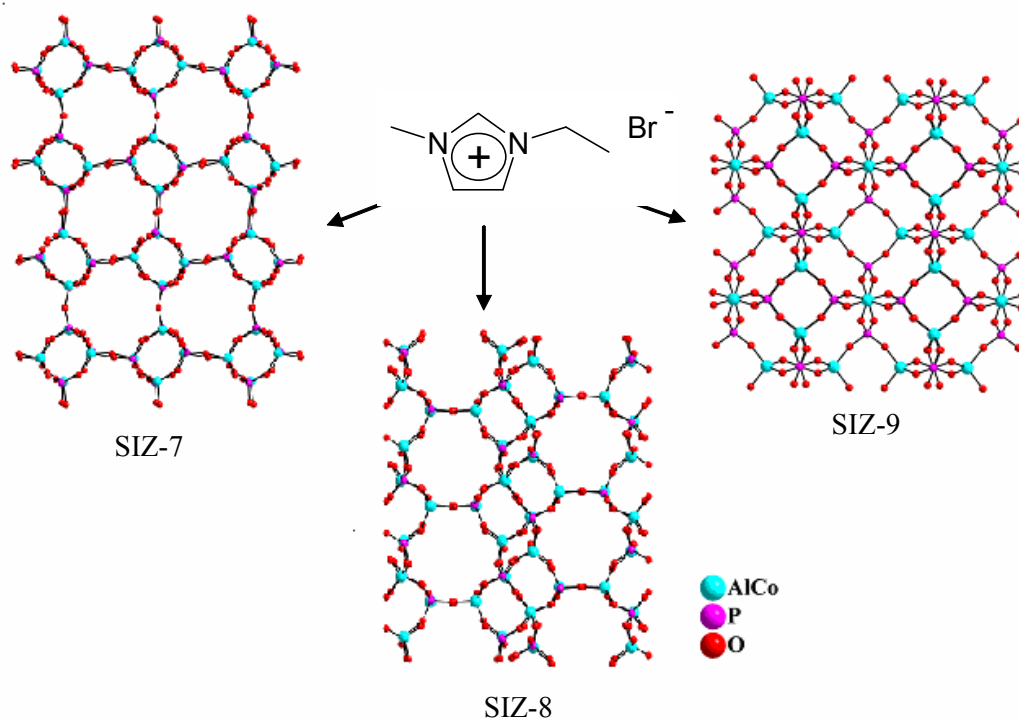


Figure 5.8: The three 3-dimensional Co-AIPO structures synthesised using 1-ethyl-3-methylimidazolium bromide as the solvent.

Figure 5.8 shows the three Co-AIPO structures synthesised ionothermally using the ionic liquid 1-ethyl-3-methylimidazolium bromide as the solvent. SIZ-7, 8 and 9 all have different framework topologies to those reported for the AlPOs in Chapter 4. This indicates that the cobalt hydroxide added to the synthesis mixture may contribute an additional structure directing effect on top of that supplied by the organic cation of the ionic liquid.

Zeolite synthesis, is in general, very sensitive to the various reaction conditions including cation source, pH, water content, organic template, solvent, time, temperature, aging and stirring. The addition of cobalt hydroxide will most definitely have altered the pH and water content. The hydroxide may react with the acidic hydrogen on the imidazolium ring between the two nitrogens to produce water. Subtle changes in

reaction conditions can alter the product selectivity markedly. This makes it quite difficult to prepare pure phase samples.

The synthesis of the three Co-AIPOs is an indication that the ionothermal synthesis method is suitable for the preparation of transition metal-functionalised frameworks that may be useful for applications such as catalysis or gas adsorption. The preparation of the novel framework topology, SIZ-7, is a further indication of the potential of ionothermal synthesis in the production of new zeotype materials.

5.6: References

1. F. Corà, M. Alfredsson, C.M. Barker, R.G. Bell, M.D. Foster, I. Saadoune, A.Simperler and C.R.A. Catlow, *J. Solid State Chem.*, 2003, **176**, 49
2. M. Hartmann and L. Kevan, *Chem. Rev.*, 1999, **99**, 635
3. F. Corà, C.R.A. Catlow and A.D'Ercole, *J. Mol. Catal. A: Chem.*, 2001, **166**, 87
4. J.M. Thomas, R. Raja, G. Sankar and R.G. Bell, *Nature*, 1999, **398**, 227
5. A. Ristic, N.N. Tutar, I. Arcon, F. Thibault-Starzyk, D. Hanzel, J. Czyzniewska and V. Kaucic, *Microporous Mesoporous Mater.*, 2002, **56**, 303
6. P.Y. Feng, X.H. Bu and G.D. Stucky, *Nature*, 1997, **388**, 735
7. G. Sankar, J.K. Wyles and C.R.A. Catlow, *Top. Catal.*, 2003, **24**, 173
8. X. Bu, P. Feng and G.D. Stucky, *Science*, 1997, **278**, 2080
9. A.L. Spek, *J. Appl. Crystallogr.*, 2003, **36**, 7
10. H. Steinfink, *Acta Crystallogr.*, 1962, **15**, 644
11. K. Fischer and V. Schramm, *Adv. Chem. Ser.*, 1971, **101**, 250
12. P.A. Barrett, G.Sankar, C.R.A. Catlow and J.M. Thomas, *J. Phys. Chem.*, 1996, **100**, 8977
13. P. Concepcion, T. Blasco, J.M.L. Nieto, A. Vidal-Moya and A. Martinez-Arias, *Microporous Mesoporous Mater.*, 2004, **67**, 215
14. A. Simmen, L.B. McCusker, C. Baerlocher and W.M. Meier, *Zeolites*, 1991, **11**, 654
15. J. Chen and J. M. Thomas, *Chem. Commun.*, 1994, 603
16. S. Bachmann and J. Ch. Buih, *Microporous. Mater.*, 1999, **28**, 35

6: Variations on the imidazolium cation used as solvent and template in AlPO synthesis.

6.1: Aims

This chapter describes the work carried out which aimed to investigate the effect on the AlPO zeolite analogues produced during ionothermal synthesis when small changes to the imidazolium cation were introduced such as increased chain length and chain branching in the 3-position of the imidazolium ring.

It was hoped that small changes in the imidazolium cation would lead to the production of different AlPO framework topologies as demonstrated by Zones in the hydrothermal synthesis of high-silicate zeolites.¹ Zones reported the use of four quaternized imidazole derivatives (Chapter 4.2, Figure 4.2) as structure-directing organic cations. Each produced a different zeolite framework giving very good templating effects with close correlation between the imidazole structure and the zeolite pore size.

6.2: Introduction – Imidazolium cation variations.

As previously discussed in Chapter 1.2.3, by varying the anion and cation, the properties of an ionic liquid, including viscosity, solvating ability, catalytic activity, and melting point can be altered dramatically.^{2, 3} In this section we discuss specifically the effect of altering the alkyl chain in the 1-alkyl-3-methylimidazolium cation.⁴

Altering the length of the alkyl chain can produce major changes in the melting point and the tendency to form glasses rather than crystalline solids on cooling due to changes in the efficiency of ion packing. Recent studies have shown that, in general, increasing the alkyl chain length initially reduces the melting point of the ionic liquid, with a tendency towards glass formation for alkyl chain lengths of 4-8 carbons. On increasing the alkyl chain length further to > 8 carbons, the melting points of the salts start to increase again with increasing chain length.⁵

The initial decrease in melting point on increasing alkyl chain length can be attributed to the increased asymmetry of the cation. Asymmetry opposes strong charge ordering⁶ and causes a distortion from the ideal close-packing of the ionic charges in the solid lattice hence resulting in the depression of melting point.⁷

On increasing the alkyl chain length to > 8 carbons, the attractive van der Waals interactions increase between the long hydrocarbon chains forming a bilayer lattice.⁸ This results in better packing efficiency hence an increase in melting point on increasing alkyl chain lengths of > 8 carbons.⁷

The effects of alkyl chain branching on ionic liquid melting points have been studied by Bonhôte *et al.*⁹ and Y. Chauvin *et al.*¹⁰ It was found that on increasing the alkyl chain branching at the imidazolium ring 3-position, the melting points increased. This reflects the changes in efficiency of the crystal packing as free-rotational volume decreases and atom density increases.¹¹

6.3: Experimental – Changing the imidazolium cation

6.3.1: Synthesis of 1-propyl-3-methylimidazolium bromide (PrMIBr)

Under inert atmosphere conditions, degassed propylbromide (114 g, 0.927 mol, Avocado) was added to the redistilled N-methyl imidazole (56.3 g, 0.686 mol, Aldrich), with constant stirring. This was refluxed at 45 °C for 3 hours then allowed to cool to room temperature. The oily product was washed three times with ethyl acetate and dried under vacuum at 50 °C for 10 hours to give PrMIBr as a colourless oil. The product was stored under an inert atmosphere. Yield 83 %. ¹H-NMR (D₂O): δ 0.87 (t, 3H, CH₃, *J* = 7.4 Hz), 1.78-1.91 (m, 2H, CH₂CH₃) 3.86 (s, 3H, NCH₃), 4.13 (t, 2H, NCH₂, *J* = 7.0 Hz), 7.42 (d, 2H, NC(*H*)C(*H*)N, *J* = 12.0 Hz), 10.14 (s, 1H, NC(*H*)N) ppm. ¹³C-NMR (D₂O): δ 9.75 (s, CH₃), 22.29 (s, CH₂), 35.56 (s, NCH₃), 52.03 (s, NCH₂), 122.14, 123.42 (2 x s, NCCN), 135.83 (s, NCN) ppm. NMR comparable with literature values.^{12, 13}

6.3.2: Synthesis of 1-isopropyl-3-methylimidazolium bromide (iPrMIBr)

mp = 56-59 °C

The same synthesis procedure as for PrMIBr (section 6.3.1) was carried out using degassed isopropylbromide (102 g, 0.829 mol, Aldrich) and redistilled N-methyl imidazole (47.4 g, 0.577 mol, Aldrich). The mixture was refluxed at 50 °C for 4 hours. Ethyl acetate was added and the product precipitated out of solution. This was filtered, washed with ethyl acetate and dried under vacuum at 25 °C for 10 hours to give iPrMIBr as a white solid. Yield 81 %. ¹H-NMR (CDCl₃): δ 1.41 (d, 6H, CH(CH₃)₂, *J* = 6.7 Hz), 3.61 (s, 3H, NCH₃), 4.56-4.72 (m, 1H, NCH), 7.50 (d, 2H, NC(*H*)C(*H*)N, *J* = 9.5 Hz), 10.12 (s, 1H, NC(*H*)N) ppm. ¹³C-NMR (D₂O): δ 24.21 (s, CH(CH₃)₂), 35.50 (s, NCH₃), 54.04 (s, NCH), 122.16, 123.39 (2 x s, NCCN), 135.78 (s, NCN) ppm. NMR comparable with literature values.¹⁴

6.3.3: Synthesis of 1-butyl-3-methylimidazolium bromide (BMIBr)

The same synthesis procedure as for PrMIBr (section 6.3.1) was carried out using degassed butylbromide (29 g, 0.212 mol, Aldrich) and redistilled N-methyl imidazole (11.3 g, 0.138 mol, Aldrich). The mixture was refluxed at 50 °C for 5 hours then allowed to cool to room temperature. A pale yellow oil was produced. Yield 79 %.

¹H-NMR (D₂O): δ 0.89 (t, 3H, CH₃, *J* = 7.3 Hz), 1.22-1.33 (m, 2H, CH₂), 1.76-1.88 (m, 2H, CH₂), 3.86 (s, 3H, NCH₃), 4.17 (t, 2H, NCH₂, *J* = 7.2 Hz), 7.43 (d, 2H, NC(H)C(H)N, *J* = 15.4 Hz), 8.69 (s, 1H, NC(H)N) ppm. ¹³C-NMR (CDCl₃): δ 13.68 (s, CH₃), 20.01, 32.59 (2 x s, CH₂), 36.91 (s, NCH₃), 50.62 (s, NCH₂), 123.17, 124.49 (2 x s, NCCN), 136.44 (s, NCN) ppm. NMR data comparable with literature values.⁹

6.3.4: Synthesis of 1-pentyl-3-methylimidazolium bromide (PeMIBr)

The same synthesis procedure as for PrMIBr bromide (section 6.3.1) was carried out using degassed pentylbromide (108.9 g, 0.721 mol, Aldrich) and redistilled N-methyl imidazole (41.1 g, 0.501 mol, Aldrich). The mixture was refluxed at 60 °C for 5 hours. A pale brown oil was produced. Yield 80 %.

¹H-NMR (D₂O): δ 1.41 (t, 3H, CH₃, *J* = 7.3 Hz), 1.17-1.37 (m, 4H, CH₂CH₂), 1.78-1.89 (m, 2H, CH₂), 3.86 (s, 3H, NCH₃), 4.16 (t, 2H, NCH₂, *J* = 7.2 Hz), 7.38 (d, 2H, NC(H)C(H)N, *J* = 14.85 Hz), 8.68 (s, 1H, NC(H)N) ppm. ¹³C-NMR (D₂O): δ 13.05 (s, CH₃), 21.34, 27.47, 28.86 (3 x s, CH₂), 35.57 (s, NCH₃), 49.50 (s, NCH₂), 122.14, 123.40 (2 x s, NCCN), 135.78 (s, NCN) ppm. NMR data comparable with literature values.¹⁵

6.3.5: 1,1'-dimethyl-3,3'-hexamethylene-diimidazolium dibromide

mp = 112–116 °C ¹⁶

The same synthesis procedure as for iPrMIBr (section 6.3.2) was carried out using degassed 1,6-dibromohexane (40.36 g, 0.165 mol, Aldrich) and redistilled N-methyl imidazole (31.24 g, 0.380 mol, Aldrich). The mixture was refluxed at room temperature for 5 hours. A slightly off white solid was produced. Yield 97.5 %. ¹H-NMR (D₂O): δ 1.23 (m, 4H, 2 x CH₂CH₂), 1.76 (m, 4H, 2 x CH₂CH₂), 3.78 (s, 6H, 2 x NCH₃), 4.08 (t, 4H, 2 x NCH₂, J = 7.17 Hz), 7.34 (m, 4H, 2 x NC(H)C(H)N), 8.61 (s, 2H, 2 x NC(H)N). ¹³C-NMR (D₂O): δ 24.80, 29.00 (2 x s, CH₂), 35.57 (s, NCH₃), 49.32 (s, NCH₂), 122.10, 123.47 (2 x s, NCCN), 135.78 (s, NCN) ppm. NMR data comparable with literature values.¹⁶

6.3.6: Synthesis of zeolite analogues in sealed autoclaves

A typical synthesis procedure was as follows: a Teflon™-lined autoclave (volume 23 ml) was charged with the ionic liquid, Al[OCH(CH₃)₂]₃ (Aldrich) and H₃PO₄ (85 wt% in H₂O, Aldrich). HF (48 wt% in H₂O, Aldrich) was added if required. The stainless steel autoclave was then heated in an oven to the required temperature. The reagent masses, temperatures and length of time left in the oven needed to produce the optimum purity are as detailed in Table 6.1. These conditions were optimised by changing the reaction compositions slightly and ascertaining the product composition after each reaction.

		Mass of reagents added (g) (molar ratio of reagents)						
Product	IL	Al(OiPr) ₃	H ₃ PO ₄	HF	H ₂ O	IL	Temp (°C)	Time (hrs)
SIZ-10a	PrMIBr	0.1018 (1.0)	0.1742 (3.0)	0.015 (0.72)	* (3.8)	5.90 (58)	150	72
SIZ-10b	BMIBr	0.1040 (1.0)	0.1740 (3.0)	0.015 (0.71)	* (3.7)	4.10 (37)	200	96
SIZ-10c	PeMIBr	0.1009 (1.0)	0.1700 (3.0)	0.015 (0.73)	* (3.7)	4.58 (40)	170	240
SIZ-10d	dication	0.1017 (1.0)	0.1757 (3.1)	0.015 (0.72)	* (3.81)	4.01 (25)	170	45
SIZ-10e	iPrMIBr	0.1048 (1.0)	0.1756 (3.0)	0.015 (0.70)	* (3.69)	4.04 (38)	150	96
SIZ-11	iPrMIBr	0.1080 (1.0)	0.1748 (2.9)	0.00 (0.0)	* (2.9)	4.06 (37)	150	96

* No extra water added in these preparations. Small amounts of water present come from the aqueous HF and H₃PO₄ solutions and the ionic liquid.

Table 6.1: Synthesis details and conditions for the preparation of materials using various imidazolium based ionic liquids.

6.3.7: Experimental Details

Structural Characterisation using X-ray diffraction

Single crystal X-ray diffraction data for SIZ-10 was collected on station 9.8 at the Synchrotron Radiation Source (SRS), Daresbury Laboratories, Cheshire, UK. The structure was solved using standard direct methods and refined using least-squares minimisation techniques against F^2 . The CIF file is available for this structure on the accompanying CD. Framework phase identification was accomplished using powder X-ray diffraction (Stoe STADIP diffractometer, Cu $K\alpha$ radiation).

^{13}C , ^{31}P , ^{27}Al and ^{19}F MAS-NMR spectra

^{13}C , ^{31}P and ^{27}Al data were collected at the EPSRC Solid State NMR service facility at the University of Durham, UK on a 300 MHz Varian UNITY*Inova* with a 7.05 T Oxford Instruments magnet. ^{19}F data were collected on an Infinity plus 500 MHz spectrometer. The frequencies for data collection are 75.368 MHz (^{13}C) 121.371 MHz (^{31}P), 78.125 MHz (^{27}Al) and 125.666 MHz (^{19}F). Proton decoupled ^{13}C NMR spectra were collected with the samples spun at the magic angle at 5 kHz, a contact time of 1 ms and a recycle time of 30 s. The chemical shift reference was $(\text{CH}_3)_4\text{Si}$. ^{31}P NMR spectra were collected with proton decoupling using a recycle time of 120 s and a 20 ms acquisition time. Spectra were referenced to 85 % H_3PO_4 at 0 ppm. ^{27}Al NMR spectra were collected without ^1H decoupling using a 10 ms acquisition time and a recycle time of 0.5 s. The spectra were referenced to 1M AlCl_3 at 0 ppm. ^{19}F MAS-NMR spectra were collected with a 10 ms acquisition time and a recycle time of 60 s. The chemical shift reference was CFCl_3 and there was no decoupling used.

6.4: Results

6.4.1: Effect of lengthening ionic liquid alkyl chain on AIPO structure formation.

Increasing the alkyl chain length in the 1-alkyl-3-methylimidazolium bromide ionic liquid to 3, 4 and 5 carbons and adding no HF to the zeolite analogue reactions resulted in no AIPO framework forming. However on addition of HF, AIPO-CHA¹⁷ was synthesised. This has the same framework topology as SIZ-4 (section 4.4.3) which was synthesised using the EMIBr ionic liquid. Phase recognition was achieved by comparison of X-ray powder diffraction data (Stoe STADIP diffractometer, Cu K α radiation) with that recorded for SIZ-4. The same results were reported for the dication 1,1'-dimethyl-3,3'-hexamethylene-diimidazolium dibromide.

Single crystal data was collected on Station 9.8 at the Synchrotron Radiation Source, Daresbury, for an AIPO-CHA crystal formed using PeMIBr as the solvent and template. The template was completely resolved, (including the location of the hydrogens) and revealed to be the 1,3-dimethylimidazolium cation. As the template is different to that identified in SIZ-4 a new code, SIZ-10, was given. Crystal data and structure refinement details of SIZ-10 are given in Table 6.1. Data were also collected for an AIPO-CHA crystal formed using 1,1'-dimethyl-3,3'-hexamethylene-diimidazolium dibromide as the solvent and template. Again the template was completely resolved, revealing the 1,3-dimethylimidazolium cation.

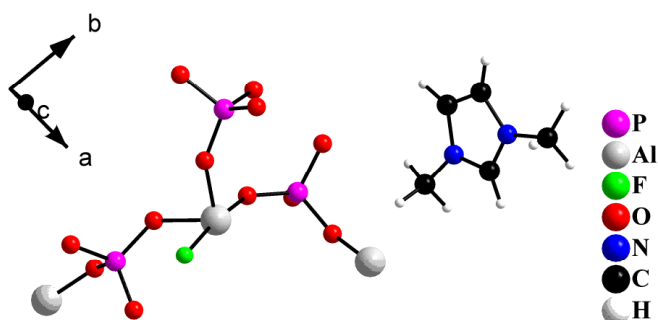


Figure 6.1: Asymmetric unit of SIZ-10

The asymmetric unit of SIZ-10 (Figure 6.1) consists of three aluminium, three phosphorus, twelve oxygen and one fluorine atom with one molecule of 1,3-dimethylimidazolium.

Table 6.2: Crystal data and structure refinement for SIZ-10

Identification code	SIZ-10
Empirical formula	$\text{Al}_3(\text{PO}_4)_3 \text{F} \cdot \text{C}_5\text{H}_9\text{N}_2$
Formula weight	481.99
Temperature	150(2) K
Wavelength	0.69330 Å
Crystal system, space group	Triclinic, P -1
Unit cell dimensions	$a = 9.074(3) \text{ \AA}$ $\alpha = 76.446(5)^\circ$ $b = 9.230(3) \text{ \AA}$ $\beta = 87.343(5)^\circ$ $c = 9.309(3) \text{ \AA}$ $\gamma = 89.388(5)^\circ$
Volume	$757.1(4) \text{ \AA}^3$
Z, Calculated density	2, 2.114 Mg/m^3
Absorption coefficient	0.527 mm^{-1}
F(000)	484
Crystal size	$0.03 \times 0.02 \times 0.01 \text{ mm}$
Theta range for data collection	$2.21 \text{ to } 29.67^\circ$
Limiting indices	$-12 \leq h \leq 12, -13 \leq k \leq 13, -13 \leq l \leq 13$
Reflections collected / unique	8652 / 4468 [R(int) = 0.0281]
Completeness to $\theta = 24.80^\circ$	98.70%
Refinement method	Full-matrix least-squares on F^2
Data / restraints / parameters	4468 / 0 / 237
Goodness-of-fit on F^2	1.041
Final R indices [$I > 2\sigma(I)$]	$R1 = 0.0403, wR2 = 0.1117$
R indices (all data)	$R1 = 0.0555, wR2 = 0.1203$
Largest diff. peak and hole	0.612 and $-0.572 \text{ e.\AA}^{-3}$

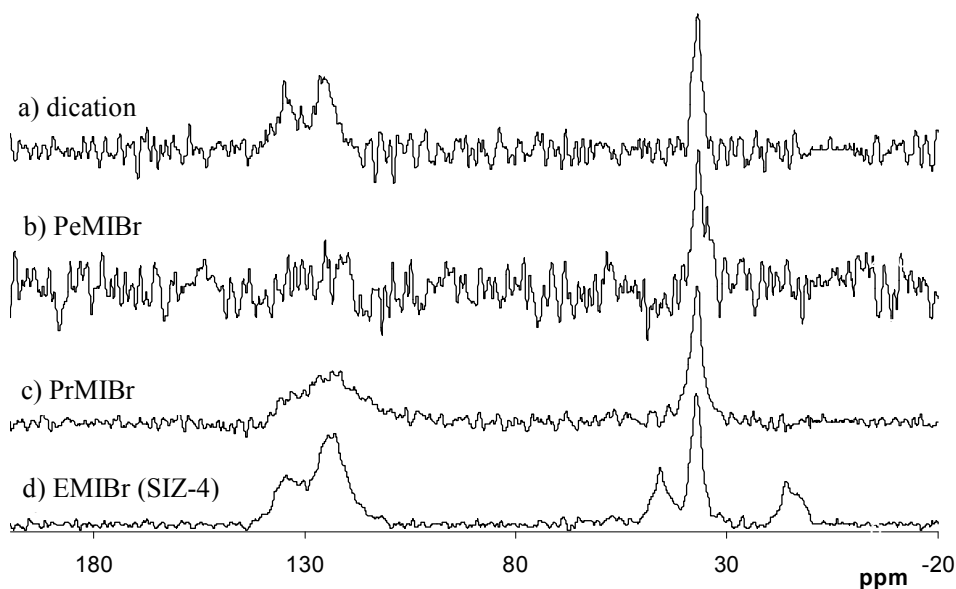


Figure 6.2: ^{13}C Solid State NMR data for AIPO-CHA synthesised using various imidazolium based ionic liquids.

^{31}P , ^{27}Al and ^{19}F MAS-NMR were collected for the various SIZ-10 samples made with the different ionic liquids. The results were comparable to those collected for SIZ-4 CHA (see section 4.4.3). ^{13}C MAS-NMR data were collected for the various SIZ-10 samples to confirm the presence of the 1,3-dimethylimidazolium cation (Figure 6.2). The peaks in the ^{13}C spectrum for SIZ-10 are broader than they might otherwise be due to instrumental problems leading to the spectra being collected with decoupling with relatively low power of about 30 kHz. The SIZ-10 made with PeMIBr is particularly poor due to a lack of sample. The NMR rotor was packed and unpacked several times and full sample recovery was not possible. However from this data it is still possible to see that the SIZ-10 samples only have one intense peak in the region of 40 ppm from the methyl carbons, hence confirming the presence of the 1,3-dimethylimidazolium cation. This can be compared to SIZ-4 sample containing the 1-ethyl-3-methylimidazolium cation which has three peaks in this region of the spectrum. (The peaks at about 130 ppm are from the imidazolium carbons.)

Yunpeng *et al.*¹⁸ have carried out similar ionothermal experiments using EMIBr and 1-hexyl-3-methylimidazolium bromide (HMIBr) as solvent and template in the synthesis of AlPOs. They reported that when using EMIBr the AEL framework was formed i.e. SIZ-3. When using HMIBr they however reported the synthesis of an unknown product. This unknown product can be identified from the powder pattern in the paper as AlPO-CHA. It is likely the 1-hexyl-3-methylimidazolium has broken down to produce the 1,3-dimethylimidazolium cation as demonstrated for PrMIBr, PeMIBr and 1,1'-dimethyl-3,3'-hexamethylene-diimidazolium dibromide.

To investigate whether the bulk solvent ionic liquid was breaking up under the reaction conditions to form the 1,3-dimethylimidazolium cation, the AlPO syntheses were repeated and the resulting solvent tested by ¹H solution state NMR. The ¹H NMR for the dication and ionic liquids with alkyl chain lengths of 3, 4 and 5 carbons showed the bulk of the solvent to have stayed intact, indicating that the templating must be by a minor amount of the 1,3-dimethylimidazolium cation. From the ¹H NMR taken after the AlPO had formed, the amount of 1,3-dimethylimidazolium left was 3 – 4 % of the initial imidazolium ionic liquid solvent. It must however be noted that some of the 1,3-dimethylimidazolium cations will have been consumed in the formation of the AlPO-CHA structure.

6.4.2: Effect of ionic liquid alkyl chain branching on AIPO structure formation.

iPrMIBr was used to investigate the effect of ionic liquid alkyl chain branching on the AIPO structures formed. Without the addition of HF, the SIZ-6 AIPO framework topology (section 4.4.5) was formed. On addition of HF the SIZ-10 AIPO-CHA framework (section 6.4.1) was formed. Phase recognition was achieved by comparison of X-ray powder diffraction data (Stoe STADIP diffractometer, Cu K α radiation) with that recorded for SIZ-6 and SIZ-10.

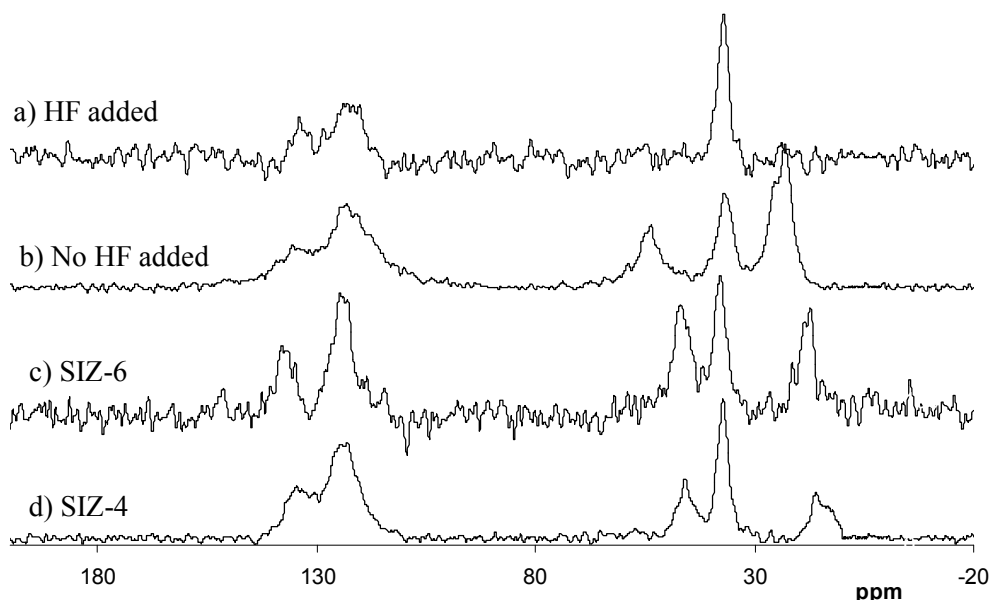


Figure 6.3: ^{13}C Solid State NMR data

- a) AIPO-CHA (SIZ-10) topology synthesised using iPrMIBr
- b) SIZ-6 (SIZ-11) topology synthesised using iPrMIBr
- c) SIZ-6 synthesised using EMIBr
- d) SIZ-4 synthesised using EMIBr

In order to identify the template, ^{13}C MAS-NMR data was collected for the samples made with and without HF using the ionic liquid iPrMIBr. From Figure 6.3 it can clearly be seen that there are 3 peaks between the region of 15-50 ppm for SIZ-4 and SIZ-6 which have previously been identified (Chapter 4) as the methyl and ethyl carbons from the 1-methyl-3-ethylimidazolium cation. However for the structure formed using iPrMIBr and no HF there are still three peaks but two are shifted slightly.

The lone methyl peak has remained in the same position at about 37.7 ppm but the other two peaks have shifted hence showing the presence of the intact 1-isopropyl-3-methylimidazolium cation in the SIZ-6 AIPO framework topology . This structure will be called SIZ-11.

With the addition of HF there is only one peak in the region from 15-50 ppm. This is the same ^{13}C MAS-NMR spectra as for SIZ-10 hence indicating that again the template has broken down on the addition of HF to form the 1,3-dimethylimidazolium cation. The HF appears to facilitate the alkyl transfer in the ionic liquid at the temperatures required for ionothermal synthesis.

6.5: Discussion and Conclusion

It is clear from both the single crystal XRD and NMR results that the SDAs occluded in the SIZ-10 materials are not the original cations from the ionic liquid but 1,3-dimethylimidazolium cation formed at some point *in situ* during the reaction process. It also appears that the addition of fluoride as a mineraliser seems to aid in the formation of this cation compared to reactions containing no fluoride where either no materials are formed or materials (e.g. SIZ-11) are formed occluding the original ionic liquid cation.

The stability of ionic liquids is currently of great interest as it impacts their potential applications greatly. The thermal stability of imidazolium-based ionic liquids has recently been studied by Chowdhury *et al.*¹⁹ using FTIR spectroscopy and time-of-flight mass spectrometry studies. They show that heating several ionic liquids to 435 °C at rates of 2000 K/s leads to the breakage of the N-alkyl bonds in these materials and that this reaction is susceptible to catalytic enhancement. It seems likely that in the presence of fluoride some of the N-alkyl bonds in the imidazolium cations are broken and also reformed under ionothermal synthesis conditions, and that the 1,3-dimethylimidazolium cations are formed *via* a metathesis of the alkyl groups. It may be that the cages in the CHA topology are too small to accommodate cations larger than the 1-ethyl-3-methylimidazolium cations and that the formation of this framework is only favorable in the presence of either the 1,3-dimethylimidazolium or the 1-ethyl-3-methylimidazolium cations. This would explain why the SIZ-10 and SIZ-4 structures are the only phases to be formed in the presence of fluoride.

A recent publication by Xu *et al.* reports the use of BMIBr as solvent and template in the microwave enhanced synthesis of a mixture of AlPO-5 (AFI) and AlPO-11 (AEL) at

ambient pressure.²⁰ These results have also been produced on the bench top in a round bottom flask using an oil bath to heat the reaction.²¹ The template in both structures is confirmed by ¹³C MAS-NMR to be the 1-butyl-3-methylimidazolium cation. These reactions are carried out at generally higher temperatures (190 °C – 280 °C) for much shorter lengths of time (0.5 – 4 hours) than we have used in our experiments. The appearance of larger pore frameworks such as AFI rather than CHA seems to be consistent with the idea that the 1-butyl-3-methylimidazolium cation is too large to act as an SDA for the CHA framework.

AEL and AFI ALPO structures are however possible to form using BMIBr in an autoclave if reactions are carried out for shorter periods of time (4 hours). The product however is not very crystalline. On longer heating (4 days) the product formed was the SIZ-10 CHA. This result demonstrates that the AEL and AFI structures can be formed in the sealed autoclaves, but after several days the product is the SIZ-10 CHA. Tests were carried out to see the effects of heating the reactions in glass beakers for up to four days however the products formed remained the AEL and AFI ALPO topologies. This is probably due to a metathesis reaction not being possible in an open vessel. Any methyl bromide (boiling point = 4 °C) or butyl bromide (boiling point = 102 °C) produced would evaporate hence the production of the 1,3-methylimidazolium cation is unlikely in an open vessel.

It is apparent that despite the large number of ionic liquids available, they will not all necessarily produce new zeotype structures. The synthesis of zeolites, is in general, very sensitive to the various reaction conditions including the type of reaction vessel used and the nature of the heat source. The framework topology CHA appears to be a default structure in the autoclave work, possibly due to a seeding effect due to the

porous nature of the Teflon™ liners. The fact that the SIZ-4 and SIZ-10 CHA frameworks have different templates points to the organic acting more as a space-filler than a structure directing agent according to the definition by Davis and Lobo.²² The same is true of SIZ-6 and SIZ-11, where the organic cation is 1-methyl-3-ethylimidazolium and 1-isopropyl-3-methylimidazolium respectively. This work however does show some interesting findings about the effect of HF on ionothermal synthesis and extends the possibilities of the ionothermal synthesis method by adding further reaction variables such as quantity of HF added, type of reaction vessel and choice of heating method.

6.6: References

1. S. I. Zones, *Zeolites*, 1989, **9**, 458
2. H. Tokuda, K. Hayamizu, K. Ishii, M. Susan and M. Watanabe, *J. Phys. Chem. B*, 2004, **108**, 16593
3. H. Tokuda, I. Kunikaza, M. Susan, S. Tsuzuki, K. Hayamizu and M. Watanabe, *J. Phys. Chem. B*, 2006, **110**, 2833
4. H. Tokuda, K. Hayamizu, K. Ishii, M. Susan and M. Watanabe, *J. Phys. Chem. B*, 2005, **109**, 6103
5. J.D. Holbrey and K.R. Seddon, *J. Chem. Soc., Dalton Trans.*, 1999, 2133
6. J.N.A. Canongia Lopes and A. A. H. Padua, *J. Phys. Chem. B*, 2006
7. A.S. Larsen, J.D. Holbrey, F.S. Tham and C.A. Reed, *J. Am. Chem. Soc.*, 2000, **122**, 7264
8. A. Downard, M.J. Earle, C. Hardacre, S.E.J. McMath, M. Nieuwenhuyzen and S.J. Teat, *Chem. Mater.*, 2004, **16**, 43
9. P. Bonhote, A.-P. Dias, N. Papageorgiou, K. Kalyanasundaram and M. Gratzel, *Inorg. Chem.*, 1996, **35**, 1168
10. Y. Chauvin, A. Hirschauer and H. Olivier, *J. Mol. Cat.*, 1994, **92**, 155
11. P. Wasserscheid and T. Welton, 'Ionic Liquids In Synthesis', Wiley-VCH, 2003. Ch. 3
12. V. P. W. Böhm and W. A. Herrman, *Chem. Eur. J.*, 2000, **6**, 1017
13. N. Leadbeater, H.M. Torenus and H. Tye, *Tetrahedron*, 2003, **59**, 2253
14. A. Fuentes, R. Matinez-Palou, H.A. Jimenez-Vazquez, F. Delgado, A. Reyes and J. Tamariz, *Monatsh. Chem.*, 2005, **136**, 177
15. R.S. Varma and V.V. Namboodiri, *Chem. Commun.*, 2001, 643

16. L. C. Branco, J.N. Rosa, J.J. M. Ramos and C.A.M. Afonso, *Chem. Eur. J.*, 2002, **8**, 3671
17. M.M. Harding and B.M. Kariuki, *Acta Crystallogr. Sect. C: Cryst. Struct. Commun.*, 1994, 852
18. Y.P. Xu, Z.J. Tian, Z.S. Xu, B.C. Wang, P. Li, S.J. Wang, Y. Hu, Y.C. Ma, K.L. Li, Y.J. Liu, J.Y. Yu and L. W. Lin, *Chin. J. Catal.*, 2005, **26**, 446
19. A. Chowdhury and S. T. Thynell, *Thermochim. Acta*, 2006, **443**, 159
20. Y.P. Xu, Z.J. Tian, S.J. Wang, Y.Hu, L. Wang, B.C. Wang, Y.C. Ma, L. Hou, J.Y. Yu and L.W. Lin, *Angew. Chem. Int. Ed.*, 2006, **45**, 1
21. L. Wang, Y. Xu, Y. Wei, J. Duan, A. Chen, B. Wang, H. Ma, Z. Tian and L. Lin, *J. Am. Chem. Soc.*, 2006, **128**, 7432
22. M.E. Davis and R.F. Lobo, *Chem. Mater.*, 1992, **4**, 756

7: Effect on AlPO synthesis of changing the ionic liquid anion.

7.1: Aims

This chapter describes the work carried out which aimed to investigate the effect, if any, on the AlPO zeolite analogues produced during ionothermal synthesis, when the ionic liquid anion is varied from Br⁻. Initial investigations started by studying the phosphorus hexafluoride anion, PF₆⁻. This anion was chosen initially due to its ease of preparation and its production of hydrophobic ionic liquids.¹ It would also be interesting to see if the ionic liquid could act not just as solvent and template, but as the phosphorus and fluoride source too. Experiments were also carried out using the anion bis((trifluoromethyl)sulfonyl)amide, [(CF₃SO₂)₂N]⁻ due to this anion producing ionic liquids with high thermal stabilities.²

7.2: Introduction – Ionic Liquid Anions

As previously discussed in Chapter 1.2.3, by varying the anion and cation, the properties of an ionic liquid, including viscosity, solvent properties, catalytic activity, and melting point can be altered dramatically.^{3, 4} In this section we discuss specifically the effect of altering the ionic liquid anion species,⁵ however it must be noted that the relationship between anion and cation size, their interactions and the physico-chemical properties of ionic liquids are far from understood.⁶

The general trend seen in ionic liquids is that increasing the anion size reduces the melting point of the ionic liquid salt. This is due to a reduction in the Coulombic

attraction contribution to the lattice energy of the crystal and an increasing covalency of the ions.⁷ Anions with greater charge diffusion/delocalisation also result in lower melting points due to the decreased interaction between the cation and anion compared to ionic compounds composed of the more charge-localized anions. An example of this is the trihalide anions versus the halide anions.⁶

Despite these trends in anion size and ionic liquid melting point, there are exceptions. The anion and cation contributions cannot be taken in isolation. Hydrogen bonding interactions seen in the crystal structures of [EMIM]X (X = Cl, Br, I)⁸ help explain the increased melting points seen for these salts. However some ionic liquids containing strongly H-bonding anions such as [CH₃COO]⁻ have melting points similar to those of ionic liquids containing anions that are highly delocalized and unable to H-bond such as [(CF₃SO₂)₂N]⁻.⁷

Replacing the Br⁻ anion with anions such as BF₄⁻, PF₆⁻ and (CF₃SO₂)₂N⁻ dramatically decreases the water solubility. However even after a moderate drying process these hydrophobic ionic liquids still often contain as much as 500 ppm water.¹ Many studies have been carried out on the effect of different anions on the ionic liquids thermal stability. To date, (CF₃SO₂)₂N⁻ has been found to be one of the anions which produces the more thermally stable ionic liquids, with many being stable to well over 500 °C.² Other properties can be altered by changing the ionic liquid anion, hence the name “designer solvents” is often used to describe the ionic liquids.⁹ A further discussion on these other properties is however beyond the scope of this Thesis.

7.3: Experimental

7.3.1: Synthesis of 1-ethyl-3-methylimidazolium phosphorus hexafluoride (EMIPF₆)

EMIPF₆ was synthesised according to the literature.¹ EMIBr (58 g, 0.304 mol, prep. - Chapter 4.3.1) was placed in a plastic container and dissolved in about 250 ml distilled water. HPF₆ (86 g, 0.354 mol, 60 wt% in H₂O, Aldrich) was added dropwise and a white precipitate formed. The liquid phase was decanted and a further 250 ml distilled water added and the mixture stirred vigorously. This step was repeated until the liquid phase measured about pH = 7. The EMIPF₆ was dried at 40 °C on a vacuum line for 7 hours and stored under Argon. Yield 48 %, melting point 59-62 °C.¹⁰

7.3.2: Synthesis of 1-ethyl-3-methylimidazolium bis((trifluoromethyl)sulfonyl)amide (EMITf₂N)

EMITf₂N was synthesised according to the literature.¹ EMIBr (15 g, 0.079 mol, prep. - Chapter 4.3.1) was placed in a plastic container and dissolved in about 30 ml distilled water. LiTf₂N (25 g, 0.087 mol) was dissolved in about 40 ml distilled water and added drop wise to the EMIBr solution. A colourless oil was produced and the top aqueous phase decanted. The oil was washed vigorously several times with distilled water until the washings showed the presence of no Br⁻ when tested with AgNO₃. The EMITf₂N was dried at 50 °C on a vacuum line for 3 hours and stored under Argon. Yield 70 %.

7.3.3: Synthesis of zeolite analogues in sealed autoclaves

A typical synthesis procedure was as follows: a TeflonTM-lined autoclave (volume 23 ml) was charged with the ionic liquid, Al[OCH(CH₃)₂]₃ (Aldrich) and H₃PO₄ (85 wt% in H₂O, Aldrich). HF (48 wt% in H₂O, Aldrich) was added if required. The stainless steel autoclave was then heated in an oven to the required temperature for 96 hours. The reagent masses and temperatures needed to produce these products are as detailed in Table 7.1. The product was dissolved in methanol, filtered then suspended in water, sonicated then filtered under suction and washed with water and acetone.

Product	IL	Mass of reagents added (g) (molar ratio of reagents)					Temp (°C)
		Al(OiPr) ₃	H ₃ PO ₄	HF	H ₂ O	IL	
β -NH ₄ AlF ₄	EMIPF ₆	0.100(1.0)	0.174 (3.1)	0 (0)	* (2.9)	1.62 (13)	190
Al(H ₂ PO ₄) ₂ F	EMITf ₂ N	0.103 (1.0)	0.176 (2.9)	0.015 (0.69)	* (3.6)	4.00 (27)	170

* No extra water added in these preparations. Small amounts of water present come from the aqueous HF and H₃PO₄ solutions and the ionic liquid.

Table 7.1: Synthesis details and conditions for the preparation of materials using the ionic liquids EMIPF₆ and EMITf₂N

7.3.4: Experimental Details

Structural Characterisation using X-ray diffraction

Single crystal X-ray diffraction data for $\text{Al}(\text{H}_2\text{PO}_4)_2\text{F}$ was collected at station 9.8 at the Synchrotron Radiation Source (SRS), Daresbury Laboratories, Cheshire and $\beta\text{-NH}_4\text{AlF}_4$ was collected using a Rigaku rotating anode single-crystal X-ray diffractometer at the University of St Andrews. The structures were solved using standard direct methods and refined using least-squares minimisation techniques against F^2 . Full details of the data collection and refinement can be found in the accompanying CIF files.

CHN Elemental Analysis

Elemental analysis was carried out using a Carlo Erba 1106 CHN Elemental Analyser.

Elemental analysis using a scanning electron microscope

A Jeol JSM-5600 scanning electron microscope (SEM) integrated with an Energy Dispersive X-rays (EDX) system for analytical elemental analysis was used to confirm the presence of fluorine in the $\beta\text{-NH}_4\text{AlF}_4$ and the $\text{Al}(\text{H}_2\text{PO}_4)_2\text{F}$ structure.

7.4: Results

7.4.1: β -NH₄AlF₄

β -NH₄AlF₄ is the same material as that previously synthesised and reported by Herron *et al.*¹¹ They characterised this material by powder diffraction at room temperature and reported it as having a space group of I4/mcm. Ionothermal syntheses of this product produced large single crystals (cubic 0.15 mm) suitable for data collection on the Rigaku rotating anode single-crystal X-ray diffractometer at the University of St Andrews. The data collection was initially collected at 150 K. This resulted in a space group of P4₂/ncm. A further data set was collected at room temperature (298 K) and this resulted in a space group of I4/mcm. Crystal data and structure refinement details of β -NH₄AlF₄ are given in Table 7.2.

Table 7.2: Crystal data and structure refinement for β -NH₄AlF₄ collected at 298 and 93 K.

Identification code	β -NH ₄ AlF ₄ Temp = 298(2) K	β -NH ₄ AlF ₄ Temp = 93(2) K
Empirical formula	10NH ₄ AlF ₄	10NH ₄ AlF ₄
Formula weight	1210.22	1210.22
Wavelength	0.7107 Å	0.7107 Å
Crystal system, space group	Tetragonal, I 4/mcm	Tetragonal, P 4₂/ncm
Unit cell dimensions	a = 11.642(5) Å α = 90.000 ° b = 11.642 Å β = 90.000 ° c = 12.661(5) Å γ = 90.000 °	a = 11.616(3) Å α = 90.000 ° b = 11.616 Å β = 90.000 ° c = 12.677(3) Å γ = 90.000 °
Volume	1716.0(12) Å ³	1710.5(7) Å ³
Z, Calculated density	2, 2.342 Mg/m ³	2, 2.350 Mg/m ³
Absorption coefficient	0.533 mm ⁻¹	0.534 mm ⁻¹
F(000)	1200	1200
Crystal size	0.1 x 0.08 x 0.08 mm	0.15 x 0.15 x 0.15 mm
Theta range for data collection	2.47 to 25.30 °	2.48 to 25.28 °
Limiting indices	-10 ≤ h ≤ 14 -13 ≤ k ≤ 14 -14 ≤ l ≤ 14	-13 ≤ h ≤ 13 -10 ≤ k ≤ 13 -14 ≤ l ≤ 14
Reflections collected/unique	5008 / 437 [R(int) = 0.0203]	9085 / 827 [R(int) = 0.0233]
Completeness to theta = 25.30 °	97.50%	98.20%
Data/restraints/parameters	437 / 4 / 61	827 / 7 / 104
Goodness-of-fit on F ²	1.146	1.134
Final R indices [I > 2σ(I)]	R1 = 0.0451, wR2 = 0.1276	R1 = 0.0438, wR2 = 0.1380
R indices (all data)	R1 = 0.0453, wR2 = 0.1278	R1 = 0.0443, wR2 = 0.1387
Largest diff. peak and hole	1.820 and -0.356 eÅ ⁻³	1.648 and -0.387 eÅ ⁻³

The space group identification for the two data sets was confirmed by checking the systematic absences in the reflections and these showed unambiguously the I centring for the room temperature phase ($h + k + l = 2n + 1$ absent). This observed phase transition at low and room temperature appears to be similar to that reported by Bulou *et al.*¹² for the α -NH₄AlF₄ structure with a tetragonal unit cell of $a = 5.0875(1)$, $c = 12.7313(3)$ Å. This structure is made of layered corner-linked [AlF₆] octahedra connected to form 4-rings. This is in contrast to the β -NH₄AlF₄ layered structure where the corner-linked [AlF₆] octahedra connect to form 3-, 4-, and 5-rings (Figure 7.1). The layers in the β -NH₄AlF₄ structure are stacked with adjacent layers having the 5 and 3-membered rings overlaid on one another. Between the layers are the ammonium cations. In the α -NH₄AlF₄ structure, at room temperature, the NH₄⁺ are statistically distributed over two different orientations and the space group is I4/mcm. In the low temperature phase, there is ordering of the NH₄⁺ and the space group is P4₂/mbc.

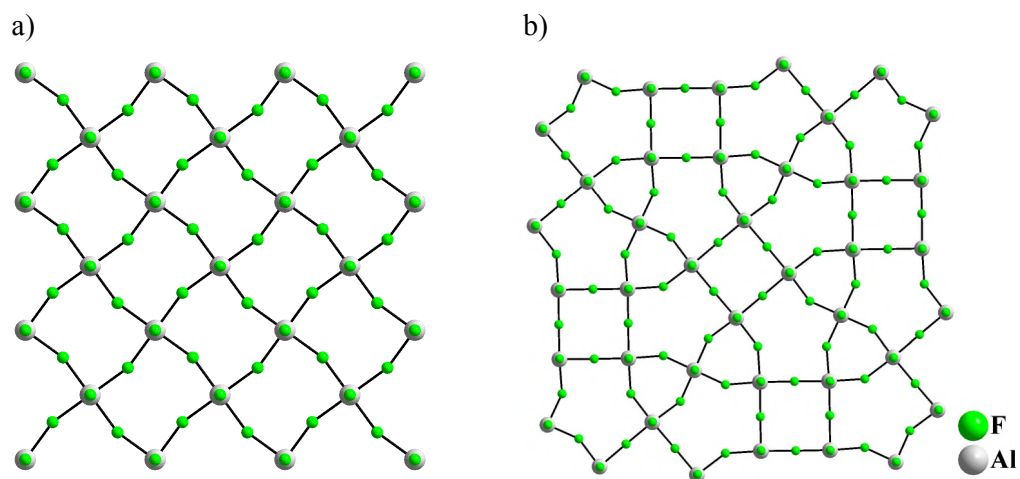


Figure 7.1: Ball and stick diagram of a layer along the c -axis from room temperature
a) α -NH₄AlF₄ b) β -NH₄AlF₄

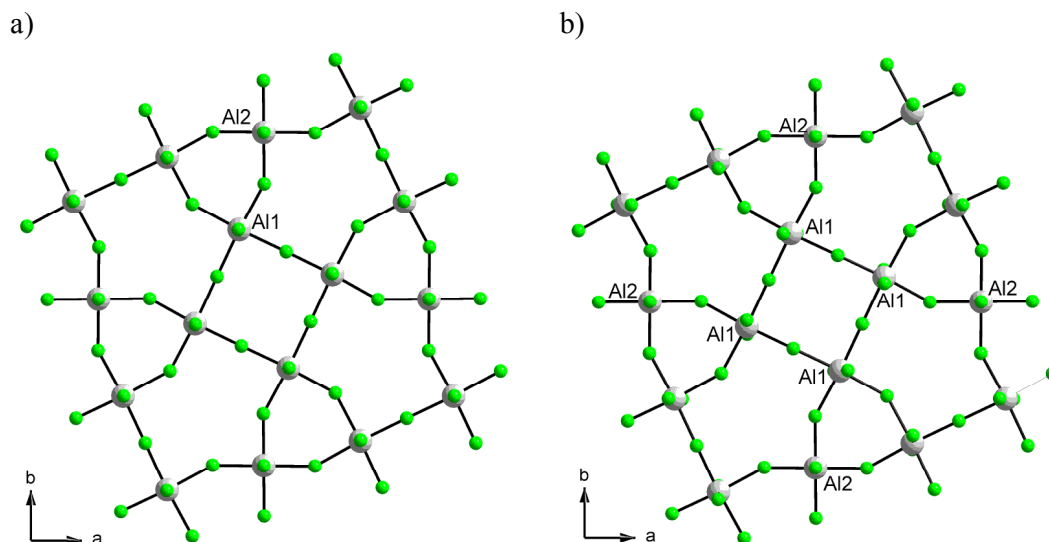


Figure 7.2: Ball and stick diagram showing the slight framework distortion from a) room temperature to b) low temperature.

Figure 7.2 shows the slight framework distortion which occurs during the phase transition from room temperature to low temperature. The Al1 octahedra tilt slightly, hence the hanging Al-F bonds are no longer parallel to the c -axis. This is in contrast to the room temperature structure where both the Al1 and Al2 are parallel to the c -axis.

It is however the orientation of the hydrogen atoms around the nitrogens which leads to the phase change from low temperature to room temperature. At low temperature the asymmetric unit contains three independent nitrogen sites (N1, N2, N3) however at room temperature the asymmetric unit only contains two independent nitrogen sites (N4, N5). Figure 7.3 shows the arrangement of the nitrogens between the AlF_4 layers. At low temperature N1, N2 and N3 are surrounded by ordered hydrogens i.e. ordered NH_4^+ groups. The data is of high enough quality for the individual hydrogen atoms to be located from the difference Fourier maps. Each site is crystallographically independent of the others due to the orientation of the hydrogens. At room temperature the N4 is surrounded by ordered hydrogens but for the N5 atom the hydrogen atoms are disordered. It is the disorder around the N5 atom which breaks the symmetry of the room temperature space group.

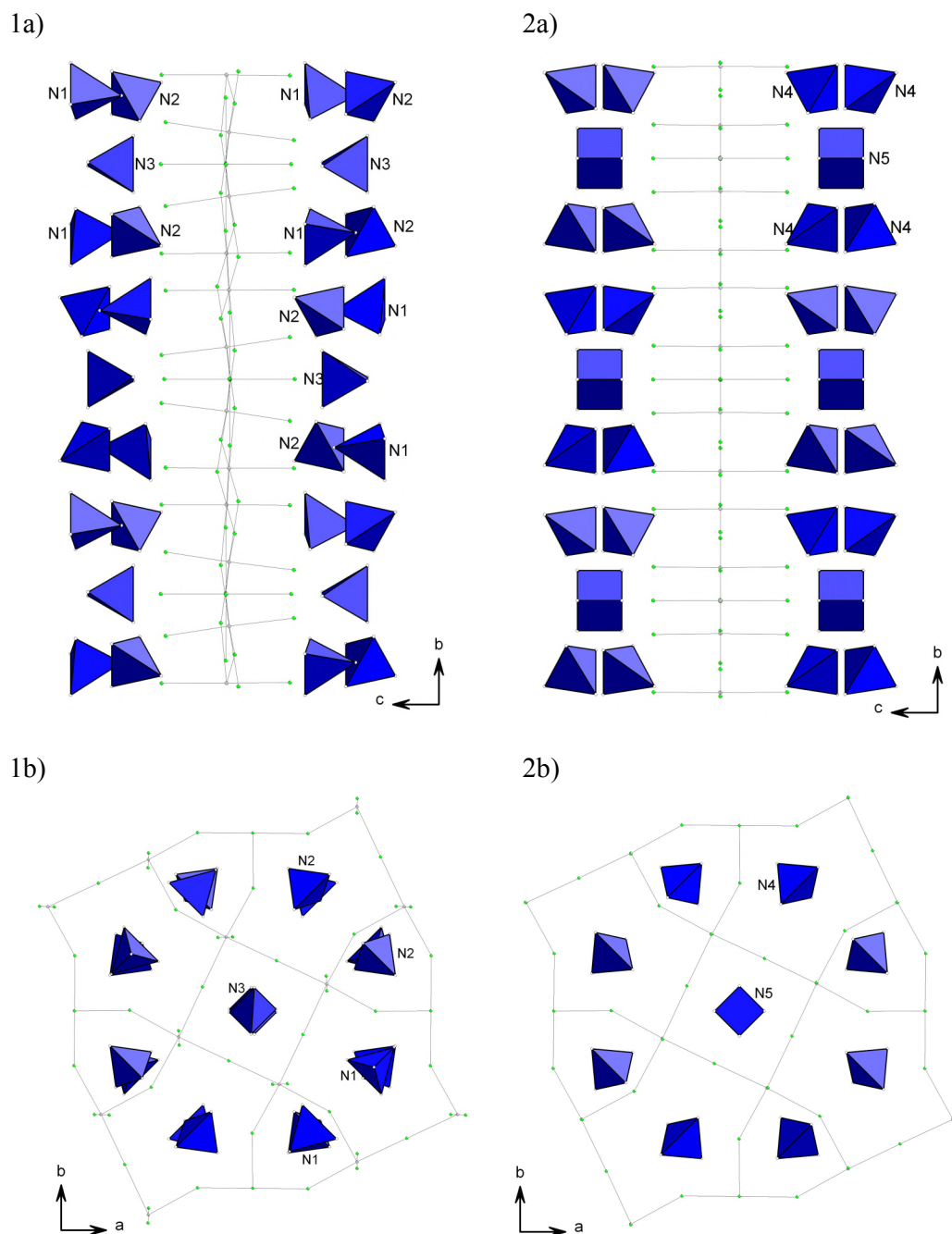


Figure 7.3: Diagram to show the orientation of the crystallographically different NH₄, shown as polyhedra, in 1a, 1b, the low temperature data, 2a, 2b the room temperature data.

To confirm the presence of fluorine in the β -NH₄AlF₄ structure, the crystals were analysed using EDX. This gave an atomic ratio of Al:F of 1:3.7. This result confirms the layers in the structure to be AlF₄. CHN was carried out to confirm the presence of ammonium. The values were as follows; C = 0.08, H = 2.95, N = 10.85 % which are not too dissimilar to the calculated values of C = 0.00, H = 3.33, N = 11.57 %.

7.4.2: Al(H₂PO₄)₂F

A novel 1-dimensional structure type, Al(H₂PO₄)₂F, was synthesised and its structure solved using single crystal X-ray diffraction on Station 9.8 at the Synchrotron Radiation Source, Daresbury. Crystal data and structure refinement details for Al(H₂PO₄)₂F are given in Table 7.3.

Table 7.3: Crystal data and structure refinement for Al(H₂PO₄)₂F

Identification code	Al(H₂PO₄)₂F
Empirical formula	Al(H ₂ PO ₄) ₂ F
Formula weight	239.95
Temperature	150(2) K
Wavelength	0.69990 Å
Crystal system, space group	Monoclinic, P 2 ₁ /c
Unit cell dimensions	a = 8.449(2) Å alpha = 90 ° b = 4.784(1) Å beta = 99.491(3) ° c = 15.767(3) Å gamma = 90 °
Volume	628.6(2) Å ³
Z, Calculated density	4, 2.536 Mg/m ³
Absorption coefficient	0.730 mm ⁻¹
F(000)	480
Crystal size	0.04 x 0.02 x 0.001 mm
Theta range for data collection	3.23 to 25.84 °
Limiting indices	-10<=h<=9 - 5<=k<=5 -19<=l<=18
Reflections collected / unique	4222 / 1261 [R(int) = 0.0656]
Completeness to theta = 25.84 °	99.70%
Refinement method	Full-matrix least-squares on F ²
Data / restraints / parameters	1261 / 28 / 125
Goodness-of-fit on F ²	1.023
Final R indices [<i>I</i> >2sigma(<i>I</i>)]	R1 = 0.060, wR2 = 0.1320
R indices (all data)	R1 = 0.0714, wR2 = 0.1439
Largest diff. peak and hole	0.720 and -0.649 eÅ ⁻³

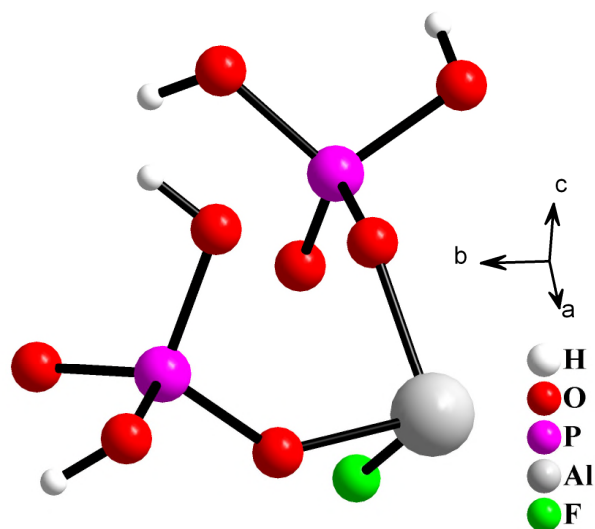
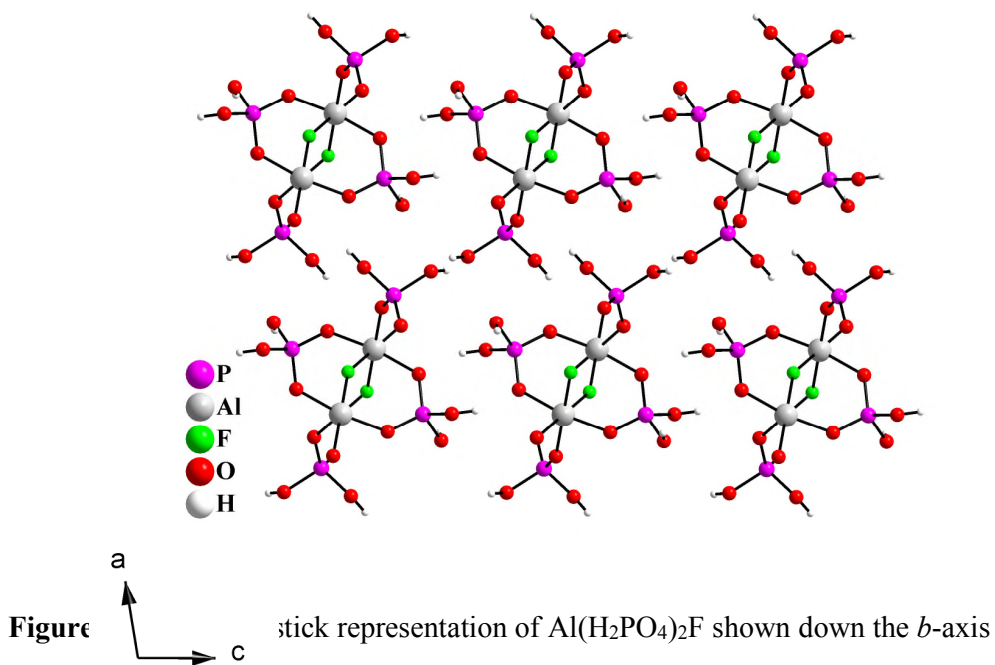


Figure 7.4: Asymmetric unit of $\text{Al}(\text{H}_2\text{PO}_4)_2\text{F}$

The asymmetric unit of $\text{Al}(\text{H}_2\text{PO}_4)_2\text{F}$ (Figure 7.4) consists of one aluminium, two phosphorus, eight oxygen, one fluorine and four hydrogen atoms. This gives an empirical formula of $\text{Al}(\text{H}_2\text{PO}_4)_2\text{F}$. The structure is made up of chains lying parallel to the *b*-axis (Figure 7.5), joined together through hydrogen bonding. The absence of template was confirmed *via* CHN analysis which gave C = 0.12, H = 1.23 and N = 0.0%. The calculated H = 1.67 %.



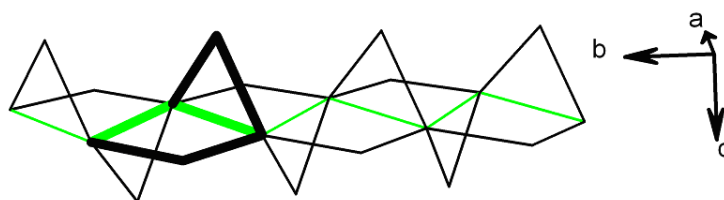


Figure 7.6: A line diagram representing the chain structure of $\text{Al}(\text{H}_2\text{PO}_4)_2\text{F}$. Each black line represents an Al-O-P linkage and each green line represents an Al-F-Al linkage.

The chains are made up of phosphorus atoms tetrahedrally bonded to four oxygens, two of which are terminal P-OH. The other two oxygens are bonded to octahedrally coordinated aluminium (AlO_4F_2). There exists an infinite zig-zagging Al-F-Al linkage in the chain parallel to the *b*-axis, represented in Figure 7.6 as a green line. The chain structure is made up of squares joined together running parallel to the *b*-axis. The corners of these squares consist of three aluminium and one phosphorus atoms. Parallel to the *c*-axis, running along the Al-F-Al zig-zagging linkage, are triangles. These are situated alternately above and below the chain made up of squares. The corners of these triangles consist of two aluminium and one phosphorus.

Figure 7.7 shows the SEM image of the $\text{Al}(\text{H}_2\text{PO}_4)_2\text{F}$ crystals. The crystals were analysed using EDX to confirm the presence of fluorine. The reported atomic percentages are O = 68.43, F = 7.74, Al = 8.60 and P = 15.23 %. These values are comparable with the calculated values of O = 66.67, F = 8.33, Al = 8.33, P = 16.67 %.

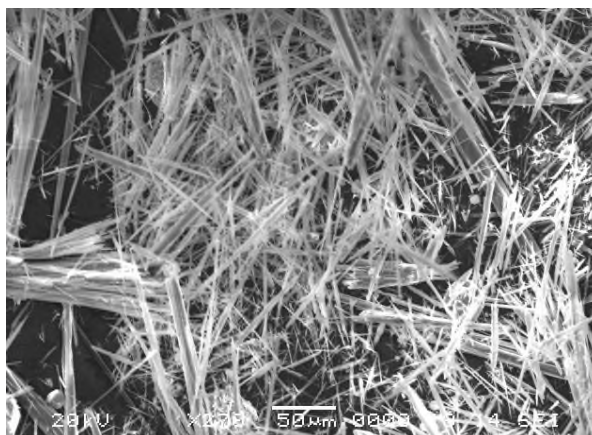


Figure 7.7: SEM image of $\text{Al}(\text{H}_2\text{PO}_4)_2\text{F}$ crystals

7.5: Conclusion and Discussion

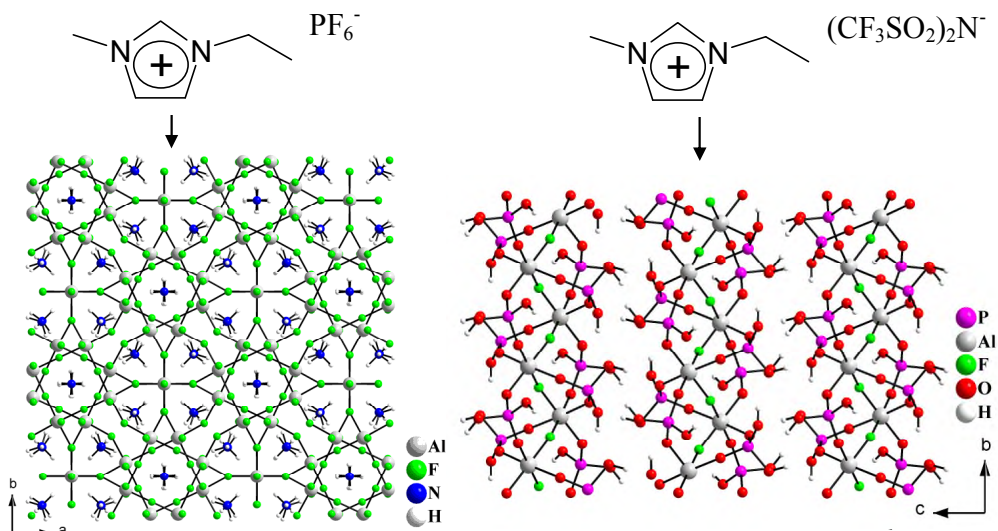


Figure 7.8: The two structures synthesis by changing the anion of the ionic liquid.

The $\beta\text{-NH}_4\text{AlF}_4$ structure (Figure 7.8) was unexpected. In this particular synthesis, phosphoric acid was added to the reaction mixture. In previous experiments where the ionic liquid, EMIPF₆ was to act as the phosphorus source, no crystalline material was synthesised. With the addition of phosphoric acid it was hoped that an AIPO framework would form, however the $\beta\text{-NH}_4\text{AlF}_4$ structure resulted. This raises many questions about the reaction conditions required to produce AIPOs using ionic liquids as the solvent and template. One issue with using the PF_6^- anion is the formation of HF. Ionic liquids containing the PF_6^- anion are sparingly water soluble. In the presence of water, PF_6^- can undergo hydrolysis to produce HF and PO_4^{3-} .¹ It would appear from the necessity to add phosphoric acid to this reaction that the water present in the phosphoric acid is in fact necessary to catalyse the formation of HF. The exact quantity of water present in the reaction is difficult to control, making reproducibility tricky. The quantity of water will affect the amount of HF present in the reaction, hence the pH. It is likely that large amounts of HF may lead to the break up of the imidazolium cation, hence the template for this structure is the ammonium cations.

Whilst this work raises many interesting questions, it was decided that as an initial test for the effect on AlPO synthesis of changing the ionic liquid anion, PF_6^- was not ideal. The production and disposal of large quantities of HF was also a consideration when the decision to terminate this work was made.

The formation of the new chain structure $\text{Al}(\text{H}_2\text{PO}_4)_2\text{F}$ (Figure 7.8), from the ionic liquid EMITf_2N , was also unexpected. This is the first aluminophosphate to be made without the incorporation of a structure directing agent when using an ionic liquid as the solvent. Again this work leads on to several questions being asked about the conditions required to make three dimensional aluminophosphate structures that incorporate the ionic liquid cation into the pores. One idea for why the cation may not have been incorporated into this structure could be due to the size of the anion. The idea behind ionothermal synthesis was to potentially remove the competition between template-framework and solvent-framework interactions that are present in hydrothermal preparations. However if the anion in the ionic liquid is large and bulky, this too could act to prevent favourable template-framework interactions hence hindering the formation of a three-dimensional framework.

Another possibility could be that EMITf_2N is not a polar enough solvent to facilitate ionothermal synthesis. It was observed that the starting materials of $\text{Al}[\text{OCH}(\text{CH}_3)_2]_3$, H_3PO_4 (85 wt% in H_2O) and HF (48 wt% in H_2O) formed a gel at the bottom of the autoclave, which did not dissolve into the EMITf_2N . The $\text{Al}(\text{H}_2\text{PO}_4)_2\text{F}$ crystalline product formed on the surface of this gel and berlinite formed in the centre. The two crystalline phases were separated by sonication. It would appear that this synthesis may predominantly be a solid-phase transformation rather than a solution-mediated transformation as seen for SIZ-1, SIZ-3, SIZ-4 and SIZ-6.

This research is in the early stages and there are many more anions to be tested before any unequivocal conclusions can be drawn about ionothermal synthesis and the effect of anion size. When changing the anion many different reaction conditions are altered. All of these factors must be taken into consideration when continuing the investigation into effect of the ionic liquid anion on ionothermal synthesis. The one conclusion however that we can draw from the work carried out in this chapter is that the anion does affect the reaction synthesis hence the final product produced. The evidence for this comes from the production of two very different materials to those made using the imidazolium ionic liquid with the Br⁻ anion.

7.6: References

1. J.G. Huddleston, A.E. Visser, W.M. Reichert, H.D. Willauer, G.A. Broker and R.D. Rogers, *Green Chem.*, 2001, **3**, 156
2. J.M. Crosthwaite, M.J. Muldoon, J.K. Dixon, J.L. Anderson and J.K. Brennecke, *J. Chem. Thermodyn.*, 2005, **37**, 559
3. H. Tokuda, I. Kunikaza, M. Susan, S. Tsuzuki, K. Hayamizu and M. Watanabe, *J. Phys. Chem. B*, 2006, **110**, 2833
4. H. Tokuda, K. Hayamizu, K. Ishii, M. Susan and M. Watanabe, *J. Phys. Chem. B*, 2005, **109**, 6103
5. H. Tokuda, K. Hayamizu, K. Ishii, M. Susan and M. Watanabe, *J. Phys. Chem. B*, 2004, **108**, 16593
6. A. Bagno, C. Butts, C. Chiappe, F. D'Amico, J.C.D. Lord, D. Pieraccini and F. Rasrelli, *Org. Biomol. Chem.*, 2005, **3**, 1624
7. P. Wasserscheid and T. Welton, 'Ionic Liquids In Synthesis', Wiley-VCH, 2003, Ch. 3
8. A. Elaiwi, P.B. Hitchcock, K.R. Seddon, N. Srinivasan, Y.M. Tan, T. Welton and J.A. Zora, *J. Chem. Soc., Dalton Trans.*, 1995, 3467
9. M. Freemantle, *Chem. Eng. News*, 1998, **76**, 32
10. P.J. Dyson, D.J. Ellis, D.G. Parker and T. Welton, *Chem. Commun.*, 1999, 25
11. N. Herron, D.L. Thorn, R.L. Harlow, G.A. Jones, J.B. Parise, J.A. Fernandez-Baca and T. Vogt, *Chem. Mater.*, 1995, **7**, 75
12. A. Bulou, A. Leble and A.W. Hewat, *Mater. Res. Bull.*, 1982, **17**, 391

8: Urea/ Choline Chloride eutectic mixture as solvent in the synthesis of AlPOs.

8.1: Aims

This chapter describes the work carried out which aimed to investigate the use of a urea/choline chloride eutectic mixture as the solvent in the synthesis of aluminophosphate zeolite analogues. No organic structure directing agent (SDA) was added to the synthesis hence it was envisaged that a component of the eutectic mixture would be required to act as the SDA.

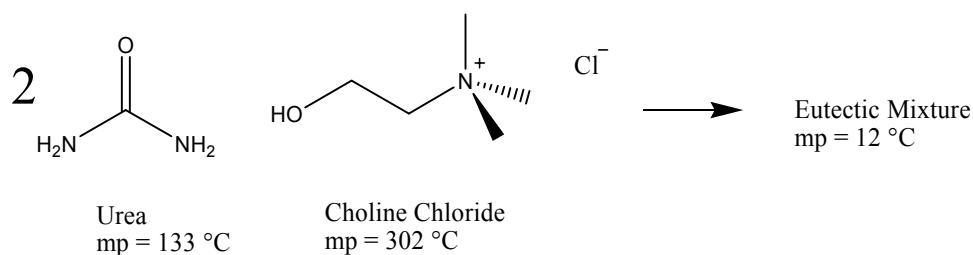
8.2: Introduction – Eutectic Mixtures verse Ionic Liquids

Eutectic mixtures display unusual solvent properties that are very similar to those shown by the ionic liquids. High solubilities can be observed (depending on the eutectic mixture used) for inorganic salts, salts that are sparingly soluble in water, aromatic acids, and amino acids. Due to the high anion concentration, these mixtures can also dissolve several metal oxides.¹ Eutectic mixtures are made using simple organic halide salts (e.g. choline chloride) and complexing agents (e.g. urea) that form a hydrogen bond. It is this complexing agent that decreases the interaction between the anion and cation and therefore lowers the mixture's melting point.

Advantages of using eutectic mixtures over ionic liquids is their ease of preparation in pure state and their relative non reactivity with water. Many are biodegradable and the toxicological properties of the components are often well characterised. Eutectic mixtures based on urea and choline chloride are also far less costly than ionic liquids. These properties make eutectic mixtures a versatile alternative to ionic liquids.

8.3: Experimental

8.3.1: Synthesis of choline chloride/urea eutectic mixture



The eutectic mixture was prepared from choline chloride and urea in a 1:2 ratio according to the literature.¹ To a round bottomed flask was added urea (30 g, 0.500 mol) and choline chloride (35 g, 0.250 mol, Sigma). This was heated to 80 °C with constant stirring under an inert atmosphere until a homogeneous liquid formed. This was cooled to room temperature to give the product as a colourless oil. For ease of handling the product was cooled to below 12 °C to form a solid.

8.3.2: Synthesis of zeolite analogues in sealed autoclaves

A typical synthesis procedure was as follows: a Teflon™-lined autoclave (volume 23 ml) was charged with the eutectic mixture, $\text{Al}[\text{OCH}(\text{CH}_3)_2]_3$ (Aldrich) and H_3PO_4 (85 wt% in H_2O , Aldrich). Distilled water or HF (48 wt% in H_2O , Aldrich) were added if required. The stainless steel autoclave was then heated in an oven to the required temperature. The reagent masses, temperatures and length of time left in the oven needed to produce the pure phase materials are as detailed in Table 8.1. After cooling the autoclave to room temperature the product was suspended in distilled water, filtered by suction and washed with acetone. The products were all colourless, crystalline solids.

Product	Mass of Reagents (g) (Molar ratio of reagents)					Temp (°C)	Time (hrs)
	Al(OiPr) ₃	H ₃ PO ₄	HF	H ₂ O	EU		
SIZ-2	0.1007 (1.0)	0.171 (3.0)	0.00 (0.0)	* (2.9)	5.13 (40)	180	72
ALPO-CJ2 [†]	0.1059 (1.0)	0.175 (2.9)	0.00 (0.0)	0.557 (6.2)	4.91 (37)	180	72
ALPO-CJ2 [#]	0.1024 (1.0)	0.178 (3.1)	0.015 (0.7)	* (3.8)	5.32 (41)	180	72

* No extra water added in these preparations. Small amounts of water present come from the aqueous HF and H₃PO₄ solutions and the ionic liquid. [†] No added fluoride. [#]Fluoride added

Table 8.1: Synthesis details and conditions for the preparation of materials using the ionic Eutectic Mixture (EU) Urea/Choline Chloride.

8.3.3: Experimental Details

Structural Characterisation using X-ray diffraction

Single crystal X-ray diffraction data for SIZ-2 was collected on station 9.8 at the Synchrotron Radiation Source (SRS), Daresbury Laboratories. The structure was solved using standard direct methods and refined using least-squares minimisation techniques against F^2 . CIF files are available for all structures. The unit cell dimensions for AlPO-CJ2 were determined from a small number of images (a matrix). A full data set however was not collected. Phase recognition was confirmed using powder X-ray diffraction (Stoe STADIP diffractometer, Cu $K\alpha$ radiation).

^{31}P and ^{27}Al MAS-NMR spectra

Data was collected at the EPSRC Solid State NMR service facility at the University of Durham, UK on a 300 MHz Varian UNITY*Inova* with a 7.05 T Oxford Instruments magnet. The frequencies for data collection are 121.371 MHz (^{31}P) and 78.125 MHz (^{27}Al). During data collection the samples were spun at 10 kHz (for ^{31}P , ^{27}Al). ^{31}P NMR spectra were collected with proton decoupling using a recycle time of 300 s and a 20 ms acquisition time. Spectra were referenced to 85 % H_3PO_4 at 0 ppm. ^{27}Al NMR spectra were collected without ^1H decoupling using a 20 ms acquisition time and a recycle time of 1 s. The spectra were referenced to 1 M AlCl_3 at 0 ppm.

Thermal analysis

Thermal analysis experiments were carried out using a TA Instruments 2960 TGA analyser. The samples were heated under flowing nitrogen up to 1000 °C at 10 °C per minute.

CHN Elemental Analysis

Elemental analysis was carried out using a Carlo Erba 1106 CHN Elemental Analyser.

8.4: Results

8.4.1: SIZ-2

A novel structure type, SIZ-2 has been formed, and its structure solved using single crystal X-ray diffraction using Station 9.8 at the Synchrotron Radiation Source, Daresbury. Crystal data and structure refinement details of SIZ-2 are given in Table 8.2.

Table 8.2: Crystal data and structure refinement for SIZ-2.

Identification code	SIZ-2
Empirical formula	$\text{Al}_2(\text{PO}_4)_3 \cdot 3\text{NH}_4$
Temperature	150 (2) K
Wavelength	0.6886 Å
Crystal system, space group	Orthorhombic, $\text{Pna}2_1$
Unit cell dimensions	$a = 9.065(5)$ Å $\alpha = 90^\circ$ $b = 17.109(5)$ Å $\beta = 90^\circ$ $c = 8.614(5)$ Å $\gamma = 90^\circ$
Volume	$1336.0(11)$ Å ³
Z, Calculated density	4, 1.472 Mg/m ³
Absorption coefficient	0.478 mm ⁻¹
F(000)	598
Crystal size	0.06 x 0.04 x 0.01 mm
Theta range for data collection	2.54 to 30.53 °
Limiting indices	$-7 \leq h \leq 12$, $-23 \leq k \leq 22$, $-11 \leq l \leq 11$
Reflections collected / unique	7190 / 3422 [R(int) = 0.0345]
Completeness to theta = 30.53 °	90.1 %
Refinement method	Full-matrix least-squares on F ²
Data / restraints / parameters	3422 / 1 / 181
Goodness-of-fit on F ²	1.052
Final R indices [$I > 2\sigma(I)$]	R1 = 0.0564, wR2 = 0.1527
R indices (all data)	R1 = 0.0581, wR2 = 0.1542
Largest diff. peak and hole	1.465 and -0.684 e.Å ⁻³

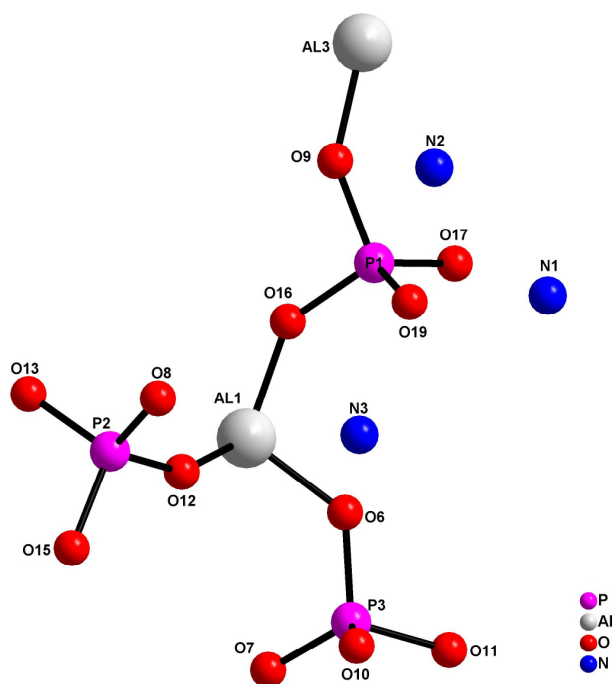


Figure 8.1: Asymmetric unit of SIZ-2

The asymmetric unit of SIZ-2 consists of two aluminium, three phosphorus, twelve oxygen, three nitrogen and twelve hydrogen. This is illustrated in Figure 8.1 where the hydrogen atoms are omitted for clarity.

The structure contains both aluminium and phosphorus in tetrahedral coordination. The Al-O-P alternation is maintained, but the chemical formula, $\text{Al}_2(\text{PO}_4)_3 \cdot 3\text{NH}_4$, indicates that SIZ-2 is an interrupted structure (i.e. P-O hanging bonds) as illustrated in Figure 8.2. The pore architecture displays three small intersecting channels parallel to the three crystallographic directions.

The pores appear to be too small to adsorb anything but the smallest molecules, but preliminary ion exchange experiments indicate that the ammonium can be at least partially exchanged for metal cations such as Cu^{2+} .

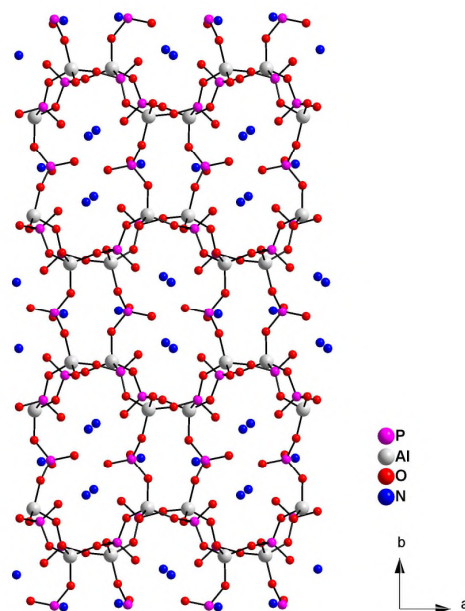


Figure 8.2: SIZ-2 structure

Elemental CHN analysis confirmed that the template located in the channels of SIZ-2 is ammonium and not water; C = 0.02, H = 2.99, N = 9.88 %. (Calc. C = 0.00, H = 3.08, N = 10.69 %.) This is formed from the partial decomposition of the urea and acts not only as a template but also balances the charge on the framework. Time studies using powder X-ray diffraction data (Figure 8.3) indicate that the crystallinity of the products reaches its maximum between 24 and 48 hours after the reactions started, with overall yields of about 70 % after 48 hours.

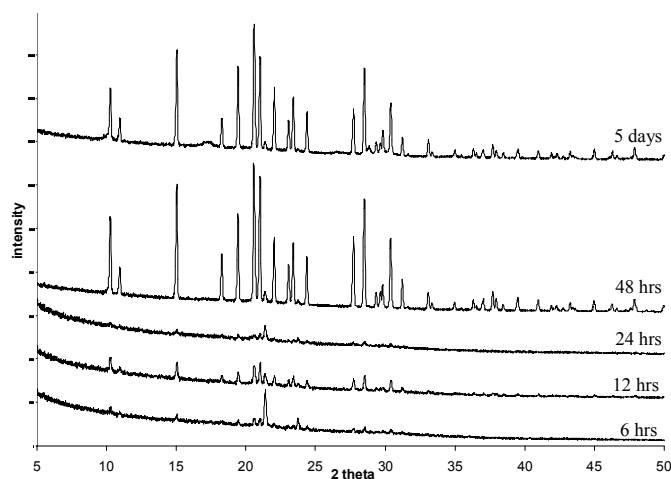


Figure 8.3: X-ray diffraction patterns of the crystallisation of SIZ-2. The maximum yield of ~70 % is reached after 12 - 48 hrs and fluctuates only slightly.

The ^1H NMR studies (Figure 8.4) of the eutectic mixture solvent recovered after the reactions show that at 12 hours the breakdown products are only just visible above background. However, after 5 days the eutectic mixture shows quite a complex ^1H NMR spectrum indicating extensive degradation of the solvent system. Clearly the nucleation and crystallisation of the materials takes place at relatively low levels of solvent degradation under conditions where the concentration of the template species is slowly increasing as more eutectic mixture decomposes.

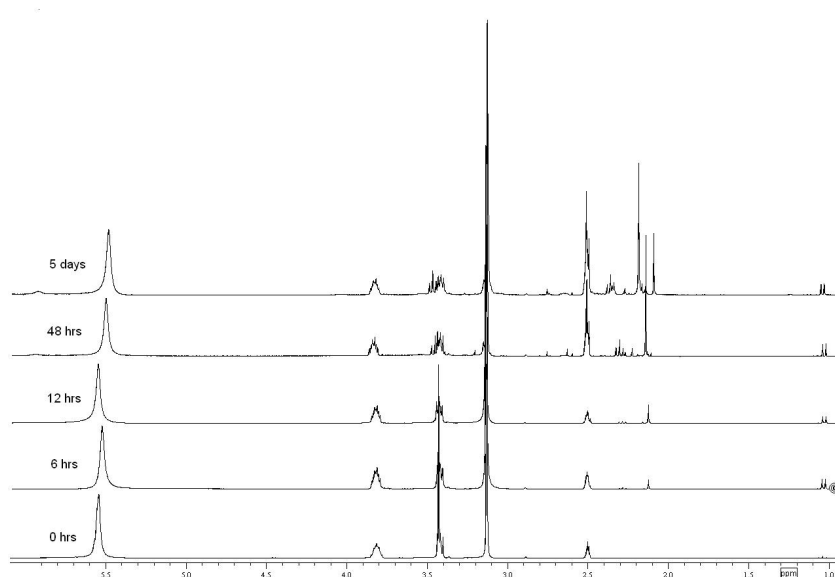


Figure 8.4: ^1H solution state NMR spectra of the urea/choline chloride eutectic mixture recovered after the crystallisation of SIZ-2. This shows the breakdown of the eutectic mixture is extensive after several days.

The SIZ-2 ^{31}P MAS-NMR spectrum (Figure 8.5a) shows two resolvable resonances at -18.4 and -10.7 ppm, plus a small amount of berlinite impurity. The resonance at -10.7 ppm shows a shoulder at the low field side indicating that it is composed of at least two resonances. This is consistent with the expected three sites from the XRD study. The ^{27}Al MAS-NMR spectrum (Figure 8.5b) shows a clear resonance for tetrahedrally bonded aluminium as well as a small peak indicating higher coordination.

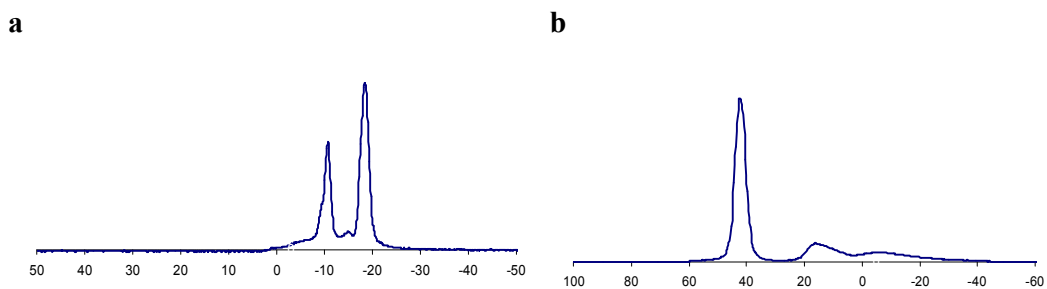


Figure 8.5: a = ^{31}P , b = ^{27}Al MAS-NMR for SIZ-2

During thermal analysis, SIZ-2 shows (Figure 8.6) an almost 10 % weight loss at just above room temperature, which is most likely due to weakly held species at the surface of the sample. An intermediate weight loss is observed at ~ 200 °C of around 10-12 % which corresponds to the loss of the ammonia (calculated 13.7 %) although it is almost impossible to resolve this weight loss from the subsequent slow weight loss that is due to the condensation reactions.

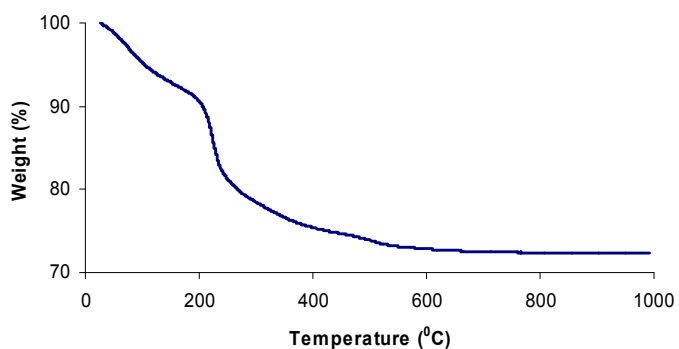


Figure 8.6: TGA experiment for SIZ-2

8.4.2: AIPO-CJ2

The unit cell dimensions for AIPO-CJ2 (orthorhombic $a = 9.40$, $b = 9.52$ and $c = 9.96\text{\AA}$) were determined from a matrix collected on Station 9.8 at the Synchrotron Radiation Source, Daresbury. A full data set however was not collected. Phase recognition was confirmed using powder X-ray diffraction (Stoe STADIP diffractometer, Cu $K\alpha$ radiation). The material is isostructural with that previously reported.² Full structural characterisation (diffraction plus NMR) of AIPO-CJ2 is given in the literature.³

AIPO-CJ2 was first synthesised by Yu *et al.*³ and the structure is shown in Figure 8.7. This structure is composed of single 4 ring units (S4R) of alternating aluminium and phosphorous atoms. The aluminium is either five or six coordinated. To the four Al-O-P bonds of the S4R unit, an OH/F bridge links both the aluminium, with one aluminium carrying a terminal fluorine. The two ammoniums act to neutralise the charge of the framework.

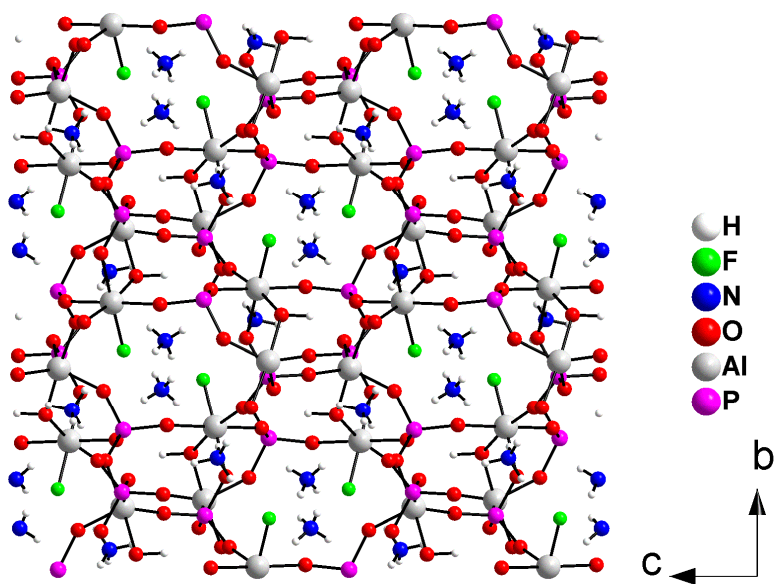


Figure 8.7: Ball and stick representation of AIPO-CJ2 along the a -axis³

The three dimensional framework has two types of channels. One is formed by 8-T (T = Al or P) rings packed along (100) and the other is formed by zigzag packing of 8-T rings along (001) axis.

Interestingly ALPO-CJ2 can be made in the presence of fluorine and no water or three times the molar ratio of water to choline chloride/urea eutectic mixture. If there is no HF used in the synthesis but equal molar water to choline chloride/urea eutectic mixture ALPO-CJ2 is also produced. This was unexpected since this structure has not been found in the literature with no F present.

8.5: Discussion and Conclusion

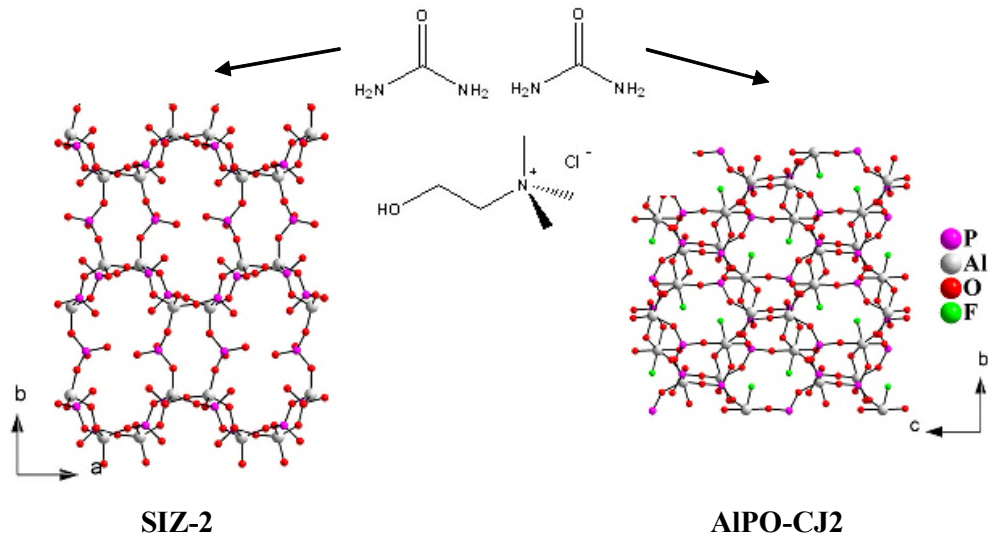


Figure 8.8: The two structures formed from the choline chloride/urea eutectic mixture.

The choline chloride/urea eutectic mixture has acted as the solvent in the formation of the new framework topology SIZ-2 and the known framework AIPO-CJ2 (Figure 8.8). Of particular interest is the fact that the urea decomposes under the reaction conditions and acts as a template delivery agent. It has been shown through SIZ-2 synthesis time studies that the nucleation and crystallisation of SIZ-2 takes place at relatively low levels of solvent degradation under conditions where the concentration of the template species is slowly increasing as more eutectic mixture decomposes.

Again it has been possible to show, as in Chapter 4, that ionothermal synthesis allows a great deal of control over the mineralisers that are present in the solvent. With little water and no HF to act as mineralisers, interrupted framework structures (SIZ-2) appear to be targeted. On addition of HF or water, condensed structures (AIPO-CJ2) are formed with no hanging P-O bonds, hence there is the possibility of selectively targeting interrupted frameworks or fully condensed zeotypes. Mineralising agents such

as fluoride help solubilise the inorganic components and catalyse T-O-T bond formation (where T are the tetrahedral framework atoms). The eutectic mixture is a good solvent on its own, but adding fluoride increases its solvating power and can change the types of framework that are formed.

8.6: References

1. A.P. Abbott, G. Capper, D.L. Davies, R.K. Rasheed and V. Tambyrajah, *Chem. Commun.*, 2003, 70
2. L. Yu, W. Pang and L. Li, *J. Solid State Chem.*, 1990, **87**, 241
3. F. Taulelle, M. Pruski, J.P. Amoureux, D. Lang, A. Bailly, C. Huguenard, M. Haouas, C. Gerardin, T. Loiseau and G. Ferey, *J. Am. Chem. Soc.*, 1999, **121**, 12148

9: Eutectic Mixtures as Template Delivery Agents.

9.1: Aims

This chapter describes the work carried out which aimed to investigate the concept of using unstable eutectic mixtures as template delivery agents in the synthesis of zeolite analogues. Deep eutectic solvents based on mixtures between derivatised ureas and choline chloride are used as the reaction media and the source of the organic template in the synthesis of aluminophosphate materials. The formation of the template by the decomposition of the derivatised urea is investigated as previously reported in Chapter 8 for the urea/choline chloride eutectic mixture.

9.2: Introduction – *In situ* generation of template

There are only a few examples in the literature of zeotypes and zeolite analogues synthesised by the *in situ* generation of a template within the reaction vessel.¹⁻⁶ These syntheses are typically a quasi nonaqueous mixture involving mainly an alkyl formamide as the solvent. The thermal decomposition of the alkyl formamide produces the template and it is this slow *in situ* liberation of the template into the reaction mixture which appears to be essential for the crystallisation.^{3,6} Any water present in the reactions stems from the aluminium and phosphorus sources and is deemed necessary for crystallisation to occur.⁷

Vidal *et al.* have produced several different layered and three-dimensional aluminophosphate structures *via* this *in situ* generation of template from the solvent and Lakiss *et al.* have also shown this synthesis route to be successful with gallophosphates (Table 9.1).

Product	Solvent	Template Formed	Ref.
AIPO-41	diisopropylformamide	diisopropylamine	1
AIPO Mu-4	diethylformamide	diethylamine	2
AIPO Mu-7	methylformamide	methylamine	3
GaPO Mu-30	cyclohexylformamide	cyclohexylamine	4

Table 9.1: Zeolite analogues formed *via* the *in situ* generation of templates from various solvents.

Paulet *et al.* synthesised a new layered fluorinated gallium phosphate (MIL-30) from a mixed water-dimethylformamide solvent.⁶ Again the alkyl formamide molecules decompose to form dimethylamine which acts as a template along side the 1,3-diaminopropane which was added to the initial reaction vessel.

Paillaud *et al.* synthesised a new fluorinated aluminophosphate (AIPO-GIS) in a mixed dimethylformamide-triethyleneglycol solvent. Once again the dimethylformamide decomposes to give the protonated template, dimethylamine. This decomposition is not unexpected since dimethylformamide is catalytically decomposed in acidic media above its melting point.⁸

9.3: Experimental

9.3.1: Synthesis of eutectic mixtures

The required amount of as bought amide and quaternary ammonium salt were measured out in a 2:1 ratio and ground in a mortar. This was then placed into a Teflon™-lined autoclave with the rest of the reactants.

	Amide	Mp (°C)	Quaternary ammonium salt	Mp (°C)	Eutectic mixture Mp (°C)
1	1,3-dimethyl urea	101-105	Tetraethylammonium bromide	285-290	20-25
2	1,3-dimethyl urea	101-105	Choline chloride	298-305	69-71
3	N,N-trimethylene urea	264-266	Choline chloride	298-305	150-155
4	Ethylene urea	129-132	Choline chloride	298-305	69-73

Table 9.2: Eutectic Mixtures

9.3.2: Synthesis of aluminophosphate zeolite analogues in sealed autoclaves

A typical synthesis procedure for aluminophosphates **1-8** was as follows: a Teflon™-lined autoclave (volume 23 ml) was charged with eutectic mixture, Al[OCH(CH₃)₂]₃ (Aldrich), and H₃PO₄ (85 wt% in H₂O, Aldrich). HF (48 wt% in H₂O, Aldrich) and distilled water were added if required. The stainless steel autoclave was then heated in an oven to the required temperature. The reagent masses, temperatures and length of time left in oven are as detailed in the tables below.

After cooling the autoclave to room temperature the product was suspended in distilled water, sonicated, filtered by suction and washed with acetone. The products were colourless, crystalline solids.

Product	Mass of reagents added (g) (molar ratio of reagents)				Temp (°C)	Time (hrs)
	Al(OiPr) ₃	H ₃ PO ₄	HF	H ₂ O		
1	0.0568 (1.0)	0.1763 (5.5)	0.00 (0.0)	* (5.3)	150	96
2	0.0534 (1.0)	0.1742 (5.8)	0.00 (0.0)	* (5.6)	200	96
3	0.1043 (1.0)	0.1237 (2.1)	0.015 (0.70)	* (2.9)	150	99

1,3-dimethyl urea (2.3 g, Avocado) / tetraethylammonium bromide (2.7 g, Avocado)

Table 9.3: Synthesis details and conditions for the preparation of materials using eutectic mixture 1.

Mass of reagents added (g) (molar ratio of reagents)						
Product	Al(OiPr) ₃	H ₃ PO ₄	HF	H ₂ O	Temp (°C)	Time (hrs)
2	0.1021 (1.0)	0.1762 (3.1)	0.015 (0.72)	* (5.1)	180	48

1,3-dimethyl urea (2.8 g, Avocado) / Choline Chloride (2.2 g, Avocado)

Table 9.4: Synthesis details and conditions for the preparation of materials using eutectic mixture 2.

Mass of reagents added (g) (molar ratio of reagents)						
Product	Al(OiPr) ₃	H ₃ PO ₄	HF	H ₂ O	Temp (°C)	Time (hrs)
4	0.1034 (1.0)	0.1710 (2.9)	0.015 (0.071)	0.4780 (56.0)	170	66
5	0.1089 (1.0)	0.1701 (2.8)	0.015 (0.67)	* (3.5)	200	96

Ethylene urea (2.8 g, Aldrich) / Choline Chloride (2.2 g, Avocado)

Table 9.5: Synthesis details and conditions for the preparation of materials using eutectic mixture 3.

Mass of reagents added (g) (molar ratio of reagents)						
Product	Al(OiPr) ₃	H ₃ PO ₄	HF	H ₂ O	Temp (°C)	Time (hrs)
6	0.1038 (1.0)	0.1776 (3.0)	0.00 (0.0)	* (2.9)	170	72
7	0.1030 (1.0)	0.1781 (3.1)	0.015 (0.71)	0.1033 (15.2)	200	96
8	0.1031 (1.0)	0.1763 (3.1)	0.00 (0.0)	0.2169 (27.24)	200	96

N,N-Trimethylene urea (3.0 g, Fluka) / Choline Chloride (2.0 g, Avocado)

Table 9.6: Synthesis details and conditions for the preparation of materials using eutectic mixture 4.

* No extra water added in these preparations. Small amounts of water present come from the aqueous HF and H₃PO₄ solutions

9.3.3: Synthesis of gallium phosphate Zeolite-A (Structure 9)

The method was followed as for the aluminophosphates but the Al[OCH(CH₃)₂]₃ was replaced by Ga₂(SO₄)₃ (Aldrich). Tetrahydro-2-pyrimidione (2.0 g, 0.020 mol, Fluka) / Choline Chloride (1.4 g, 0.010 mol, Avocado) constituted the eutectic mixture. The amount of the starting materials were 0.105 g Ga₂(SO₄)₃ and 0.173 g of H₃PO₄ (85 wt% in H₂O), molar ratio of Ga₂(SO₄)₃ :H₃PO₄ was 1:6.1. The reaction was heated at 170 °C for 72 hours.

9.3.4: Experimental Details

Structural Characterisation using X-ray diffraction

Single crystal X-ray diffraction data for all materials except **2** were collected using MoK α radiation using a Rigaku rotating anode single-crystal X-ray diffractometer at the university of St Andrews or using a wavelength of ~ 0.7 Å station 9.8 at the Synchrotron Radiation Source (SRS), Daresbury Laboratories, Cheshire, UK. The structures were solved using standard direct methods and refined using least-squares minimisation techniques against F^2 . Full details of the data collection and refinement can be found in the accompanying CIF files. Structures **5** and **7** are fully characterised in the literature hence the crystal data is only reported on the accompanying CD. Framework phase identification for **2** (which has the Mu-7 structure) was accomplished from the unit cell given by single crystal X-ray diffraction.

Preliminary MAS-NMR characterisation of the materials

MAS-NMR data (^{27}Al , ^{31}P , ^{13}C and ^{19}F) for the materials were collected at the University of St Andrews on a 500MHz Varian Infinity plus spectrometer (Structures **1** and **2**) or at the EPSRC Solid State NMR service facility at the University of Durham, UK on a 300MHz Varian UNITY*Inova* with a 7.05 T Oxford Instruments magnet.

Thermal analysis

Thermal analysis experiments were carried out using a TA Instruments 2960 TGA analyser. The samples were heated under flowing nitrogen up to 1000 °C at 10 °C per minute.

CHN Elemental Analysis

Elemental analysis was carried out using a Carlo Erba 1106 CHN Elemental Analyser.

9.4: Results

9.4.1: Structure 1

A novel, 1-dimensional structure type, **1** was synthesised and its structure solved using single crystal X-ray diffraction on Station 9.8 at the Synchrotron Radiation Source, Daresbury. Crystal data and structure refinement details for Structure **1** are given in Table 9.7.

Table 9.7: Crystal data and refinement for Structure **1**.

Identification code	Structure 1
Empirical formula	$\text{Al}_2(\text{PO}_4)_4 \cdot 4\text{CH}_3\text{NH}_3 \cdot 2\text{NH}_4$
Formula weight	598.2
Temperature	150(2) K
Wavelength	0.69330 Å
Crystal system, space group	Orthorhombic, $P 2_12_12_1$
Unit cell dimensions	$a = 8.4710(10)$ Å $\alpha = 90^\circ$ $b = 16.710(2)$ Å $\beta = 90^\circ$ $c = 17.234(2)$ Å $\gamma = 90^\circ$
Volume	$2439.5(5)$ Å ³
Z, Calculated density	4, 1.629 Mg/m ³
Absorption coefficient	0.372 mm ⁻¹
F(000)	1248
Crystal size	0.07 x 0.025 x 0.01 mm
Theta range for data collection	1.66 to 20.27 °
Limiting indices	$-8 \leq h \leq 8$, $-16 \leq k \leq 16$, $-17 \leq l \leq 17$
Reflections collected / unique	12610 / 2548 [R(int) = 0.0607]
Completeness to theta = 20.27 °	99.60 %
Absorption correction	None
Refinement method	Full-matrix least-squares on F ²
Data / restraints / parameters	2548 / 38 / 293
Goodness-of-fit on F ²	1.073
Final R indices [$I > 2\sigma(I)$]	R1 = 0.0354, wR2 = 0.0876
R indices (all data)	R1 = 0.0437, wR2 = 0.0917
Largest diff. peak and hole	0.615 and -0.250 e.Å ⁻³

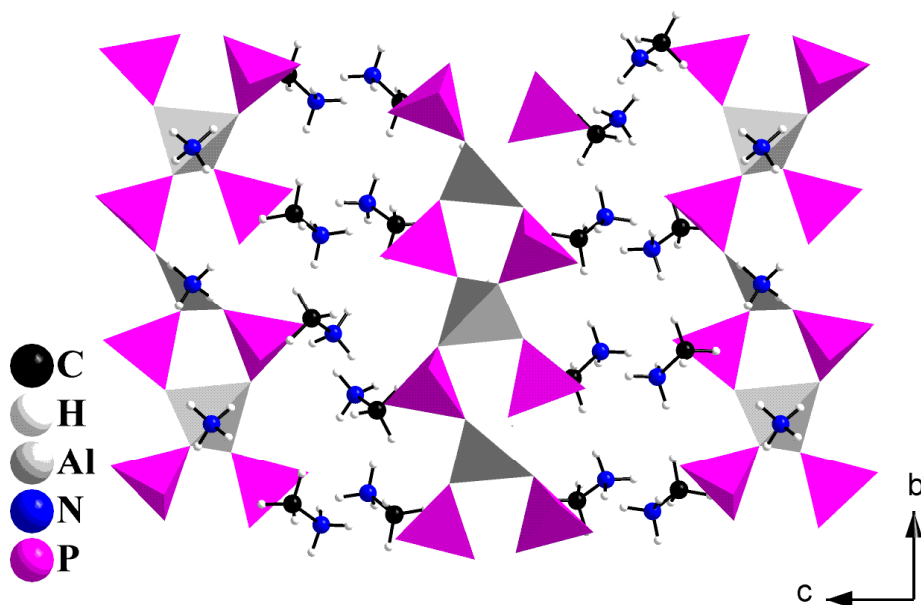


Figure 9.1: Diagram of Structure **1** along the a -axis showing the $[\text{Al}(\text{PO}_4)_2]^{3-}$ chain composition as polyhedral and the template as ball and stick diagrams.

Structure **1** has an Al:P ratio of 1:2 and is made up from corner sharing AlO_4 and PO_4 tetrahedra with a chain composition of $\infty[\text{Al}(\text{PO}_4)_2]^{3-}$. All the AlO_4 vertices are shared but each PO_4 has two terminal P-O linkages (Figure 9.1). The derivatised urea in the eutectic mixture has broken down to provide the templating agent which in turn has fragmented, leading to the coexistence of $2[\text{CH}_3\text{NH}_3]^+$ and $[\text{NH}_4]^+$. These cations hold the chains together through hydrogen bond interactions with the terminal P-O linkages. The hydrogen atoms on the templates were found from the difference Fourier maps.

MAS-NMR is consistent with Structure **1** (Figure 9.2), with the ^{27}Al NMR spectrum indicating tetrahedral coordination, the ^{31}P NMR spectrum showing several resolved resonances and shoulders consistent with four sites and the ^{13}C NMR spectrum showing one resonance in the region expected for methylammonium.

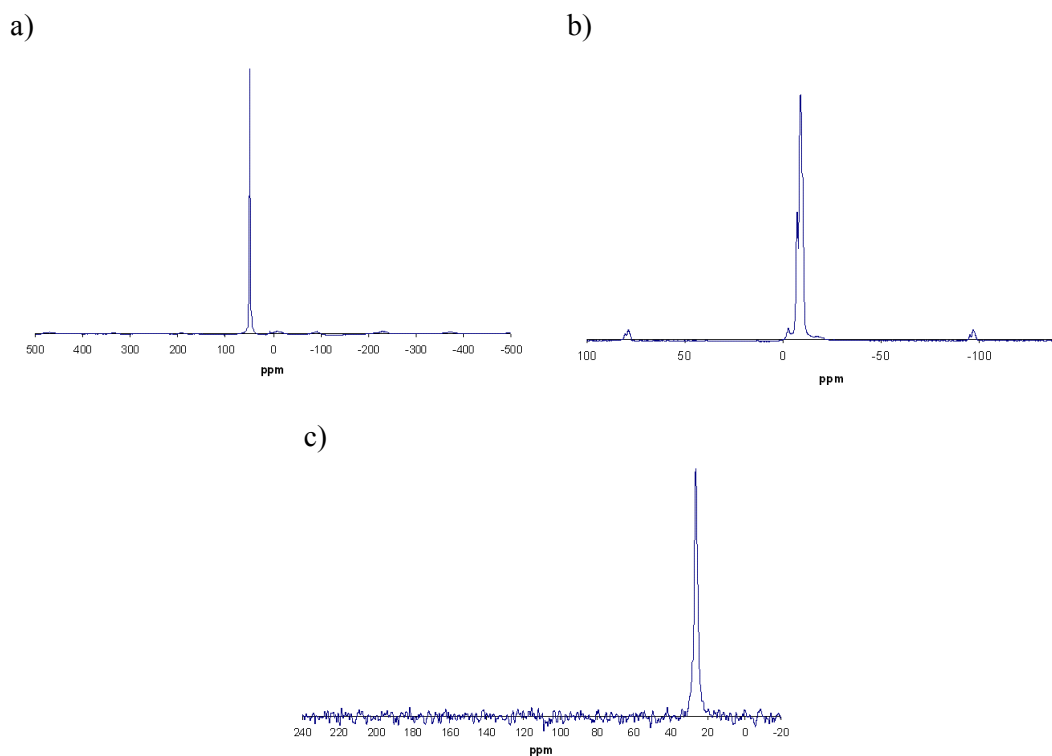


Figure 9.2: a = ^{27}Al , b = ^{31}P , c = ^{13}C MAS-NMR for Structure 1.

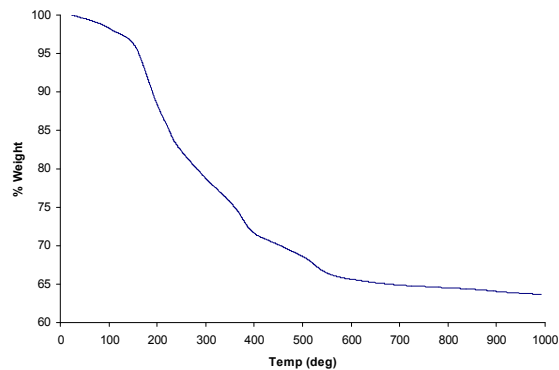


Figure 9.3: TGA experiment for Structure 1.

Structure 1 TGA data (Figure 9.3) shows a weight loss of about 29.5 % from 150 to 540°C. This is comparable to the calculated weight loss of 27.5 % for the removal of the $[\text{CH}_3\text{NH}_3]^+$ and $[\text{NH}_4]^+$ structure directing agents. The CHN data gave values of C = 8.28, H = 5.20, N = 13.00 % which are not too dissimilar to the calculated values of C = 8.03, H = 5.39, N = 14.05 %.

9.4.2: Structure 2

The unit cell dimensions for Structure 2, $\text{Al}_3(\text{PO}_4)_4 \cdot (\text{CH}_3\text{NH}_3)_3$ were determined from a matrix collected on Station 9.8 at the Synchrotron Radiation Source, Daresbury as triclinic $a = 8.350$, $b = 11.252$, $c = 11.448 \text{ \AA}$, $\alpha = 72.5$, $\beta = 89.68$, $\gamma = 85.27^\circ$. A full data set however was not collected as Structure 2 has the same framework topology and template as the two-dimensional layered aluminophosphate, Mu-7, reported and characterised by Vidal *et al.*^{3,9}

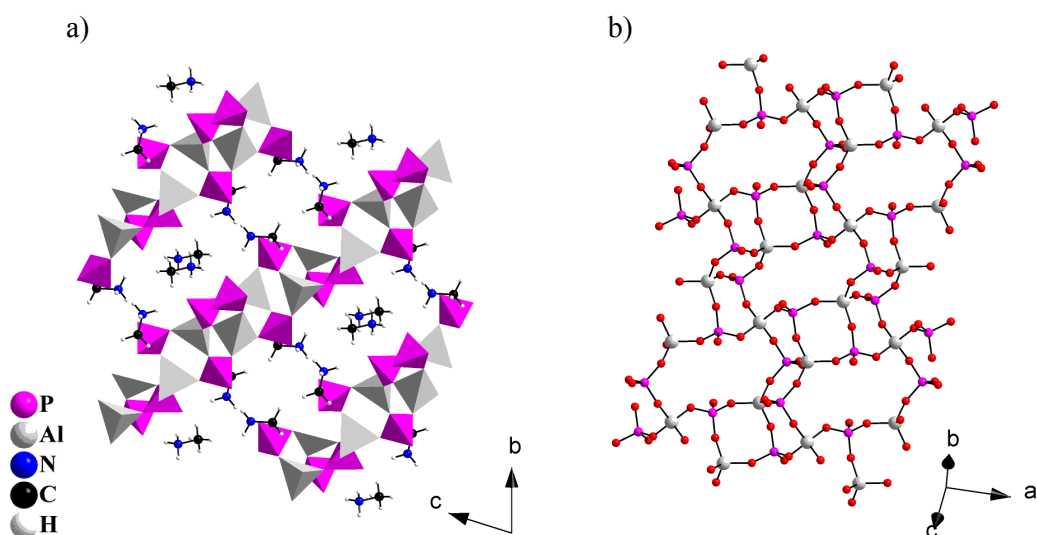


Figure 9.4: Structure 2 a) the zigzag ladder chains b) the 4x8 layer network.³

The aluminophosphate layers are built up from S4R and S8R which are joined together in the layer through zigzag ladder chains (Figure 9.4). The synthesis of Mu-7 was the first time that the aluminophosphate layered 4x8 network had been made. The synthesis was carried out in a quasi non aqueous system using methylformamide as the solvent. During the synthesis the methylformamide decomposes resulting in the *in situ* formation of methylamine as the template. In the synthesis of Structure 2 it is the *in situ* decomposition of the derivatised urea which provides the template of $[\text{CH}_3\text{NH}_3]^+$ which is located in the interlayer spaces.

Vidal *et al.* proposed a crystallisation mechanism for the formation of Mu-7³ (Figure 9.5 and 9.6) based upon the proposed mechanistic pathways postulated in earlier work by Oliver *et al.*⁷ This mechanism starts with the “parent” chain $\infty[\text{AlP}_2\text{O}_8\text{H}_2]^-$ which consists of corner-sharing $\text{Al}_2\text{P}_2\text{O}_8$ four-rings bridged through aluminium centres (i.e. Structure **1**). Hydrolysis, rotation and condensation takes place resulting in $\infty[\text{Al}_4\text{P}_4\text{O}_{20}\text{H}_4]^{4-}$ zigzag ladder type chains. The Mu-7 layers are then formed through a condensation reaction between one “parent” chain and two zigzag ladder chains.

While Vidal *et al.* felt this mechanism to be highly likely, they were unable to either isolate or detect the two kinds of chains involved in the building of the layers. The eutectic mixture method however appears to offer rather milder hydrolysis conditions than in hydrothermal or solvothermal synthesis, hence the “parent” chain was isolated at 170°C as Structure **1** and at 200 °C Structure **2** (Mu-7) was isolated. This suggests that synthesis in eutectic mixtures may be more controllable than other synthetic methods and perhaps more compounds that are not isolable under normal conditions can be recovered. Other workers have postulated different mechanisms of framework synthesis (see section 1.1.2) and the isolation of the “parent” chain in our work is not evidence either way of the mechanistic pathway (since we only characterise the final products) however it does raise some interesting points that may require further work.

9.4.3: Structure 3

A novel, 1-dimensional structure type, **3** was synthesised and its structure solved using single crystal X-ray diffraction on Station 9.8 at the Synchrotron Radiation Source, Daresbury. Crystal data and structure refinement details for Structure **3** are given in Table 9.8.

Table 9.8: Crystal data and refinement for Structure **3**

Identification code	Structure 3
Empirical formula	Al(HPO ₄) ₂ F · 2CH ₃ NH ₃
Formula weight	302.07
Temperature	150(2) K
Wavelength	0.69330 Å
Crystal system, space group	Monoclinic, P 2 ₁ /m
Unit cell dimensions	a = 8.4890(17) Å alpha = 90 ° b = 6.8360(14) Å beta = 109.69(3) ° c = 9.7440(19) Å gamma = 90 °
Volume	532.4(2) Å ³
Z, Calculated density	2, 1.884 Mg/m ³
Absorption coefficient	0.435 mm ⁻¹
F(000)	312
Crystal size	0.05 x 0.04 x 0.01 mm
Theta range for data collection	3.81 to 29.69 °
Limiting indices	-11<=h<=12 -9<=k<=9 -13<=l<=13
Reflections collected / unique	6074 / 1717 [R(int) = 0.0218]
Completeness to theta = 29.69	98.30 %
Refinement method	Full-matrix least-squares on F ²
Data / restraints / parameters	1717 / 0 / 101
Goodness-of-fit on F ²	0.854
Final R indices [I>2sigma(I)]	R1 = 0.0292, wR2 = 0.0814
R indices (all data)	R1 = 0.0356, wR2 = 0.0857
Largest diff. peak and hole	0.531 and -0.281 e. Å ⁻³

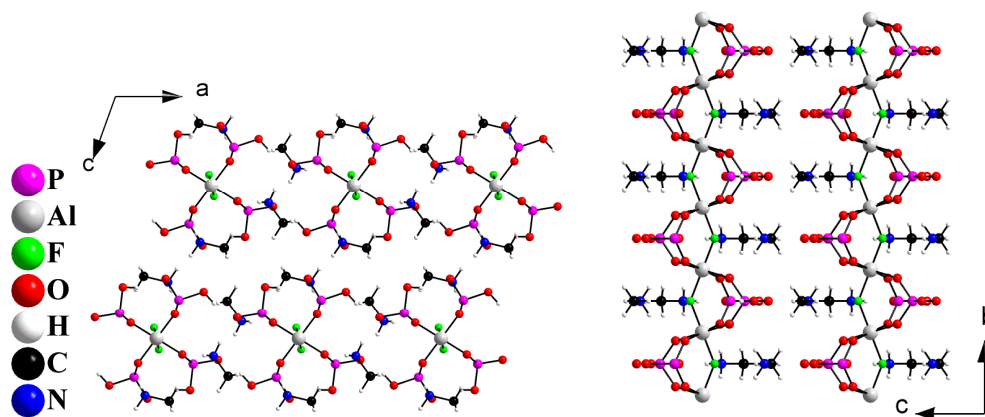


Figure 9.7: Structure 3 ball and stick diagram down the *a* and *b*-axis.

Structure 3 was synthesised with the addition of HF to the 1,3-dimethyl urea / tetraethyl ammonium bromide eutectic mixture resulting in a fluoroaluminophosphate chain with composition $\infty[\text{Al}(\text{HPO}_4)_2\text{F}]^{2-}$. Again the urea derivative breaks down *in situ* to provide the template of $[\text{CH}_3\text{NH}_3]^+$. The phosphorus atoms are tetrahedrally bonded to four oxygens, one of which is a terminal P-O and the other a terminal P-OH. The other two oxygens are bonded to octahedrally co-ordinated aluminium (AlO_4F_2). There exists an infinite Al-F-Al linkage in the chain parallel to the *b*-axis (Figure 9.7). There is some resolvable disorder of the phosphate groups in the chains. This has been omitted from Figure 9.7 for clarity.

This aluminophosphate chain framework is very similar to one synthesised by Yan *et al.*¹⁰ in a solvothermal synthesis where tetraethylene glycol was used as the solvent and hexamethyleneimine as the organic template. This gave a compound with the formula $[\text{Al}(\text{H}_2\text{PO}_4)(\text{HPO}_4)\text{F}] [\text{C}_6\text{H}_{12}\text{NH}_2]$.

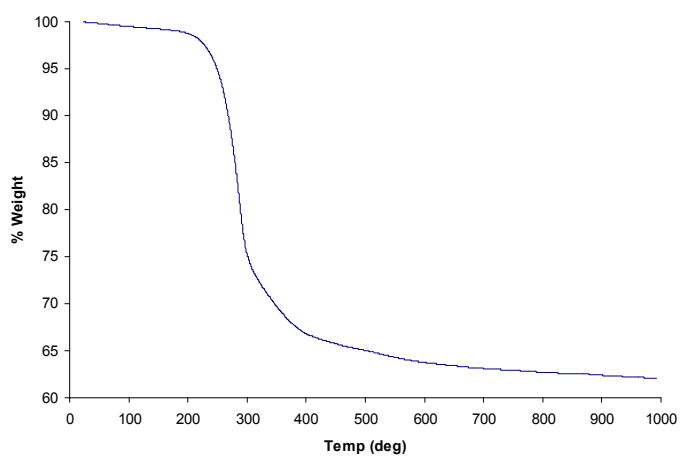


Figure 9.8: TGA experiment for Structure 3.

Structure 3 TGA data (Figure 9.8) shows a weight loss of about 31 % from 220 °C to 400 °C. This is comparable to the calculated weight loss of 28 % for the removal of the $[\text{CH}_3\text{NH}_3]^+$ and F^- . The CHN data gave values of C = 8.14, H = 4.49, N = 9.09 % which are not too dissimilar to the calculated values of C = 7.95, H = 4.67, N = 9.27 %.

9.4.4: Structure 4

Structure 4 was synthesised and solved using single crystal X-ray diffraction on Station 9.8 at the Synchrotron Radiation Source, Daresbury. Crystal data and structure refinement details for Structure 4 are given in Table 9.9.

Table 9.9: Crystal data and refinement for Structure 4

Identification code	Structure 4
Empirical formula	Al(PO ₄) ₂ (NH ₃ (CH ₃) ₂ NH ₃) (NH ₄)
Formula weight	297.08
Temperature	150(2) K
Wavelength	0.69330 Å
Crystal system, space group	Monoclinic, C 2/c
Unit cell dimensions	a = 17.584(9) Å alpha = 90 ° b = 8.047(5) Å beta = 105.647(12) ° c = 8.720(5) Å gamma = 90 °
Volume	1188.2(12) Å ³
Z, Calculated density	4, 1.661 Mg/m ³
Absorption coefficient	0.381 mm ⁻¹
F(000)	616
Crystal size	0.05 x 0.02 x 0.005 mm
Theta range for data collection	3.40 to 31.63 °
Limiting indices	-25<=h<=26 -12<=k<=12 -12<=l<=13
Reflections collected / unique	7171 / 2035 [R(int) = 0.1482]
Completeness to theta = 31.63 °	94.60 %
Absorption correction	None
Refinement method	Full-matrix least-squares on F ²
Data / restraints / parameters	2035 / 0 / 74
Goodness-of-fit on F ²	0.997
Final R indices [I>2sigma(I)]	R1 = 0.0545, wR2 = 0.1422
R indices (all data)	R1 = 0.0645, wR2 = 0.1456
Largest diff. peak and hole	0.741 and -0.737 e Å ⁻³

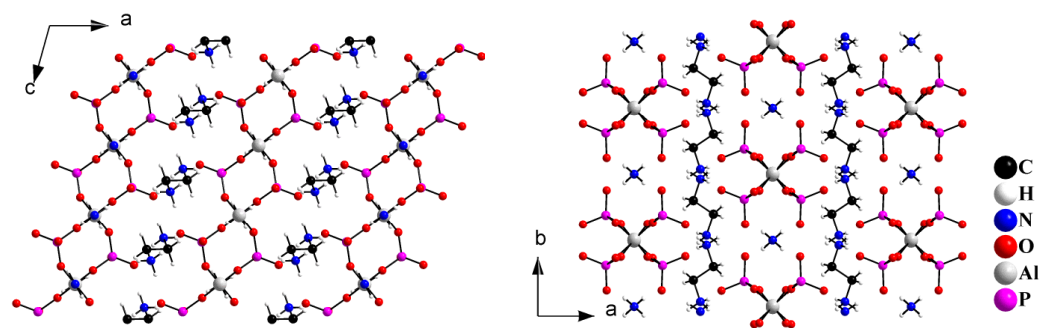


Figure 9.9: Ball and stick diagram of Structure 4 down the *b* and *c*-axis.

The data shows Structure 4 to be of the same chain composition, $\infty[\text{Al}(\text{PO}_4)_2]^{3-}$, as Structure 1 (Section 9.4.1) with corner sharing 4-membered rings (Figure 9.9). The derivatised urea in the eutectic mixture has broken down to provide the templating agent which in turn has fragmented, leading to the coexistence of $[\text{NH}_3(\text{CH}_3)_2\text{NH}_3]^{2+}$ and $[\text{NH}_4]^+$. These cations hold the chains together through hydrogen bond interactions with the terminal P-O linkages.

9.4.5: Structure 5

Structure **5** was solved using single crystal X-ray diffraction on Station 9.8 at the Synchrotron Radiation Source, Daresbury. The data showed Structure **5** to be polymorphic to Structure **4** (Section 9.4.4). The main difference is the symmetry of the structure, which means the chains are stacked in a slightly different way to that seen in **4** Figure 9.10. The unit cell dimensions for Structure **5**, $\text{Al}(\text{PO}_4)_2 \cdot (\text{NH}_3(\text{CH}_3)_2\text{NH}_3)(\text{NH}_4)$ were determined as orthorhombic $a = 19.961(5)$, $b = 8.018(5)$, $c = 8.732(5)$ Å.

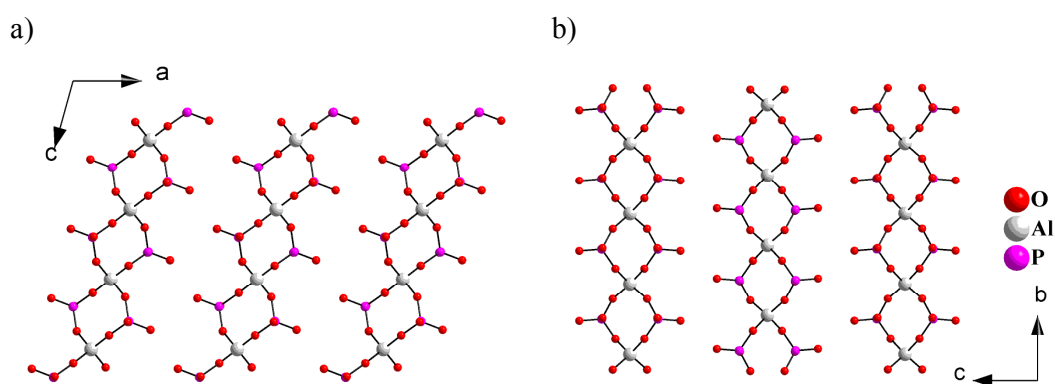


Figure 9.10: Diagram showing the AlPO chain stacking in a) Structure **4** b) Structure **5**

Structure **4** was isolated at a lower temperature than Structure **5** and only Structure **5** was synthesised phase pure. This indicates that Structure **5** is the thermodynamically more stable compound.

Structure **5** is isostructural with the one-dimensional chain aluminophosphate previously reported and characterised by Gao *et al.*¹¹ Gao's material was synthesised from a nonaqueous system of ethylene glycol with ethylenediamine as the template. In Gao's synthesis it is the ethylenediamine which is fragmented to give the ammonium ion.

9.4.6: Structure 6

Structure **6** has the same 2-dimensional layered framework topology as the $[\text{Al}_3\text{P}_4\text{O}_{16}]$ $1.5(\text{NH}_3(\text{CH}_2)_4\text{NH}_3)$ structure, previously synthesised under hydrothermal conditions by Thomas *et al.*¹² However in Structure **6** the organic template is produced from the *in situ* breakdown of the derivatised urea in the eutectic mixture to give $[\text{NH}_3(\text{CH}_2)_3\text{NH}_3]^{2+}$. Structure **6** was solved using single crystal X-ray diffraction on Station 9.8 at the Synchrotron Radiation Source, Daresbury. Crystal data and structure refinement details for Structure **6** are given in Table 9.10.

Table 9.10: Crystal data and refinement for Structure **6**

Identification code	Structure 6
Empirical formula	$2(\text{Al}_3\text{P}_4\text{O}_{16})_3 \cdot 3(\text{NH}_3(\text{CH}_2)_3\text{NH}_3)$
Formula weight	1150.07
Temperature	150(2) K
Wavelength	0.71073 Å
Crystal system, space group	Trigonal, P-3c1
Unit cell dimensions	$a = 12.8874(3)$ Å $\alpha = 90^\circ$ $b = 12.8874(3)$ Å $\beta = 90^\circ$ $c = 18.3844(9)$ Å $\gamma = 120^\circ$
Volume	$2644.30(16)$ Å ³
Z, Calculated density	2, 1.158 Mg/m ³
Absorption coefficient	0.382 mm ⁻¹
F(000)	908
Crystal size	0.04 x 0.04 x 0.04 mm
Theta range for data collection	2.87 to 30.86 °
Limiting indices	$-15 \leq h \leq 0$ $0 \leq k \leq 18$ $0 \leq l \leq 26$
Reflections collected / unique	2703 / 2703 [R(int) = 0.0000]
Completeness to theta = 30.86 °	96.70 %
Refinement method	Full-matrix least-squares on F ²
Data / restraints / parameters	2703 / 0 / 70
Goodness-of-fit on F ²	1.076
Final R indices [$I > 2\sigma(I)$]	R1 = 0.0674, wR2 = 0.2045
R indices (all data)	R1 = 0.0776, wR2 = 0.2084
Largest diff. peak and hole	1.116 and -1.018 eÅ ⁻³

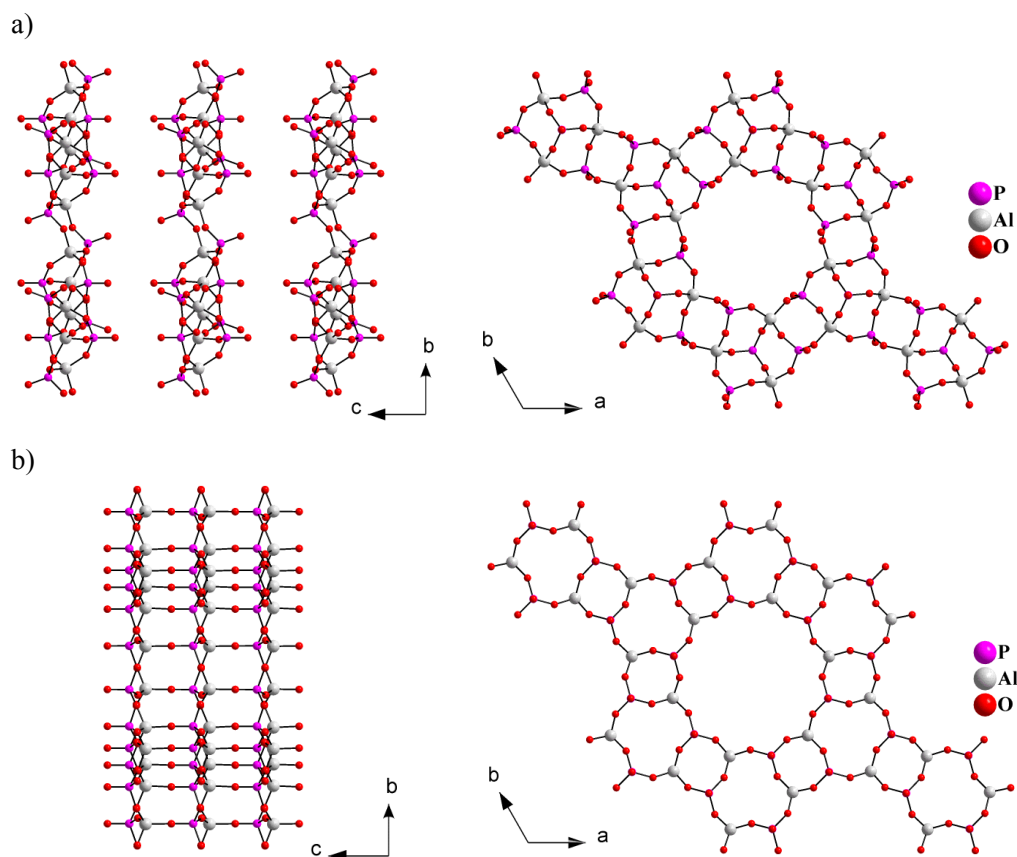


Figure 9.11: Ball and stick diagram to illustrate the similarities between a) Structure **6** and b) AlPO-5.

Structure **6** is a porous capped-AlPO-5-like layer structure, $[\text{Al}_3\text{P}_4\text{O}_{16}]^{-3}$, made up of single 4, 6 and 12 rings. Figure 9.11 illustrates the similarities between Structure **6** and AlPO-5.¹³ Structure **6** is a 2-dimensional layered structure composed of a central circular 12-membered ring, surrounded by a series of alternating 4-rings and capped 6-membered rings.

The organic template is again produced from the *in situ* breakdown of the amide in the eutectic mixture to give $[\text{NH}_3(\text{CH}_2)_3\text{NH}_3]^{2+}$. Some propylene diammonium cations could be located crystallographically but not all those required to balance the charge on the inorganic layers. However, there is still much space in the pore structure to accommodate further template molecules which may have been too disordered to locate through SCXD.

9.4.7: Structure 7

Structure 7 was solved using single crystal X-ray diffraction on Station 9.8 at the Synchrotron Radiation Source, Daresbury. The data showed Structure 7, $\text{Al}(\text{HPO}_4)(\text{PO}_4)(\text{NH}_3(\text{CH}_2)_3\text{NH}_3)$, to be triclinic with $a = 8.255$, $b = 8.614$, $c = 8.831 \text{ \AA}$, $\alpha = 112.02$, $\beta = 107.69$, $\gamma = 97.67^\circ$. This proved to be isostructural with the one-dimensional chain aluminophosphate previously reported and characterised by Ayi *et al.*¹⁴. This was the first time that the chain composition $\infty[\text{Al}(\text{HPO}_4)(\text{PO}_4)_2]^{2-}$ had been observed. The synthesis was carried out in aqueous conditions with 1,3-diammoniumpropane phosphate as the phosphorus source and templating agent.

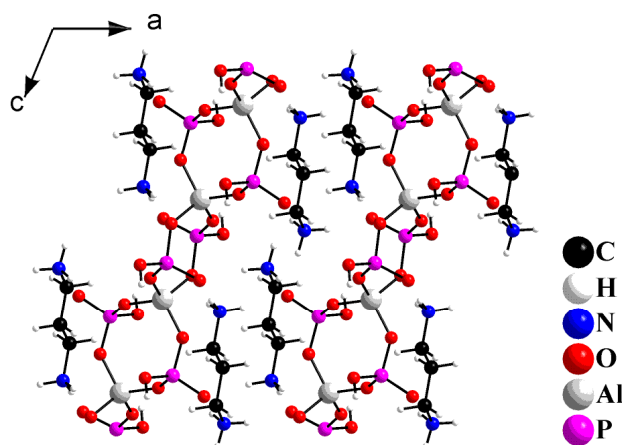


Figure 9.12: Ball and stick diagram of Structure 7 showing both the chains and template.

The Structure 7 chains are made from corner sharing AlO_4 and PO_4 tetrahedra as in Structures 1, 4 and 5. However the arrangement of the individual tetrahedra is such that every other four-membered ring in the chain is formed by either a PO_4 or a HPO_4 unit. Again the eutectic mixture amide has broken down to give the template, $[\text{NH}_3(\text{CH}_2)_3\text{NH}_3]^{2+}$. The template is crystallographically well ordered and fully resolved from the SCXD data. The cations charge balance the chain and hold the chains together through hydrogen bonding interactions with the terminal P-O linkages.

9.4.8: Structure 8

A novel, 2-dimensional structure type, **8** was synthesised and its structure solved using single crystal X-ray diffraction on Station 9.8 at the Synchrotron Radiation Source, Daresbury. Crystal data and structure refinement details for Structure **8** are given in Table 9.11.

Table 9.11: Crystal data and refinement for Structure **8**

Identification code	Structure 8
Empirical formula	$2\text{Al}_3(\text{PO}_4)_4 \cdot 3(\text{NH}_3(\text{CH}_2)_3 \text{NH}_3)$
Formula weight	1131.93
Temperature	423(2) K
Wavelength	0.69330 Å
Crystal system, space group	Triclinic, P-1
Unit cell dimensions	a = 11.026(4) Å alpha = 76.487(6) ° b = 14.598(5) Å beta = 84.144(6) ° c = 15.216(5) Å gamma = 73.376(6) °
Volume	2280.2(14) Å ³
Z, Calculated density	2, 1.649 Mg/m ³
Absorption coefficient	0.423 mm ⁻¹
F(000)	1136
Crystal size	0.05 x 0.02 x 0.01 mm
Theta range for data collection	1.34 to 31.31 °
Limiting indices	-15<=h<=16, -21<=k<=21 -22<=l<=22
Reflections collected / unique	27002 / 14357 [R(int) = 0.0809]
Completeness to theta = 31.31 °	89.20 %
Absorption correction	None
Refinement method	Full-matrix least-squares on F ²
Data / restraints / parameters	14357 / 0 / 415
Goodness-of-fit on F ²	0.936
Final R indices [I>2sigma(I)]	R1 = 0.0735, wR2 = 0.1927
R indices (all data)	R1 = 0.0974, wR2 = 0.2058
Largest diff. peak and hole	1.262 and -0.758 eÅ ⁻³

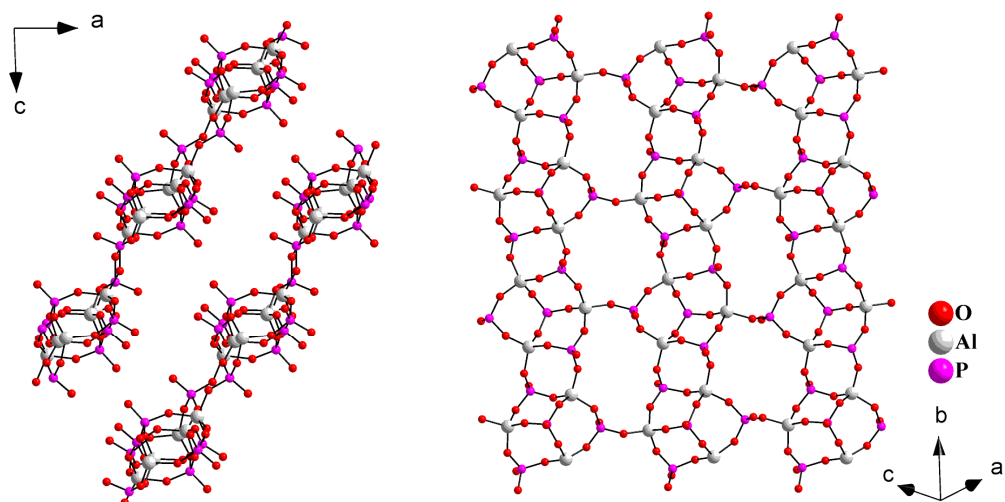


Figure 9.13: Ball and stick diagram showing the layers in Structure **8**

Structure **8** is a porous layered structure made up of a single 4, 6, and 8 rings. Within the sheets there are two distinctly different eight membered windows, one approximately circular and the other elliptical in shape (Figure 9.13). The network is made from a chain comprising of capped 6-rings joined by 4-rings. While Structure **8** has not been synthesised before the same layered structure has been isolated previously in several nonaqueous systems.¹⁵⁻¹⁸

The organic template is again produced from the *in situ* breakdown of the derivatised urea in the eutectic mixture to give $[\text{NH}_3(\text{CH}_2)_3\text{NH}_3]^{2+}$. Some propylene diammonium cations could be located crystallographically but not all those required to balance the charge on the inorganic layers. However, there is still much space in the pore structure to accommodate further template molecules.

9.4.9: Structure 9

Structure 9 was solved using MoK α radiation with a Rigaku rotating anode single-crystal X-ray diffractometer at the University of St Andrews. Interestingly this structure has the same framework topology as Zeolite A,¹⁹ but has been synthesised in the absence of F⁻. Crystal data and structure refinement details for Structure 9 are given in Table 9.12.

Table 9.12: Crystal data and refinement for Structure 9

Identification code	Structure 9
Empirical formula	4Ga(PO ₄) O
Formula weight	674.76
Temperature	150(2) K
Wavelength	0.71073 Å
Crystal system, space group	Cubic, F m-3c
Unit cell dimensions	a = 24.0030(13) Å alpha = 90 ° b = 24.003 Å beta = 90 ° c = 24.003 Å gamma = 90 °
Volume	13829.2(4) Å ³
Z, Calculated density	24, 1.945 Mg/m ³
Absorption coefficient	4.823 mm ⁻¹
F(000)	7677
Crystal size	0.07 x 0.07 x 0.07 mm
Theta range for data collection	2.40 to 28.58 °
Limiting indices	-32<=h<=32 -32<=k<=32 -32<=l<=32
Reflections collected / unique	30913 / 801 [R(int) = 0.0477]
Completeness to theta = 28.58 °	99.10%
Absorption correction	None
Refinement method	Full-matrix least-squares on F ²
Data / restraints / parameters	801 / 0 / 36
Goodness-of-fit on F ²	1.163
Final R indices [I>2sigma(I)]	R1 = 0.0391, wR2 = 0.0955
R indices (all data)	R1 = 0.0414, wR2 = 0.0972
Largest diff. peak and hole	0.837 and -0.583 eÅ ⁻³

The high cubic symmetry of the material precludes the location of the template and the final refinement used the data from the program SQUEEZE to exclude the scattering contribution from electron density within the pores. No fluoride ions were added to the synthesis of this material and chemical analysis and the lack of signal in ^{19}F MAS-NMR confirm that the atom at the centre of the D4R unit is not fluoride. This appears to be the first reporting of Zeolite A with oxygen in the centre of the D4R.

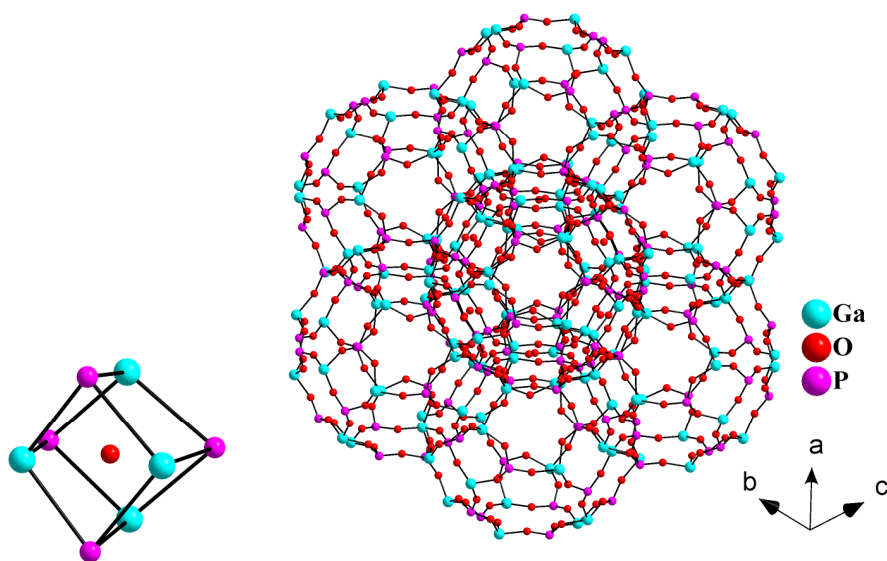


Figure 9.14: Structure **9** showing the oxygen at the centre of the D4R unit (all other oxygens omitted for clarity) and the full structure including all oxygens.

9.5: Discussion and Conclusions

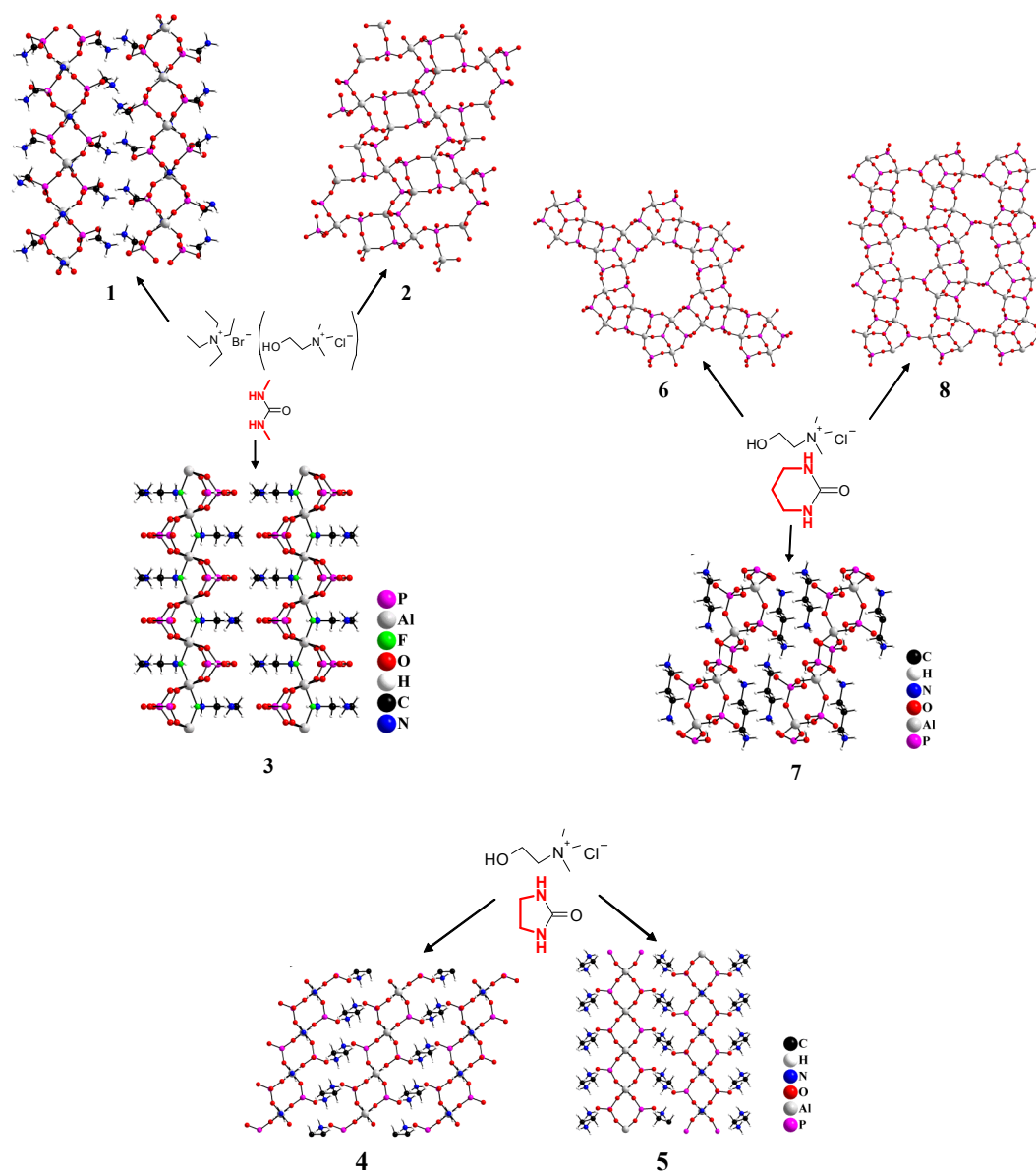


Figure 9.15: Summary of the AIPOs formed using eutectic mixtures as template delivery agents.

Figure 9.15 illustrates the different structures formed from three eutectic mixtures being used as solvent and template delivery agents. The use of eutectic mixtures allows the control of mineraliser concentration, e.g. water and HF to be retained while also providing a new mechanism by which the template is delivered to the reaction mixture. This synthesis technique has proved to be very versatile, delivering a number of

different templates to aid in the preparation of both AlPOs and GaPOs. Several hundred functionalised ureas are commercially available and many of these will probably be suitable for this type of work, illustrating the scope of this methodology. The ease of preparation of eutectic mixtures and the different chemistry involved, as evidenced by, for example the non-fluoride preparation of gallium phosphate Zeolite-A, indicate that this route may be particularly useful for targeting materials that are difficult to prepare in traditional hydrothermal synthesis.

The work in this chapter also illustrates that the template comes from the urea part of the eutectic mixture, as this is the only way in which the chemical structure of the templates can be explained. In work based on the urea/choline chloride mixture there was the possibility that the ammonium ions could originate from either the urea or the choline chloride. This issue is resolved in this work.

9.6: References

1. L. Vidal, C. Pray and J. Patarin, *Microporous Mesoporous Mater.*, 2000, **39**, 113
2. L. Vidal, V. Gramlich, J. Patarin and Z. Gabelica, *Eur. J. Solid State Inorg. Chem.*, 1998, **35**, 545
3. L. Vidal, C. Marichal, V. Gramlich, J. Patarin and Z. Gabelica, *Chem. Mater.*, 1999, **11**, 2728
4. L. Lakiss, A. Simon-Masseron, V. Gramlich and J. Patarin, *Solid State Sci.*, 2005, **7**, 141
5. J.L. Paillaud, B. Marler and H. Kessler, *Chem. Commun.*, 1996, 1293
6. C. Paulet, T. Loiseau and G. Ferey, *J. Mater. Chem.*, 2000, **10**, 1225
7. S. Oliver, A. Kuperman and G.A. Ozin, *Angew. Chem. Int. Ed.*, 1998, **37**, 46
8. A.B. Thomas and E.G. Rochow, *J. Am. Chem. Soc.*, 1957, **79**, 1843
9. L. Vidal, V. Gramlich, J. Patarin and Z. Gabelica, *Chem. Lett.*, 1999, **28**, 201
10. W.F. Yan, J.H. Yu, Z. Shi, Y. Wang, Y.C. Zou and R.R. Xu, *J. Solid State Chem.*, 2001, **161**, 259
11. Q.M. Gao, J.S. Chen, S.G. Li, R.R. Xu, J.M. Thomas, M. Light and M.B. Hursthouse, *J. Solid State Chem.*, 1996, **127**, 145
12. J.M. Thomas, R.H. Jones, R.R. Xu, J.S. Chen, A.M. Chippindale, S. Natarajan and A.K. Cheetham, *J. Chem. Soc., Chem. Commun.*, 1992, 929
13. G.J. Klap, H. van Keningsveld, H. Graafsma and A.M.M. Schreurs, *Microporous Mesoporous Mater.*, 2000, **38**, 403
14. A.A. Ayi, A. Choudhury and S. Natarajan, *J. Solid State Chem.*, 2001, **156**, 185
15. R.H. Jones, J.M. Thomas, R.R. Xu, Q. S. Huo, A.K. Cheetham and A.V. Powell, *J. Chem. Soc., Chem. Commun.*, 1991, 1266
16. S. Oliver, A. Kuperman, A. Lough and G.A. Ozin, *Inorg. Chem.*, 1996, **35**, 6373

17. P.A. Barrett and R.H. Jones, *J. Chem. Soc., Chem. Commun.*, 1995, 1979
18. R.H. Jones, A.M. Chippindale, S. Natarajan and J.M. Thomas, *J. Chem. Soc., Chem. Commun.*, 1994, 565
19. T.B. Reed and D.W. Breck, *J. Am. Chem. Soc.*, 1956, **78**, 5972

10: Review, Conclusions and Future Work

10.1: Summary and Conclusions

“Structural and synthetic solid state chemistry has continued to flourish during 2004. A notable highlight was the use of ionic liquids and eutectic mixtures in the synthesis of the SIZ series of templated aluminophosphate and aluminofluorophosphate zeolite and zeotype materials.”

*G.B. Hix, Annual Reports on the Progress of Chemistry (2005)*¹

The work presented in this thesis shows the first research into the new methodology of ionothermal synthesis, used for the synthesis of zeolite type materials. Much of the work has now been published,²⁻⁵ leading to other research groups investigating the area of ionothermal synthesis. This section will summarise and conclude the work presented in this thesis and tie in the related work that has been published in the area of ionothermal synthesis since my first publication in *Nature*, 2004.²

The most commonly used route to molecular sieve synthesis is the hydrothermal method.⁶ This involves the mixing of the reagents in water, which acts as the solvent, then heating in a sealed autoclave at autogenous pressure for a specific time. The water does however appear to have other roles in the synthesis. It can act as a space filler in the porous lattice, it enhances the reactivity and lowers the viscosity of the mixture. So the water is not only a solvent but a reactant and a catalyst in T-O-T bond formation.⁷

The aim of the work outlined in this thesis was to synthesis zeolite analogues, primarily aluminophosphates, using ionic liquids/eutectic mixtures as both the organic template

and the solvent, hence eliminating the space filling effects in the reaction from the water. This however is not a simple task as most ionic liquids are hygroscopic and can absorb significant amounts of water from the atmosphere.⁸ Even after a moderate drying process, water can still be present.⁹ At low concentrations of water the molecules are isolated or exist in small independent clusters hence a small amount of water will not disrupt the ionic-liquid-framework interactions.¹⁰ There is however still the possibility that the low concentration of water could act as a catalyst in T-O-T bond formation (where T are the tetrahedral framework atoms).

Ionic liquids such as 1-ethyl-3-methylimidazolium bromide are relatively polar solvents, hence they solubilise the starting materials almost completely at the reaction temperatures, indicating that the synthesis mechanism is a crystallisation from solution rather than a solid-to-solid-transformation. The dependence of the products on water and HF gives some clues as to the mechanism of the reaction. With little water and no HF to act as mineralisers, interrupted framework structures such as the novel SIZ-1, SIZ-2 and SIZ-6 structures can be targeted (Chapters 4 and 8). On addition of HF or water, condensed structures, e.g. SIZ-3, SIZ-4, and SIZ-5 are formed with no hanging P-O bonds (Chapter 4). The ionic liquids are good solvents on their own, but adding fluoride or water as mineralisers appears to increase their solvating power and can change the types of framework that are formed, hence it appears possible to target the synthesis of interrupted or condensed frameworks using ionothermal synthesis.

The ionic liquid, in the production of SIZ-3 and SIZ-4, can be recycled and used for further zeolite synthesis. This not only lowers the potential cost of synthesising zeotypes ionothermally, but also eliminates the possible environmental issues involved in disposing of large solvent quantities of ionic liquids. Provisional tests carried out on

aquatic animals have shown that some ionic liquids are more toxic than conventional solvents such as methanol, dichloromethane and acetonitrile,¹¹ although this depends on the chemical structure of the ionic liquid.

Ionic liquids have negligible vapour pressure and synthetic procedures can be carried out in open vessels avoiding the high autogenous pressures (up to 15 atm at 200 °C) and associated safety concerns that accompany hydrothermal synthesis in sealed autoclaves. Again, this distinguishes ionothermal synthesis from hydrothermal methods. Pioneering work has recently been carried out by Xu *et al.*¹² using microwaves as the heat source in ionothermal synthesis due to the ionic liquids negligible vapour pressure and suitable thermal stability. Microwave heating has several advantages over conventional heating such as fast crystal growth and higher selectivity.¹³ It has been shown that SIZ-3 AEL type crystals can be grown in 20 minutes using microwave heating compared to 48 hours using conventional heating methods. The negligible vapour pressure of the ionic liquids has removed the safety concerns raised over microwave heating under hydrothermal synthesis conditions, where the pressures could reach up to 476 KPa at 150 °C.¹²

The synthesis of the three Co-AIPOs, SIZ-7, SIZ-8 and SIZ-9, is an indication that the ionothermal synthesis method is suitable for the preparation of transition metal-functionalised frameworks that may be useful for applications such as catalysis or gas adsorption (Chapter 5). The preparation of the novel framework topology, SIZ-7, is a further indication of the possible potential of ionothermal synthesis in the production of new zeotype materials. Also of interest is the sensitivity of the ionothermal synthesis technique. Previously discussed is the role of HF and water in the reaction and the ability to target interrupted of condensed frameworks using ionothermal synthesis. On

addition of cobalt hydroxide as the cobalt source, further reaction conditions will be altered such as pH and water content. The hydroxide may react with either the phosphoric acid (added as the phosphorus source) or the acidic hydrogen on the imidazolium ring, thus increasing the volume of water in the reaction. The water could then act as a catalyst in T-O-T bond formation, thus explaining why SIZ-7, SIZ-8 and SIZ-9 are all fully condensed frameworks.

Xu *et al.*¹⁴ reported the ionothermal synthesis of Si-AlPOs. This work however needs further clarification as no analysis is reported to demonstrate the amount of silicon that is incorporated into the AIPO frameworks. With the addition of tetraethylorthosilicate (TEOS) a phase change is seen, again illustrating the sensitivity to reagents of the ionothermal technique in zeotype synthesis.

Many ionic liquid cations are chemically very similar to species that are already known as good templates (alkylimidazolium-, pyridinium-based ionic liquids etc). By changing the cation slightly e.g. altering the chain on the alkyl-methylimidazolium, it was hoped that different framework topologies would result, as demonstrated in the hydrothermal synthesis work by Zones.¹⁵ However the AIPO-CHA and SIZ-6 structures appear to be default structures that form when the cation is altered slightly. The fact that the SIZ-4 and SIZ-10 CHA frameworks have different templates points to the organic acting more as a space-filler than a structure directing agent according to the definition by Davis and Lobo (section 1.1.3).¹⁶ The same is true of SIZ-6 and SIZ-11, where the organic cation is 1-methyl-3-ethylimidazolium and 1-isopropyl-3-methylimidazolium respectively (Chapter 6).

Most ionic liquids show suitable thermal stability to be utilised in ionothermal synthesis. Many are reported to be stable to almost 400 °C¹⁷ with even the worst of the common ionic liquids stable to well above the temperatures we have shown are required for successful ionothermal synthesis. However with the addition of reagents such as HF, this appears to catalyse, over the period of several days, the slow metathesis rearrangement of the alkyl-methylimidazolium bromides, hence the templating agent seen in several products is the 1,3-dimethylimidazolium cation.

Investigations carried out involving the replacement of the bromide anion with PF₆⁻ resulted in the formation of β-NH₄AlF₄ (Chapter 7). This was only formed with the addition of phosphoric acid (85 wt% in H₂O) indicating that the water was required for the PF₆⁻ to undergo hydrolysis to produce HF and PO₄³⁻ before crystallisation could take place. This work does however still leave open the question as to why the phosphorus remained in solution, but this may have to do with the quantity of HF acting as a mineraliser. The template in this reaction was ammonium. Again this appears to illustrate how the HF catalyses the decomposition of the ionic liquid over time.

In an attempt to overcome this effect of HF on the ionic liquid, the anion was changed to (CF₃SO₂)₂N⁻ (Chapter 7). To date, (CF₃SO₂)₂N⁻ has been found to be one of the anions which produces the more thermally stable ionic liquids, with many being stable to well over 500 °C.¹⁸ The product obtained using this ionic liquid however did not contain any structure directing agent. One suggestion for why the cation may not have been incorporated into this structure could be due to the size of the anion. The idea behind ionothermal synthesis was to potentially remove the competition between template-framework and solvent-framework interactions that are present in hydrothermal preparations. However if the anion in the ionic liquid is large and bulky,

this too could act to prevent favourable template-framework interactions hence hindering the formation of a three-dimensional framework. However the $(\text{CF}_3\text{SO}_2)_2\text{N}^-$ anion also produces relatively less polar solvents than the Br^- anion hence the starting materials are not soluble in this ionic liquid. This indicates a solid-phase transformation rather than a solution-mediated transformation.

Recent work by Lin *et al.*¹⁹ has taken the idea of ionothermal synthesis a step further by incorporating the technique of ionothermal synthesis and microwave heating to synthesise anionic metal-organic frameworks (MOF) templated by the ionic liquid; $(\text{EMIm})_2[\text{Ni}_3(\text{TMA})_2(\text{OAc})_2]$. This work demonstrates the future potential of ionothermal synthesis not only as a methodology for zeolite and zeotype material synthesis but rather a general technique for open-framework materials synthesis.

The use of eutectic mixtures as solvents has provided a new mechanism whereby the eutectic mixture also acts as a template delivery agent (Chapters 8 and 9). This synthesis technique has been shown to be very versatile, delivering a number of different templates to aid in the preparation of both AlPOs and GaPOs. Several hundred functionalised ureas are commercially available and many of these will probably be suitable for this type of work, illustrating the scope of this methodology. The ease of preparation of eutectic mixtures and the different chemistry involved, as evidenced by, for example the non-fluoride preparation of gallium phosphate zeolite-A, indicate that this route may be particularly useful for targeting materials that are difficult to prepare in traditional hydrothermal synthesis.

The isolation of several “parent chain” structures also points to the rather milder hydrolysis conditions than in hydrothermal or solvothermal synthesis. The control of

the addition of mineralisers such as water and HF can again be carefully monitored, with the addition of water tending to lead to the formation of two-dimensional structures. Time studies carried out on the production of SIZ-2 showed that the nucleation and crystallisation takes place at relatively low levels of solvent degradation under conditions where the concentration of the template species is slowly increasing as more eutectic mixture decomposes.

Liao *et al.*²⁰ recently reported the synthesis of a novel coordination polymer, $Zn(O_3PCH_2CO_2) \cdot NH_3$, where the solvent was the eutectic mixture choline chloride/urea, The urea partially decomposes and acts as the template delivery agent to produce the structure-directing ammonium ions. Work has also been carried out by Sheu *et al.*²¹ using a eutectic mixture of choline chloride/malonic acid as the solvent to produce two new open-framework iron oxalatophosphates; $Cs_2Fe(C_2O_4)_{0.5}(HPO_4)_2$, $CsFe(C_2O_4)_{0.5}(H_2PO_4)(HPO_4)$. This is the first report of ionothermal synthesis of organic-inorganic hybrid compounds. Both the work by Liao *et al.* and the work by Sheu *et al.* demonstrates again the versatility and ease of using eutectic mixtures as solvents for the synthesis of open-framework structures. New structures are being synthesised that have not previously been possible to make under hydrothermal or solvothermal conditions, again indicating that the eutectic mixture plays a vital role in the crystallisation.²¹

Another advantage of ionothermal synthesis is the production of crystals suitable for single crystal characterisation. Zeolites are notoriously difficult to prepare as large crystals. My experience in preparing zeotypes in this work indicates that these solvent systems are suitable for the preparation of highly ordered solids with crystals large

enough for single crystal X-ray diffraction studies at a synchrotron source. This makes the characterisation of the structural architecture very much easier than is often the case.

The methodology of ionothermal synthesis is still in its early stages, but it is however a growing field. The diversity of materials and novel structures being made is expanding with the recent synthesis of AlPOs, Co-AlPOs, GaPOs, MOF and coordination polymers. There are still many questions to be answer and potentially large amounts of work to be carried out in this new field. The following section (10.2) will cover some of the ideas for future work.

10.2: Future Work

Here I will discuss a selection of ideas for possible future work. Some preliminary experiments have been carried out for some of the ideas and these will be discussed in this section, but full structural characterisations have not been completed.

Many ionic liquid cations are chemically very similar to species that are already known as good templates (e.g. alkylimidazolium-, pyridinium-based ionic liquids etc). Work in this thesis has concentrated primarily on the alkylimidazolium-based ionic liquids however research into other ionic liquid cations including the pyridiniums and the 4-dimethyl-aminopyridiniums (DMAP) was started and initial results appear promising with the production of several AlPO and SiO crystalline materials.

The production of a new silicate polymorph framework was a break through. However further work is required as it was produced as isolated crystals amongst a lot of amorphous material. This result however is important as it shows is that it is possible to ionothermally synthesise pure silicates. Data was collected on Station 9.8 at the Synchrotron Radiation Source, Daresbury and the framework was fully identified as a new silicate polymorph framework topology, SIZ-12 (Crystallographic data can be found on the accompanying CD). Triclinic P-1, $a = 7.116 (1)$, $b = 7.622 (1)$, $c = 7.622 (2)$ Å, $\alpha = 115.198 (2)$, $\beta = 100.730 (2)$, $\gamma = 106.848 (2)$ °. There is some unidentified electron density in the pores of this material which maybe sulphur or silicon half occupying two sites.

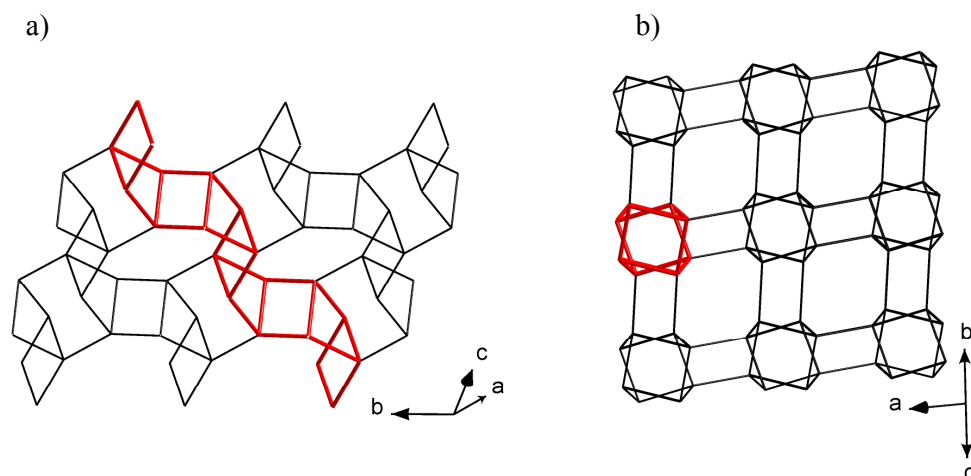


Figure 10.1: Line diagrams of SIZ-12 where each line represents a Si-O-Si linkage. a) a layer through the structure illustrating the distorted double crankshaft chain in red b) the three-dimensional structure.

The SIZ-12 structure is made up of distorted double crankshaft chains illustrated in red in Figure 10.1. These chains form a layer with each chain being a mirror image of the next to form pear shaped pores. The layers are joined together in an ABAB sequence to give a three-dimensional structure. SIZ-12 cannot be classified as a zeolite due to its lack of porosity hence it is a polymorph. SIZ-12 has a framework density of 23.92 Si/1000 Å³ which is comparable to that of quartz, cristobalite and tridymite which have framework densities of 26.52, 23.33 and 22.61 Si/1000 Å³ respectively.²²

Work is currently continuing in the group to further investigate the effects of using the pyridinium-based ionic liquids in the synthesis of GaPOs and AlPOs. This leads onto a further area of future work which is to investigate the use of ionothermal synthesis for the production of materials other than AlPOs. Most of the work in this thesis concentrated on AlPOs with some preliminary work on SiO (as illustrated above) and GaPOs (Chapter 9.4.9 LTA Zeolite A occluding oxygen).

Initial experiments carried out using the ionic liquid 1-ethyl-3-methylimidazolium bromide and the eutectic mixtures as solvent and template in the production of GaPOs

were successful with the production of several already known three-dimensional structures including ULM-3²³ and LTA Zeolite A occluding fluoride.²⁴ (Crystallographic data can be found for both these structures on the accompanying CD.) Work on the characterisation of the organic template has not yet been completed. Initial findings seem to indicate that the three-dimensional GaPO structures are easier to synthesise ionothermally than either the AlPOs or SiOs. This pattern is the same as in hydrothermal synthesis.

Preliminary work has been started using the gallophosphate double-4-ring (D4R) building unit occluding oxygen²⁵ as a starting material for the production of three-dimensional zeotype structures. The production of zeotype structures with hanging P-O bonds suggests that ionothermal synthesis may have a slower rate of hydrolysis, hence it was hoped that the D4R building units would stay intact and join together to form a three-dimensional ACO type zeotype structure. This would lead to an attractive mechanistic idea to the design and preparation of molecular sieves that has thus far appeared to be unsuccessful in hydrothermal/solvothermal synthesis.²⁶

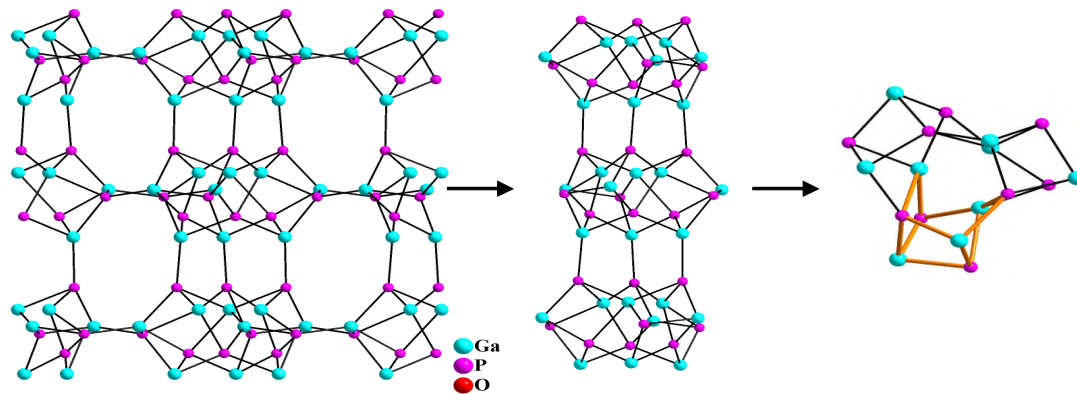


Figure 10.2: Diagram illustrating the framework topology and building unit of the GaPO synthesised from the GaPO D4R building unit.

Preliminary findings produced the GaPO framework topology illustrated in Figure 10.2. This was identified by a matrix (hexagonal $a = 12.34$, $c = 16.73$ Å) collected on Station 9.8 at the Synchrotron Radiation Source, Daresbury, however a full data set was not collected. This framework topology has been synthesised hydrothermally and its structure reported by Gunagdi *et al.*²⁷ Of particular interest is the fact that the framework is constructed of blocks of three cubes, all opened up and joined together as illustrated in Figure 10.2. This result indicates that the starting material cubes may have acted as building blocks in the formation of this structure. However, if the same reaction conditions are used but the tetrahedral framework reagent source changed to gallium sulphate and phosphoric acid, the same product is formed. This result therefore leads to many questions about the possible mechanisms by which this structure is formed. One possible method of investigating these mechanisms may be the use of *in situ* synchrotron powder X-ray diffraction studies to monitor any changes in the crystalline product produced throughout the reaction.²⁸

Another interesting idea is the use of a mixture of different ionic liquids²⁹ as solvent and template in zeolite synthesis. If we consider the results from using the EMIBr, the ionic liquid acted as template and solvent, but this ionic liquid is difficult to handle due to its hygroscopic nature. Also there are questions over its thermal stability with the addition of HF. The EMITf₂N however has a greater thermal stability and is hydrophobic but appears not to act as the template. Preliminary experiments have been carried out using a mixed solvent system of EMIBr and EMITf₂N. The resulting powder X-ray diffraction (PXRD) data is shown in Figure 10.3.

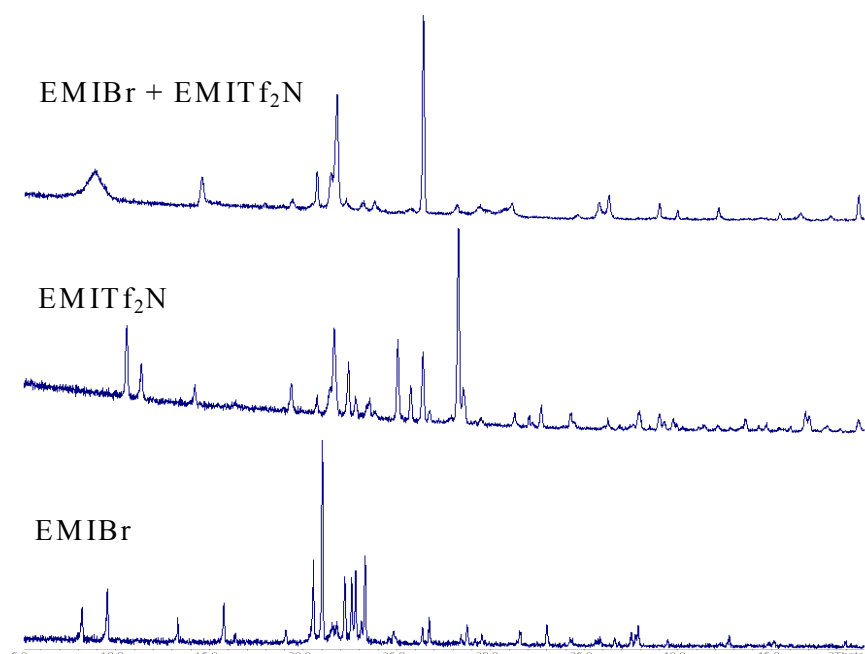


Figure 10.3: XRD data showing the different products produced using two different ionic liquids and a mixed ionic liquid system.

EMIBr produces SIZ-3 AlPO-11, EMITf₂N produces Al(H₂PO₄)₂F, and the mixture of ionic liquids appears to produce two phases. One is a crystalline dense phase and the other is partially crystalline showing a broad peak at about $2\theta = 10^\circ$. Only two experiments were tried using this mixed ionic liquid system. I believe that this idea however could lead to some interesting studies. As well as mixed anion ionic liquid systems the cations can also be mixed. This would be an interesting study to carry out to see if two products were formed using the different cation templates or if competition of templates leads to just one product being formed.

Other areas of future work include investigating the ability to induce greater selectivity hence making more of the products phase pure. It is claimed that microwave heating leads to greater selectivity^{12, 19} hence this maybe a possible method of producing phase pure materials. Microwave heating would also overcome the problems encountered from default structures being seeded in the Teflon™ liners since the microwavable vessels

are glass and disposable. Other problems may arise though such as the HF etching the glass.

Work into other inorganic porous materials is currently being undertaken in the group with the recent production of several metal organic framework (MOF) structures. This again demonstrates the versatility of the ionothermal synthesis technique.

Here I have discussed a selection of ideas for the future work and direction that the new synthesis methodology of ionothermal synthesis could take. These ideas are summarised in bullet form.

- Change the ionic liquid cation
- Change the ionic liquid anion
- Investigate mixed ionic liquid systems
- Investigate the effect of the addition of a traditional organic structure directing agent to the synthesis procedure
- Change the tetrahedral framework reagent source
- Make zeotypes phase pure, perhaps investigating further the claims that microwave heating produces greater selectivity.
- Use microwave heating in general for ionothermal synthesis of zeotypes since this method is far faster, producing typically better crystals than reactions by conventional heating methods
- Extend the methodology of ionothermal synthesis to other areas of inorganic synthesis.

10.3: References

1. G.B. Hix, *Annu. Rep. Prog. Chem., Sect. A.*, 2005, **101**, 394
2. E.R. Cooper, C.D. Andrews, P.S. Wheatley, P.B. Webb, P. Wormald and R.E. Morris, *Nature*, 2004, **430**, 1012
3. E.R. Parnham, P.S. Wheatley and R.E. Morris, *Chem. Commun.*, 2006, 380
4. E.R. Parnham and R.E. Morris, *J. Am. Chem. Soc.*, 2006, **128**, 2204
5. E.R. Parnham, E.A. Drylie, P.S. Wheatley, A.M.Z. Slawin and R.E. Morris, *Angew. Chemie.*, 2006, **118**, 1
6. R.M. Milton, U.S. 2 882 243, 1959
7. S.Y. Yang, A.G. Vlessidis and N.P. Evmiridis, *Microporous Mater.*, 1997, **9**, 273
8. L. Cammarata, S.G. Kazarian, P.A. Salter and T. Welton, *Phys. Chem. Chem. Phys.*, 2001, **3**, 5192
9. J.G. Huddleston, A.E. Visser, W.M. Reichert, E.D. Willauer, G.A. Broker and R.D. Rogers, *Green Chem.*, 2001, **3**, 156
10. C.G. Hanke and R.M. Lynden-Bell, *J. Phys. Chem. B*, 2003, **107**, 10873
11. C. Pretti, C. Chiappe, D. Pieraccini, M. Gregori, F. Abramo, G. Monni and L. Intorre, *Green Chem.*, 2006, **8**, 238
12. Y.P. Xu, Z.J. Tian, S.J. Wang, Y. Hu, L. Wang, B.C. Wang, Y.C. Ma, L. Hou, J.Y. Yu and L.W. Lin, *Angew. Chem.*, 2006, **45**, 1
13. A. Arafat, J.C. Jansen, A.R. Ebaid and H. an Bekkum, *Zeolites*, 1993, **13**, 162
14. Y.P. Xu, Z.J. Tian, Z.S. Xu, B.C. Wang, P. Li, S.J. Wang, Y. Hu, Y.C. Ma, K.L. Li, Y.J. Liu, J.Y. Yu and L. W. Lin, *Chin. J. Catal.*, 2005, **26**, 446
15. S.I. Zones, *Zeolites*, 1989, **9**, 458
16. M.E. Davis and R.F. Lobo, *Chem. Mater.*, 1992, **4**, 756

17. H.L. Ngo, K. LeCompte, L. Hargens and A.B. McEwen, *Thermochim Acta.*, 2000, **357**, 97
18. J.M. Crosthwaite, M.J. Muldoon, J.K. Dixon, J.L. Anderson and J.F. Brennecke, *J. Chem. Thermodyn.*, 2005, **37**, 559
19. Z. Lin, D.S. Wragg and R.E. Morris, *Chem. Commun.*, 2006, 2021
20. J.H. Liao, P.C. Wu and Y.H. Bai, *Inorg. Chem. Commun.*, 2005, 390
21. C.Y. Sheu, S.F. Lee and K.H. Lii, *Inorg. Chem.*, 2006, **45**, 1891
22. M.A. Camblor, L.A. Villaescusa and M.J. Diaz-Cabanas, *Topics in Catalysis*, 1999, **9**, 59
23. L. Beitone, J. Marrot, T. Loiseau and G. Ferey, *Microporous Mesoporous Mater.*, 2002, **56**, 163
24. M.M. Mertens, C. Schottdaric, P. Reinert and J.L. Guth, *Microporous Mater.*, 1995, **5**, 91
25. D.S. Wragg and R.E. Morris, *J. Phys. Chem. Solids*, 2001, **62**, 1493
26. R.E. Morris, *J. Mater. Chem.*, 2005, **15**, 931
27. Y. Guangdi, F. Shahua and X. Ruren, *Chem. Commun.*, 1987, 1254
28. R.I. Walton, T. Loiseau, D. O'Hare and G. Ferey, *Chem. Mater.*, 1999, **11**, 3201
29. K. Hayamizu, Y. Aihara, H. Nakagawa, T. Nukuda and W.S. Price, *J. Phys. Chem. B*, 2004, **108**, 19527